Tidal-Flow, Circulation, and Flushing Changes Caused by Dredge and Fill in Tampa Bay, Florida

By CARL R. GOODWIN

Prepared in cooperation with the
U.S. Army Corps of Engineers
and the Tampa Port Authority

U.S. GEOLOGICAL SURVEY WATER-SUPPLY PAPER 2282

DEPARTMENT OF THE INTERIOR
DONALD PAUL HODEL, Secretary

U.S. GEOLOGICAL SURVEY
Dallas L. Peck, Director

UNITED STATES GOVERNMENT PRINTING OFFICE: 1987

For sale by the Books and Open-File Reports Section, U.S. Geological Survey, Federal Center, Box 25425, Denver, CO 80225

Library of Congress Cataloging in Publication Data

Goodwin, Carl R.
Tidal-flow, circulation, and flushing changes caused by dredge and fill in Tampa Bay, Florida.

(U.S. Geological Survey water-supply paper ; 2282)
Bibliography: p.
Supt. of Docs. no.: I 19.13:2282
1. Tides—Florida—Tampa Bay—Data processing. 2. Tides—Florida—Tampa Bay—Mathematical models. 3. Oceanic circulation—Florida—Tampa Bay—Data processing. 4. Oceanic circulation—Florida—Tampa Bay—Mathematical models. 5. Dredging—Florida—Tampa Bay. 6. Fills (Earthwork)—Florida—Tampa Bay. I. United States. Army. Corps of Engineers. II. Tampa Port Authority. III. Title. IV. Series.
GC334.G66 1987 551.46'34 84-600408

CONTENTS

FIGURES

TABLES

Tidal-Flow, Circulation, and Flushing Changes Caused by Dredge and Fill in Tampa Bay, Florida

By Carl R. Goodwin

Abstract

Tampa Bay, Florida, underwent extensive physical changes between 1880 and 1972 because of construction of causeways, islands, channels, and shoreline fills. These changes resulted in a progressive reduction in the quantity of tidal water that enters and leaves the bay. Dredging and filling also changed the magnitude and direction of tidal flows in large parts of the bay.

A two-dimensional, finite-difference, hydrodynamic model was used to simulate flood, ebb, and residual transport of both water and a dissolved constituent for the physical conditions that existed in Tampa Bay during 1880 and 1972 and for the conditions that are likely to exist in 1985. The calibrated and verified model was used to hindcast water- and constituent-transport changes caused by construction in the bay between 1880 and 1972. The model was used also to forecast changes that can be expected to occur as a result of a major Federal dredging project scheduled for completion in 1985.

The model forecasted transport changes caused by the Federal dredging project to be much less areally extensive than the corresponding transport changes caused by construction in Tampa Bay between 1880 and 1972. Dredging-caused changes of more than 50 percent in flood and ebb transport were computed to occur over only 8 or 9 square miles of the bay's 390-square-mile surface area between 1972 and 1985. The model computed that construction between 1880 and 1972 caused changes of similar magnitude over 58 square miles of the bay. Dredging-caused changes of more than 50 percent in residual transport were computed to occur over 58 square miles of the bay between 1972 and 1985. According to the model simulation, construction between 1880 and 1972 caused changes of similar magnitude over 167 square miles.

Computations reveal historical tide-induced circulation patterns. The patterns consist of a series of about 20 interconnected circulatory features that range in diameter from 1 to 6 miles. Dredging- and construction-caused changes in size, position, shape, and intensity of the circulatory features increase tide-induced circulation and flushing throughout most of the bay. As a result of past and projected physical changes, the bay can and will more rapidly transfer waterborne constituents that have landward sources to the Gulf of Mexico. Conversely, the bay can and will more rapidly transfer constituents that have their source in the Gulf into the upper parts of the bay.

Model results show that the bay can be functionally subdivided into eight circulation zones. The zones near the entrances to Tampa Bay and the major bay subunits, Hillsborough Bay and Old Tampa Bay, have several times greater average circulation than do adjacent and more landward zones. Circulation generally decreases from the Gulf of Mexico to the head of Hillsborough and Old Tampa Bays, with a striking exception in zone 3 in mid-Tampa Bay. This 10-mile section of the bay has significantly lower average circulation than that of adjacent zones, particularly for conditions in 1880. The section is thought to be a circulation constriction that reduces the potential transport of dissolved and suspended constituents.

Circulation in the constricted section was computed as having increased 6 percent because of dredge and fill construction between 1880 and 1972. An additional increase of 21 percent, due to the Federal dredging project, is calculated. With these increases, this zone acts as less of a constriction than it did in 1880. This and other circulation increases may have contributed to increased bay salinity and to more rapid flushing of constituents from the bay to the Gulf of Mexico.

INTRODUCTION

Dredge, fill, and other construction activities have created many physical features in Tampa Bay that were not present before about 1880. These features include tens of miles of ship channels, many square miles of islands and submerged dredged-material disposal sites, four major bridges and causeways that span the bay, and numerous residential and commercial shoreline landfills. Most construction occurred between 1880 and 1972, and peak activity occurred in the 1950's and 1960's. Before this study, the cumulative impacts of these features on movement of water and waterborne constituents in the bay were not well understood, and impacts of proposed future physical changes could not be anticipated or compared with past changes.

A Federal dredging project to widen and deepen the main ship channel in Tampa Bay was started in 1976. By 1985, the anticipated end of the project, approximately 70 million yd^3 of bay bottom will have been moved and

deposited as large islands or in submerged disposal areas along the 35-mi channel. Before dredging began, the magnitude of the project and lack of information regarding possible changes in tidal flow, circulation, and flushing caused considerable concern regarding potential adverse environmental effects. A need for predictive and comparative information on flow, circulation, and flushing was recognized.

Changes in water circulation can have an impact on the overall health and ecological stability of estuaries. In general, increases in estuarine circulation result in more rapid net movement of dissolved and suspended constituents from regions of high concentration to regions of low concentration. Changes in circulation in an estuary, therefore, can cause long-term changes in the distribution and concentration levels of all waterborne material.

Long-term changes in many physical, chemical, and biological properties of estuarine water can induce ecological shifts that may destroy natural checks and balances within estuaries that have evolved over many hundreds or thousands of years. The need to assess the impact of dredge and fill projects on water circulation, as a means to help forecast the ecological shifts that might result, led to this study. The study was undertaken by the U.S. Geological Survey, initially in cooperation with the Tampa Port Authority and subsequently in cooperation with the U.S. Army Corps of Engineers.

Purpose and Scope

This study addresses the effects of dredge and fill on tidal flow, circulation, and flushing in Tampa Bay. The objectives of the study were as follows:

1. to develop methods by which tidal-flow, circulation, and flushing changes due to physical alterations of estuaries can be quantified and compared;
2. to determine tidal-flow, circulation, and flushing changes caused by the cumulative impact of construction in Tampa Bay from 1880 to 1972 (that is, prior to a large Federal dredging project to widen and deepen the main ship channel in Tampa Bay);
3. to determine tidal-flow, circulation, and flushing changes between 1972 and 1985 caused by the Federal dredging project; and
4. to compare and evaluate tidal-flow, circulation, and flushing changes caused by the Federal dredging project and all prior construction in Tampa Bay.

The circulation mechanism investigated in this report is a tidal "pumping" action caused by interaction between tidal flow and an irregular bottom configuration (Fischer and others, 1979). After a tidal cycle, a water parcel will return to the same position that it occupied at the start of the cycle if tidal inflow (flood) and tidal outflow (ebb) patterns in an estuary are exactly the same and if other flow-inducing mechanisms are not operating. If flood and ebb patterns differ, the water parcel will not return to its initial position but will be displaced by some distance from its starting position. The net displacement of every water parcel over successive tidal cycles is a result of circulation caused by tidal pumping. Different flood and ebb patterns are caused by the irregular physical dimensions of an estuary. These dimensions include the estuary's general shape and bottom configuration and the size and shape of islands, peninsulas, channels, shoals, and marshes.

Circulation and flushing in estuaries can be influenced by physical alterations created by construction of channels, islands, causeways, and shoreline dredge and fill areas. Computer simulation techniques can be used to investigate the nature and extent of this influence. This report presents information on (1) computer simulation modeling of tidal flow, circulation, and flushing in estuaries and (2) tidal-flow, circulation, and flushing changes in Tampa Bay due to dredge and fill.

Methodology

To meet study objectives, detailed hydrodynamic simulation models of water and constituent motion were created for three levels of development in Tampa Bay. The levels represent (1) conditions that existed in 1880 before any significant alterations were made to the bay, (2) conditions that existed in 1972 before start of the recent ship-channel dredging, and (3) conditions that are expected to exist in 1985 after completion of ship-channel dredging. Results from the models were analyzed and compared by using vector maps, vector-change maps, and circulation and flushing summary diagrams to determine the nature and degree of changes in tidal flow, circulation, and flushing among the 1880, 1972, and 1985 levels of development.

Because study conclusions depend on numerical simulations of water and constituent motion in Tampa Bay, effort was directed to develop a close match between (1) measured physical dimensions of the bay and their numerical representation in the model and (2) other measurable phenomena and corresponding model computations. Bathymetric field measurements were made to supplement available depth information. Measurements of water levels were made at many sites along the bay's shoreline. The magnitude and direction of tidal currents were measured at several sites within the bay. Constituent motion, in the form of turbidity plumes, was obtained from satellite imagery.

Description of Study Area

Tampa Bay is a shallow, Y-shaped embayment along the west-central coast of peninsular Florida (fig. 1), one of the most rapidly growing regions of the State. The bay occupies parts of Hillsborough, Manatee, and Pinellas Counties. It is bordered by the major cities of

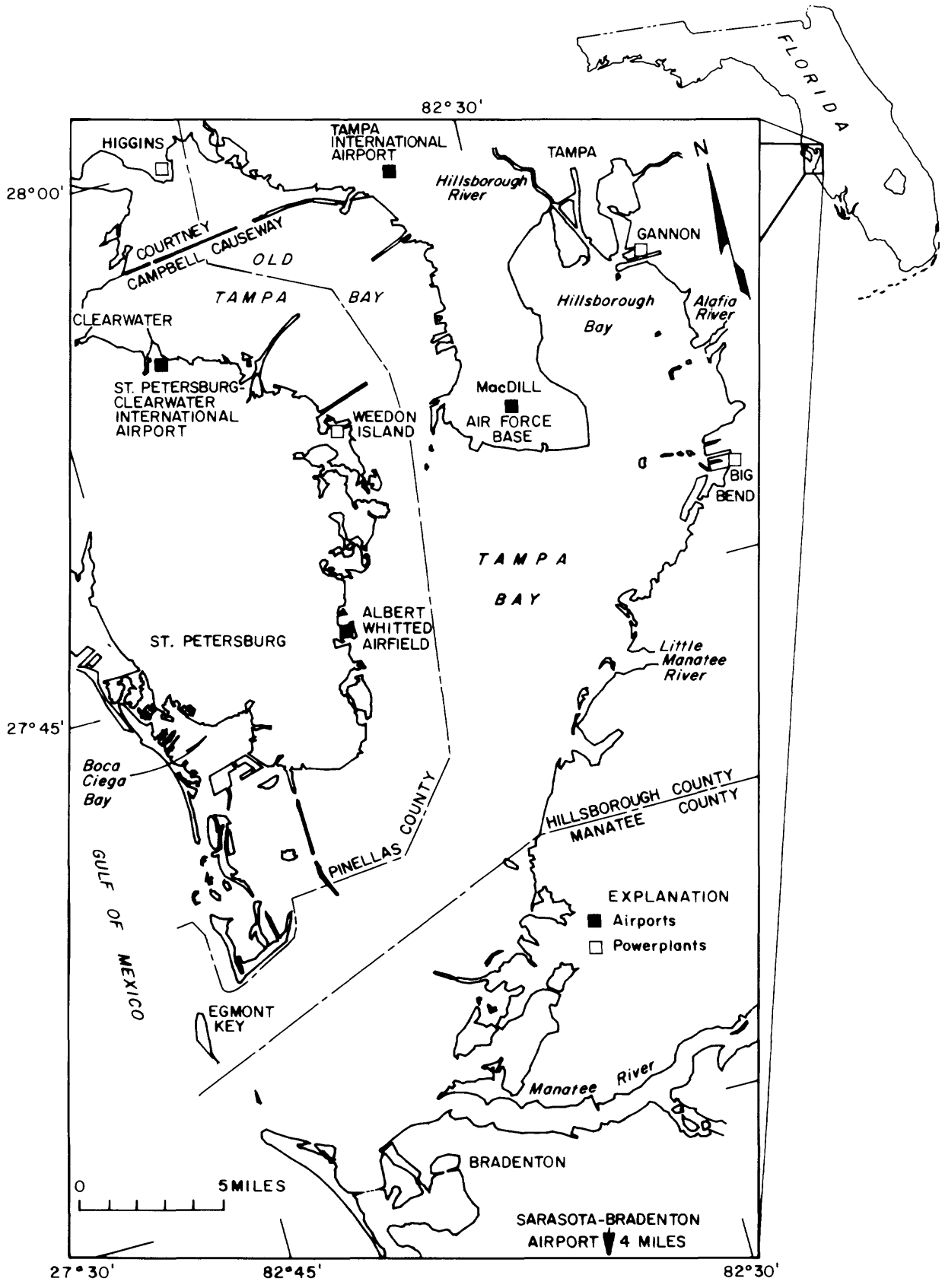

Figure 1. Location of Tampa Bay study area.

Tampa, St. Petersburg, Clearwater, and Bradenton. The population of the three-county area in 1982 was approximately 1.6 million, with a growth rate of about 42,000 residents yearly since 1970 (Thompson, 1980).

Tampa Bay has a total surface area of about 390 mi^2 (Lewis and Whitman, 1985) and is the largest estuary in Florida. Its average depth is about 12 ft. The maximum depth, about 90 ft, is off the northern tip of Egmont Key at the mouth of Tampa Bay.

The Tampa Bay area has a subtropical climate that is characterized by long, warm, humid summers and mild winters. Total rainfall averages about 53 in./yr (Heath and Conover, 1981). More than half of the rainfall occurs from June through September, primarily from thunderstorms.

Tributary inflow to Tampa Bay averages about 1,900 ft^3/s, mainly from the Hillsborough, Alafia, Little Manatee, and Manatee Rivers. Tributary inflow, municipal and industrial discharge, and runoff from adjacent urban and agricultural basins into the bay contain a variety of dissolved and suspended organic and inorganic constituents. Many constituents settle to the bottom of the bay. These constituents are subject to benthic processes. Some constituents, however, remain dissolved. These are distributed by water circulation throughout the bay. The dissolved constituents undergo various chemical and biological processes before being flushed into the Gulf of Mexico.

Seasonal variations in freshwater runoff cause measurable changes in the concentration and distribution of salinity and other constituents in bay waters (Goetz and Goodwin, 1980, p. 20). However, tide and wind actions combine to inhibit formation of salinity differences with depth under most conditions. The bay is predominantly well mixed vertically and has little density stratification.

Water motion is dominated by tides that typically convey about 21, 3, and 5 billion ft^3 of water during each flood and ebb cycle at the mouths of Tampa Bay, Hillsborough Bay, and Old Tampa Bay, respectively. The magnitude of water-level fluctuations that are attributable to the effects of the sun (diurnal)—one high and one low tide per day—and moon (semidiurnal)—two equal high and low tides per day—is approximately equal. The result is a highly variable tide that exhibits predominantly diurnal characteristics on some days and semidiurnal characteristics on others. Most of the time, the tides are a mixture of both and result in two unequal high tides and two unequal low tides each day (fig. 2).

The physical dimensions of Tampa Bay have been altered many times since the late 1800's. Most changes have resulted from man's desire to develop and expand port and other commercial facilities, to improve navigation, to allow entry of deeper draft vessels, to provide for motor vehicle transportation across the bay, to build waterfront residences, to construct power generating stations, and to develop recreational areas. Table 1 presents a summary of many of the physical changes that have occurred in the bay. Locations of the changes are shown in figures 3 and 4. Figure 4 also shows the four major subareas of Tampa Bay (lower Tampa Bay, middle Tampa Bay, Old Tampa Bay, and Hillsborough Bay), as modified from Lewis and Whitman (1985), Goetz and Goodwin (1980, p. 3), and Saloman and others (1964, p. 4).

Table 2 gives the approximate water-surface area, volume, and average depth of each major subarea for physical conditions in 1880, 1972, and 1985. The values are for a water-surface altitude equal to the National Geodetic Vertical Datum (NGVD) of 1929. The total surface area of Tampa Bay shown in table 2 differs from that given by Lewis and Whitman (1985) because of small dif-

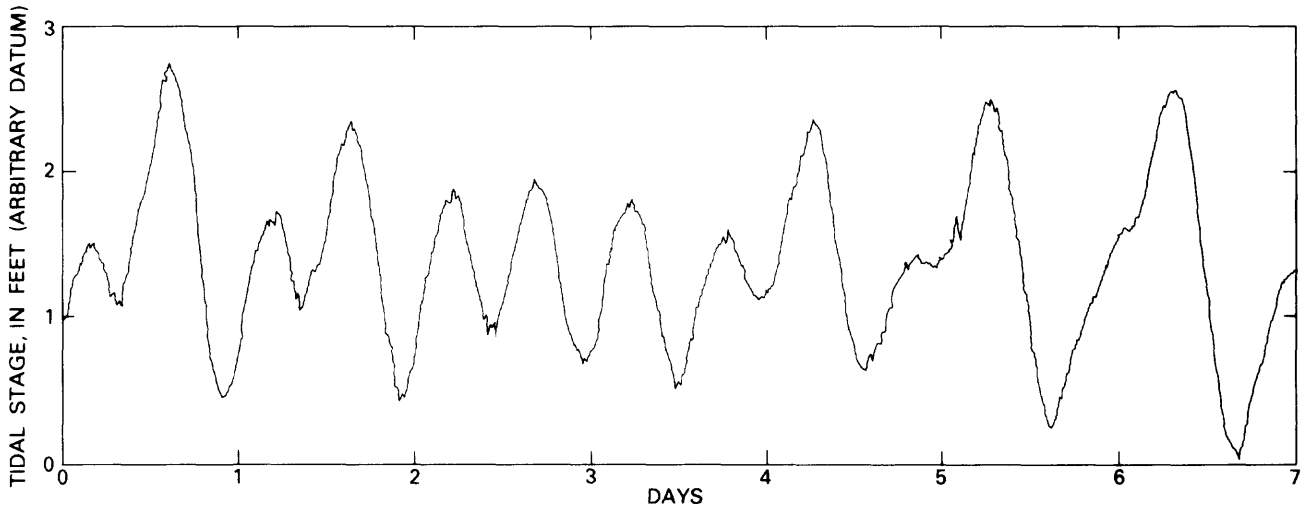

Figure 2. Diurnal and semidiurnal characteristics of typical tides in Tampa Bay.

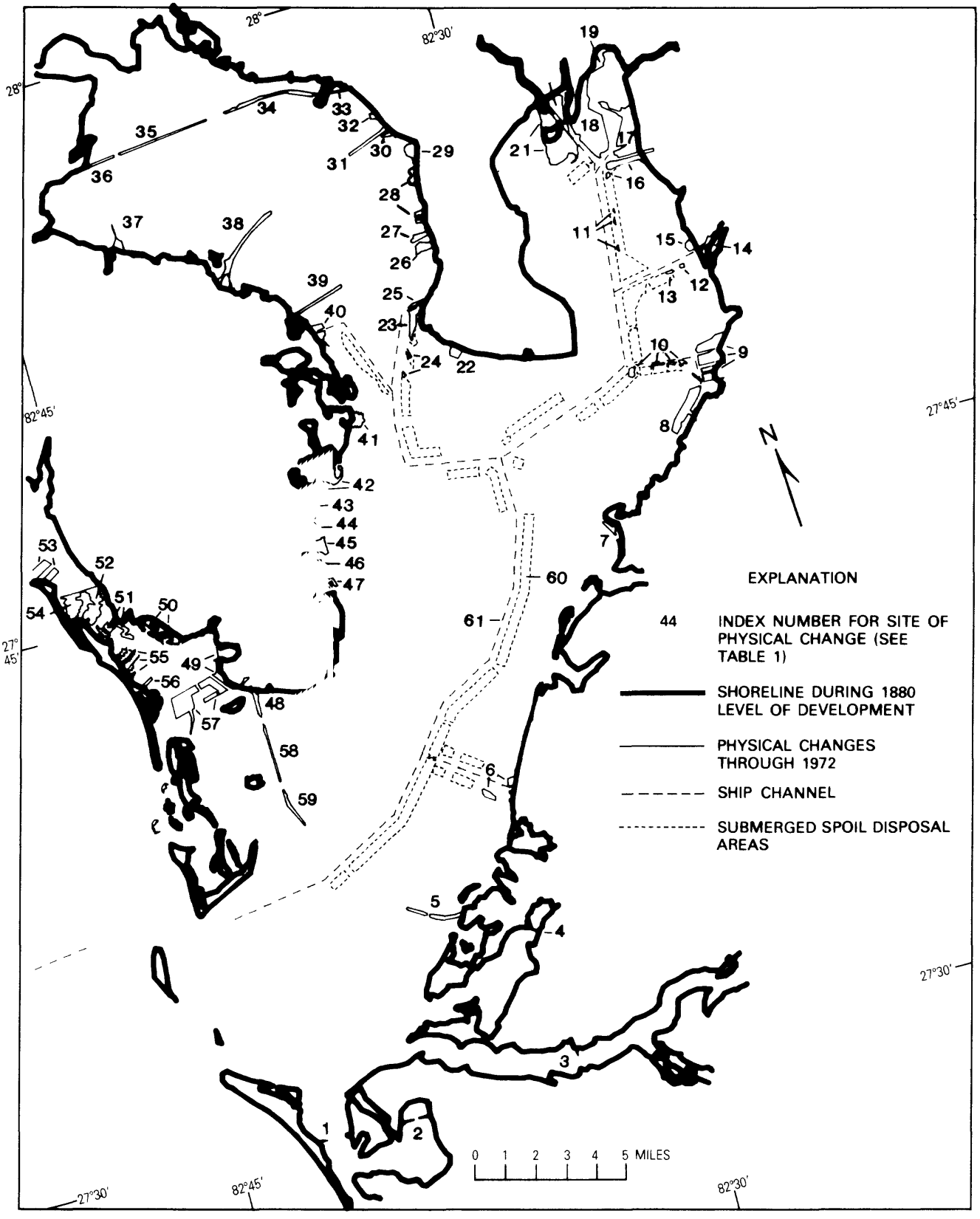

Figure 3. Locations where physical changes were made to Tampa Bay between 1880 and 1972.

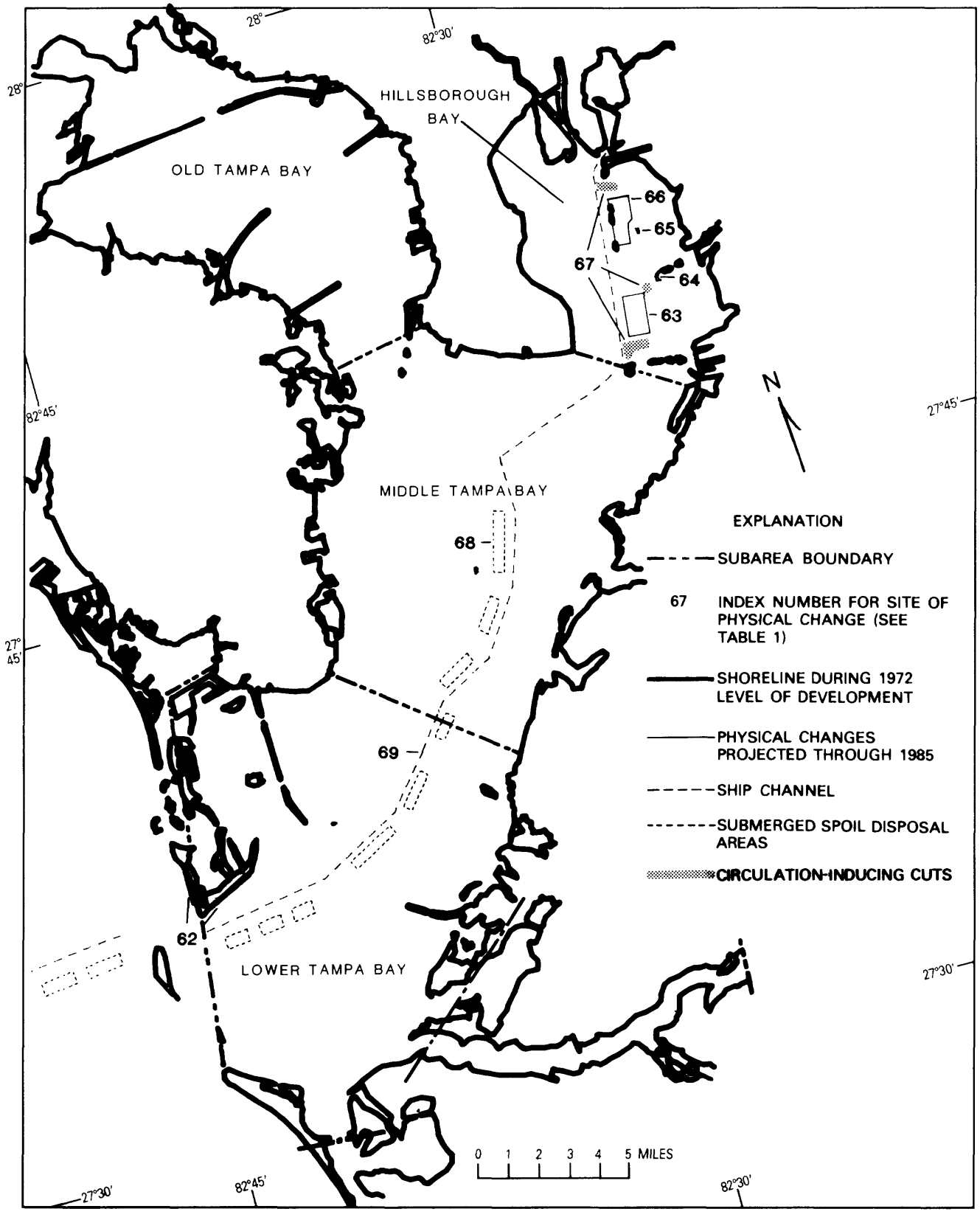

Figure 4. Locations of major subareas and areas of physical change projected for Tampa Bay between 1972 and 1985.

Table 1. Physical changes made in Tampa Bay since 1880

Index no. (see figs. 3 and 4)	Description	Approximate surface area (square miles)
1	Causeway	0.04
2	Causeway and residential	.07
3	Causeway and commercial	.13
4	Causeway and residential	.14
5	Causeway	.22
6	Commercial and spoil disposal	.15
7	Residential	.14
8	Residential	.59
9	Commercial	.76
10	Spoil disposal	.11
11	Spoil disposal	.06
12	Spoil disposal and bird sanctuary	.02
13	Spoil disposal and bird sanctuary	.04
14	Spoil disposal	.05
15	Commercial	.05
16	Commercial and spoil disposal	.23
17	Commercial and causeway	.86
18	Commercial and residential	1.56
19	Commercial	.23
20	Residential and commercial	.30
21	Residential	1.18
22	Military	.12
23	Spoil disposal	.24
24	Spoil disposal	.03
25	Commercial	.08
26	Commercial	.23
27	Causeway and military	.11
28	Residential	.18
29	Residential	.25
30	Commercial and residential	.03
31	Causeway	.13
32	Commercial	.06
33	Causeway	.02
34	Causeway and beach	.19
35	Causeway	.17
36	Causeway	.09
37	Commercial	.15
38	Causeway	.54
39	Causeway	.20
40	Commercial	.27
41	Residential	.12
42	Residential	.12
43	Residential	.10
44	Commercial	.08
45	Commercial	.23
46	Commercial	.03
47	Residential	.09
48	Causeway	.13
49	Residential	.43
50	Residential	.40
51	Causeway and residential	.40
52	Residential	.39
53	Residential	.36
54	Causeway and residential	.29
55	Residential	.21
56	Residential	.04
57	Causeway and residential	.79
58	Causeway	.19
59	Causeway	.19
60	Submerged spoil disposal	8.59
61	Ship-channel construction	4.69
62	Spoil disposal and beach nourishment	.16
63	Spoil disposal	.81
64	Spoil disposal	.02
65	Spoil disposal	.02
66	Spoil disposal	.98
67	Circulation-inducing cuts	.47
68	Submerged spoil disposal	3.12
69	Ship-channel widening	.94

ferences in the boundary definition of lower Tampa Bay. The percentage change in each physical characteristic from 1880 to 1972, from 1972 to 1985, and from 1880 to 1985 also are given. The largest percentage changes in surface area, volume, and depth were for Hillsborough Bay. Between 1972 and 1985, only Hillsborough Bay and lower Tampa Bay subareas sustained any changes in the physical characteristics that are given in table 2.

Decreases in surface area (see table 2) reflect construction of islands, causeways, and other fills. Increases in water volume occurred because (1) the source of material for most fill construction was the bay bottom and (2) only part of the dredged material became new emergent upland and represents the net gain in water volume of the bay. Under these conditions, the average depth also increased because larger water volumes are divided by smaller surface areas.

Dredging and filling from 1880 to 1985 will have reduced the surface area of the entire Tampa Bay system by 3.6 percent. By 1985, water volume will have increased in Tampa Bay by 1.3 percent, and the average depth will have increased by 4.4 percent.

Changes to the physical characteristics of Tampa Bay influence the quantity of water that enters and leaves each

Table 2. Physical characteristics of major subareas of Tampa Bay and of Tampa Bay overall for 1880, 1972, and projected 1985 levels of development

[See figure 4 for location of major subareas. Values are for a water-surface altitude equal to the National Geodetic Vertical Datum of 1929]

Physical characteristic	Area	Level of development			Percentage change		
		1880	1972	1985	1880 to 1972	1972 to 1985	1880 to 1985
Approximate surface area, in mi².	Lower Tampa Bay	128.4	126.1	125.9	− 1.8	−0.2	− 1.9
	Middle Tampa Bay	111.2	109.5	109.5	− 1.5	0	− 1.5
	Old Tampa Bay	77.8	74.8	74.8	− 3.8	0	− 3.8
	Hillsborough Bay	42.7	38.8	36.9	− 9.1	−4.9	−13.6
	Tampa Bay (total)	360.1	349.2	347.1	− 3.0	− .6	− 3.6
Water volume, in mi²-ft.	Lower Tampa Bay	1,572	1,578	1,578	+ .4	0	+ .4
	Middle Tampa Bay	1,475	1,481	1,481	+ .4	0	+ .4
	Old Tampa Bay	689	695	695	+ .9	0	+ .9
	Hillsborough Bay	352	373	388	+ 6.0	+4.0	+10.2
	Tampa Bay (total)	4,088	4,127	4,142	+ 1.0	+ .4	+ 1.3
Average depth, in ft.	Lower Tampa Bay	12.2	12.5	12.5	+ 2.4	0	+ 2.4
	Middle Tampa Bay	13.3	13.5	13.5	+ 1.5	0	+ 1.5
	Old Tampa Bay	8.9	9.3	9.3	+ 4.5	0	+ 4.5
	Hillsborough Bay	8.2	9.6	10.5	+17.1	+9.4	+28.0
	Tampa Bay (overall)	11.4	11.8	11.9	+ 3.5	+ .8	+ 4.4
Approximate tidal prism,[1] in mi²-ft.	Lower Tampa Bay	248	246	246	− .8	0	− .8
	Middle Tampa Bay	237	235	235	− .8	0	− .8
	Old Tampa Bay	190	187	187	− 1.6	0	− 1.6
	Hillsborough Bay	99	95	93	− 4.0	−2.1	− 6.1
	Tampa Bay (total)	774	763	761	− 1.4	− .3	− 1.7

[1]The volume of water that enters or leaves a tidal water body between high slack water and low slack water.

part of the bay on every tidal cycle. This quantity is called the tidal prism and is defined as the volume of water that enters or leaves a tidal water body between high slack water and low slack water. Tidal prism is approximately equal to the surface area times a representative tidal range of the water body. Even though the total volume of water in Tampa Bay is slightly increased due to dredging and filling, the tidal prism is reduced (see table 2). This apparent anomaly is explained by the reduced surface area of the bay due to filling within the intertidal zone (between the limits of high tide and low tide altitudes).

The following sketch shows an extreme example of the impact that reduced surface area can have on tidal prism for hypothetical prismatic estuaries having the same total water volume at high tide.

Surface area = $2AC$	Surface area = AC
Total volume = ABC	Total volume = ABC
Tidal prism $\cong 2aAC$	Tidal prism $\cong aAC$

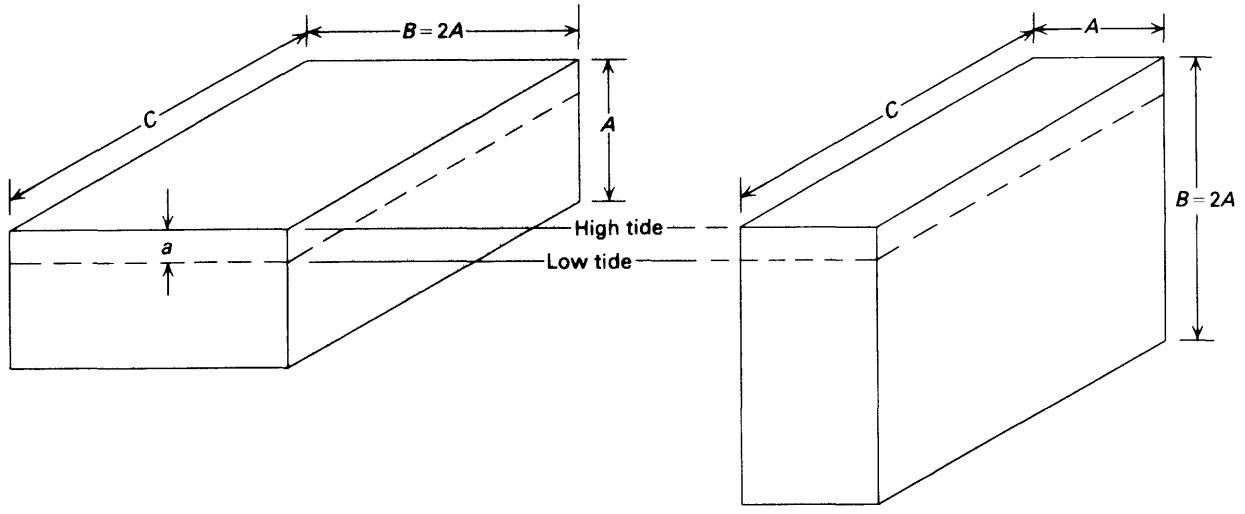

The tidal prism and associated percentage changes for Tampa Bay and for each major bay subarea are given in table 2.

Tidal prism reductions from 1880 to 1985 are expected to be 1.7 percent for Tampa Bay as a whole, 0.8 percent for lower Tampa Bay, 0.8 percent for middle Tampa Bay, 1.6 percent for Old Tampa Bay, and 6.1 percent for Hillsborough Bay. These changes indicate that, as a result of dredge and fill construction, overall tidal exchange throughout the bay is marginally reduced, and, consequently, less potential for tidal mixing and flushing exists. Modeling results from this study show, however, that dredge and fill also cause circulation increases that more than overcome the effects of reduced flushing potential in most parts of Tampa Bay.

Previous Studies

This report follows a series of investigations that were either directly or indirectly concerned with tidal effects in Tampa Bay. As background and reference information, many of these studies are briefly described and discussed herein.

Studies of tidal motion in Tampa Bay were first undertaken by the National Ocean Service (NOS), formerly the U.S. Coast and Geodetic Survey, as part of its mission to chart the coastline of the United States. Because water depths are measured from a constantly changing water surface, referencing water-surface altitudes to a meaningful navigational datum, normally mean lower low water (MLLW), is essential to the chartmaking process. MLLW is defined as the average of the lowest low-water height of each tidal day observed over a tidal epoch of 18.6 years. Shorter periods of observations must be corrected by comparison with simultaneous observations at a long-term control station. Tidal stage data were first collected by the NOS in Tampa Bay in 1878. A continuous recording tide gage has been operating at St. Petersburg since 1947.

By analyzing tide data in terms of harmonic constituents, the NOS has predicted tides (U.S. Department of Commerce, 1982a) each year since 1939. Tidal currents at selected locations also have been predicted each year since 1950 (U.S. Department of Commerce, 1982b). Maps designed to extend tidal current predictions to unmeasured locations also have been published (U.S. Department of Commerce, 1951). The most recent NOS survey, 1963, of tidal currents in Tampa Bay was described and summarized by Dinardi (1978). His report included data for 39 current-meter sites and for photogrammetrically tracked drogues and foam patches. Data from Dinardi (1978) were used to confirm tide-induced, residual velocities computed during this study.

A study was conducted by the Federal Water Pollution Control Administration to determine the source of obnoxious odors in Hillsborough Bay (U.S. Department of the Interior, 1969). As part of the study, tidal current data were collected within an hour of predicted times of maximum current at 24 sites. Generalized floodtide and ebbtide current patterns were approximated for use in a two-dimensional, constituent-transport model having 40 segments or cells. Little information was developed during this study regarding tidal circulation and flushing in Hillsborough Bay.

In two master's theses prepared at the University of South Florida, R. D. Ghioto (written commun., March 1973) and D. H. Cote (written commun., June 1973) developed and applied a two-dimensional, hydrodynamic model of tidal flow in Tampa Bay that was based on an algorithm by Reid and Bodine (1968). Residual tidal current patterns were determined by Cote by integrating tidal currents at each ½-mile grid site over a 14-day lunar tidal cycle. The resulting vector map indicated that several gyres or net rotational features existed in the bay that appeared to contribute to bay circulation and flushing characteristics. Results from a similar model reported by Ross (1973) showed a different gyre pattern than that computed by Cote. Such differences confirm that circulation and residual tidal current computations are sensitive to one or more of the following items:

1. choice of hydrodynamic model,
2. schematization of bottom configuration,
3. grid size,
4. location of seaward boundary, and
5. choice of tidal boundary function.

It is important to note that there are no fixed patterns of circulation in any estuary. Fischer and others (1979) point out that circulation is an ever-changing quantity that evolves in response to changing tide, wind, and other driving forces. Determination of a truly representative or average circulation pattern must be deferred until exhaustive measurements and computations are undertaken. Until then, reasonable estimates of representative conditions will differ because of computational sensitivity to the above items.

This study extends the work of Ghioto (written commun., 1973), Cote (written commun., 1973), and Ross (1973) in several ways. Special emphasis is given to model calibration and verification. Observed and computed data are closely matched to assure that model computations represent conditions in the real system. The modeled area in this study is significantly larger than that of the previous models so that interactions between Tampa Bay and the Gulf of Mexico can be included. Also, the entire bay is modeled at a finer grid size than the previous models to provide greater resolution of circulation features.

Computer studies of tidal mixing in upper Old Tampa Bay were conducted at the University of South Florida by Ross and Anderson (1972). A two-dimensional, hydrodynamic model having a grid size of ¼ mile was developed. The model covered the northern two-thirds of the bay. An effective method was used to determine changes in flushing characteristics caused by various alteration options to the Courtney Campbell Causeway. High and low uniform constituent concentrations were initially assigned to the water on the landward and seaward sides of the causeway, respectively. The mass of constituent transferred during one tidal cycle was used as a basis for flushing comparison between alternatives.

Goodwin (1977) compared computed residual tidal currents in Hillsborough Bay for islands of various configurations constructed from materials dredged from the ship channel. He concluded that circulation patterns could be modified by changes in island configurations, but that little potential existed for improving overall circulation between waters of Hillsborough Bay and Tampa Bay. Preliminary circulation results from a detailed model of Hillsborough Bay (Goodwin, 1980) showed complex net tidal currents that had not been previously detected. Comparisons were made between computed flow and circulation patterns for conditions both before and after the Federal dredging project begun in 1976.

Giovannelli (1981) used the results of Goodwin (1980) as input to a salt-transport model to analyze specific conductance changes in Hillsborough Bay off the mouth of the Alafia River. He found that a 17-fold increase in river discharge (40–680 ft^3/s) produced a 25-percent reduction in the specific conductance (40,000–30,000 μmho/cm) of bay water near the river mouth. Specific conductance at the river mouth was reduced by more than 70 percent. This reduction in specific conductance indicates significant mixing of river water with Hillsborough Bay water near the Alafia River.

Acknowledgments

We are grateful to the Tampa Port Authority, particularly Delmar Drawdy, for initiation and cooperative financing of this study from 1971 to 1973. We are also grateful to the U.S. Army Corps of Engineers, Jacksonville District, for continuation of the study and financial support through 1984.

Large computer simulation runs that culminated this study were made possible by the Defense Communications Agency (DCA) Hybrid Simulation Facility at Reston, Va. Without assistance from DCA, a full-scale study could not have been made.

Initial model calibration by Jan Leendertse of the Rand Corporation and Robert Baltzer of the U.S. Geological Survey research staff on a precursor of the models described in this report is gratefully acknowledged. Enhancement of satellite imagery by Gerald Moore of the Earth Resources Observation Systems Data Center is also appreciated.

DESCRIPTION OF COMPUTER SIMULATION SYSTEM

The model used in this study can simulate water and constituent motion in well-mixed estuaries, embayments, and other coastal areas. Equations that describe the physical laws governing water and constituent motion in two dimensions are applied between every location where simulated information is desired. These equations are solved at successive small time steps to provide a close approximation of the time history of water level, water transport, and constituent transport at each corresponding location in the real system.

The following sections describe the equations, numerical procedures, input requirements, and operational aspects of the simulation system.

Governing Equations

Water motion in estuaries is governed by the physical laws of conservation of momentum and conservation of mass. The two-dimensional estuarine simulation system (SIMSYS2D) applied in this study uses vertically integrated forms of equations that describe conservation of mass and momentum, as given by Leendertse and Gritton (1971, p. 8):

$$\frac{\partial \zeta}{\partial t}+\frac{\partial (HU)}{\partial x}+\frac{\partial (HV)}{\partial y}=0 \qquad (1)$$

$$\frac{\partial U}{\partial t}+U\frac{\partial U}{\partial x}+V\frac{\partial U}{\partial y}-fV+g\frac{\partial \zeta}{\partial x}+g\frac{U(U^2+V^2)^{0.5}}{C^2H}-\frac{1}{\varrho H}\tau_x^s=0 \qquad (2)$$

$$\frac{\partial V}{\partial t}+U\frac{\partial V}{\partial x}+V\frac{\partial V}{\partial y}+fU+g\frac{\partial \zeta}{\partial y}+g\frac{V(U^2+V^2)^{0.5}}{C^2H}-\frac{1}{\varrho H}\tau_y^s=0 \qquad (3)$$

where

- f = the Coriolis parameter, $2\omega \sin\phi$ (s^{-1}), where ω = the angular velocity of the Earth around its axis (radians per second) and ϕ = geographical latitude (degrees);
- g = acceleration of gravity, in foot per second squared;
- ϱ = water density, in pound·second^2 per foot^4;
- ζ = water-level altitude with respect to the reference plane, in feet;
- $H = h$ (distance from the reference plane to the embayment bottom, in feet) + ζ = water depth, in feet;

C = Chezy roughness coefficient, in foot$^{0.5}$ per second;
τ_x^s = surface wind-stress component in the x direction, in pound per square foot;
τ_y^s = surface wind-stress component in the y direction, in pound per square foot; and
t = time, in seconds.

The variables U and V are the vertically averaged velocities of flow defined as:

$$U = \frac{1}{H}\int_{-h}^{\zeta} u\, dz \tag{4}$$

$$V = \frac{1}{H}\int_{-h}^{\zeta} v\, dz \tag{5}$$

where u and v are the point-flow velocities in the positive x and y directions, respectively, and dz is the differential in the vertical direction. The wind-stress components are given by Dronkers (1964, p. 188) as:

$$\tau_x^s = \theta \varrho_a w^2 \sin \psi \tag{6}$$

and

$$\tau_x^s = \theta \varrho_a w^2 \cos \psi \tag{7}$$

where

θ = wind-stress coefficient $\cong 0.0026$, from Leendertse and Gritton (1971, p. 9), nondimensional,
ϱ_a = air density, in pound·second^2 per foot^4,
w = wind velocity, in foot per second, and
ψ = angle between wind vector and y axis, in degrees.

Equation 1 expresses continuity of mass in two dimensions. Equations 2 and 3 express continuity of momentum in the x and y Cartesian coordinate directions, respectively. These equations assume that water density is constant both horizontally and vertically, that vertical flow components do not exist, and that horizontal flow components do not vary vertically. The model is limited in application to areas that are vertically and horizontally well mixed. However, this type of model has been successfully applied where gradually varying horizontal density gradients occur.

Transport of dissolved constituents is governed by large-scale advective or translatory motion of water and by fine-scale dispersive or mixing action caused by presence of turbulence superimposed on the average flow. Transport of dissolved constituents is governed by the conservation of solute mass. Transport incorporates advective and dispersive concepts and allows for constituent sources and sinks as given by Leendertse and Gritton (1971, p. 4) for two-dimensional flow (equation 8):

$$\frac{\partial(HP)}{\partial t} + \frac{(HUP)}{\partial x} + \frac{\partial(HVP)}{\partial y} - \frac{\partial\left(HD_x \frac{\partial P}{\partial x}\right)}{\partial x} - \frac{\partial\left(HD_y \frac{\partial P}{\partial y}\right)}{\partial y} - HS_A = 0 \tag{8}$$

where

D_x = dispersion coefficient, flow in the x direction, in square feet per second;
D_y = dispersion coefficient, flow in the y direction, in square feet per second; and
S_A = source and sink function, including the rate of injection of constituent A.

As with the velocities U and V, P is the vertically integrated average mass concentration of the constituent given by

$$P = \frac{1}{H}\int_{-h}^{\zeta} p_A\, dz \tag{9}$$

where p_A is the local mass concentration of a particular constituent substance, A.

Holley (1969, p. 628) noted that, except in regions of large constituent concentration gradients, mass transport by longitudinal dispersion is often very small compared with mass transport by advection. Leendertse (1970, p. 13) reasoned that, if this were true, small errors in assigning values to the longitudinal dispersion coefficient would not substantially change the solutions obtained. He then assumed that dispersion could be adequately defined by two components, an isotropic component representing the effect of lateral mixing and a directional component approximating longitudinal effects. The dispersion coefficients, D_x and D_y, used in SIMSYS2D are given by Leendertse (1970, p. 14 and 54) as:

$$D_x = \mathrm{d}HU\mathrm{g}^{0.5}C^{-1} + D_w \tag{10}$$

$$D_y = \mathrm{d}HV\mathrm{g}^{0.5}C^{-1} + D_w \tag{11}$$

where

D_w = a diffusion coefficient representing wave, wind, and lateral mixing effects, in square feet per second, and
d = an empirical dimensionless constant similar to that presented by Elder (1959).

Numerical Procedures

Partial differential equations 1, 2, 3, and 8 describe general relations that exist among the many forces that control water and solute motion. Because the equations cannot be solved analytically for most real-world conditions, procedures have been devised that provide approximate solutions by using computers to rapidly perform an enormous quantity of numerical computations.

The numerical procedure used in SIMSYS2D is summarized below and is presented in detail by Leendertse and Gritton (1971, p. 15). Equations 1, 2, 3, and 8 can be approximated over a region in time and space by a large number of difference equations. Each difference equation is similar in form to the parent differential equation but is applicable at only one point in time and space and is separated from all other points by finite time and space increments. Such a finite-difference approximation

is valuable because, by using the approximation, a differential equation is reduced to multiple interrelated algebraic equations involving quantities at defined locations.

Each difference equation contains known and unknown terms. As long as the number of equations equals the number of unknown terms, the system is solvable. The method of solution for the unknown terms involves a point-to-point, repeating, stepwise procedure that incorporates previously computed values and input data as appropriate.

A space-staggered grid scheme (fig. 5) is used in the SIMSYS2D model. Water levels (ζ) and solute mass density (P) are defined at integer values of m and n. The reference water depths (h), measured from the NGVD of 1929, are defined at points midway between integer values of both m and n. Velocities in the y direction (V) are defined at points midway between integer values of n and at integer values of m. Velocities in the x direction (U) are defined at points midway between integer values of m and at integer values of n.

The grid extends to the boundaries of the modeled area in the positive and negative x and y directions. On land areas, reference water depths (h) are replaced by land altitudes ($-h$), and water velocities are computed only at times when water levels exceed land altitudes. Time (t) also is simulated in a stepwise manner, with computational elements defined at integer points and midway between integer points. Simulation time extends from the beginning to the end of each period of interest.

Leendertse and Gritton (1971, p. 11) give a complete description of how equations 1, 2, 3 and 8 are structured at each (x, y, t) point and how unknowns in each equation are solved. An overview of the solution scheme is given also by Cheng and Casulli (1982, p. 1655).

Input Requirements

Three categories of input data are needed to operate SIMSYS2D:

1. definition of intrinsic characteristic and initial conditions,
2. definition and characteristics of the fixed boundary (bay bottom and land surface), and
3. definition of the driving functions of tide, wind, tributary inflow, and constitutent sources.

The first category includes the density of water, dispersion coefficients (see equations 10 and 11), starting constituent concentration distributions, and starting water-surface altitudes. The lateral dispersion coefficient (D_w) and starting concentrations can be specified as unique values at each cell in the model.

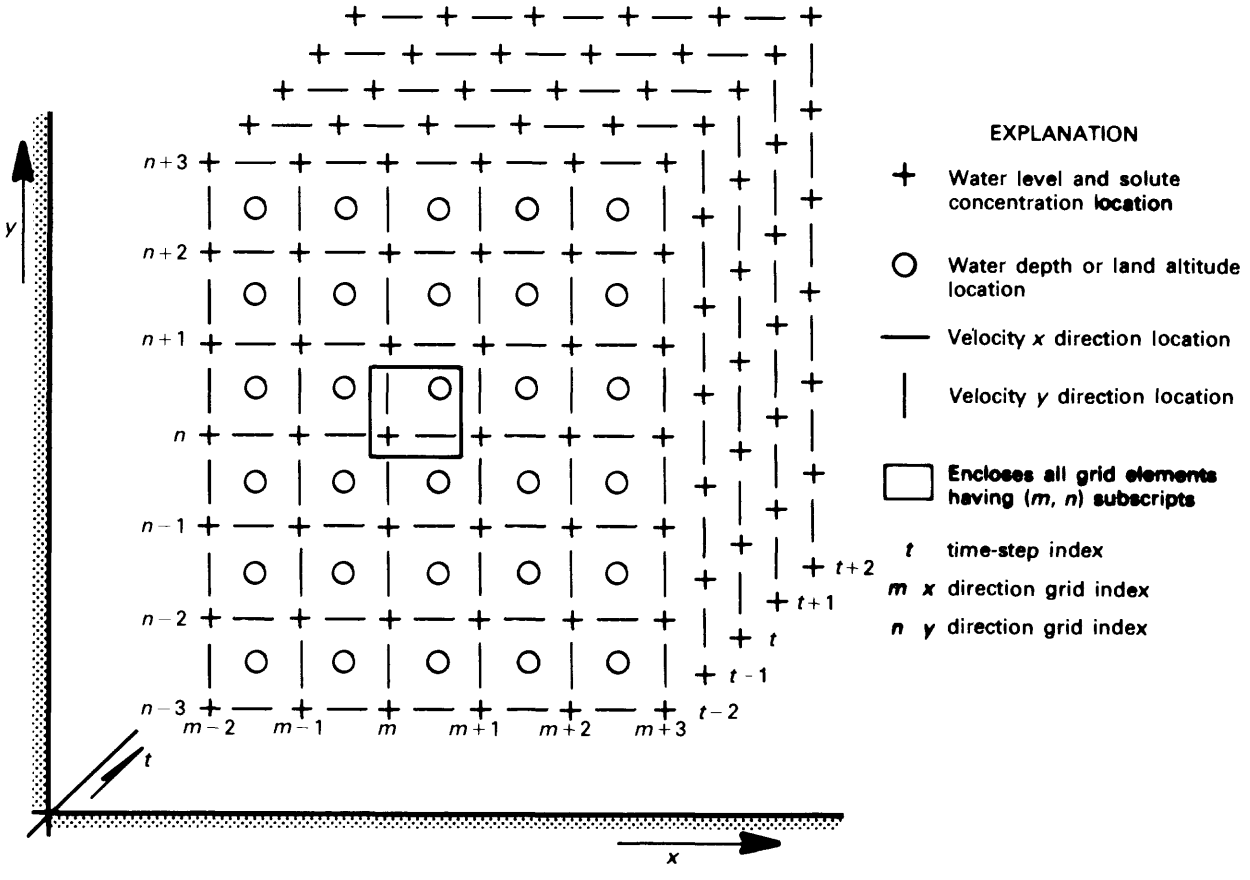

Figure 5. Finite-difference scheme for computer simulation model (modified from Leendertse and Gritton, 1971).

The second category includes information on the physical size and dimensions of the estuarine basin. Basin geometry is defined by specifying a water depth or land altitude at each model cell. The resistance to water flowing over the bottom is defined by specifying values for Manning's roughness coefficient (n) at each cell.

The third category includes information that can be entered as functions of time. Tidal fluctuations are defined at the ocean boundary. Speed and direction of the wind is defined at the water surface. The rates of water and of constituent inflows are defined at appropriate locations to simulate rivers, sewage outfalls, dye injections, and so forth.

Operations

SIMSYS2D is composed of several interrelated programs and files, as shown in figure 6. The system has four main sections that have distinctly different functions.

The INPUT DATA PROCESSOR (IDP) scans the user-prepared input data file, often several thousand card images in size, and checks for many potential format and logic errors. This step detects as many errors as possible before submitting the data to the more lengthy MIXER and simulation-computation steps. Data listings and error messages are printed to guide error correction.

With successful completion of IDP, three disk files are written for subsequent use. (1) The SIMULATION INPUT (SIMINP) file is a restructured version of the original input data that matches requirements of the computation section of the system (SIM2D). (2) The SIMPT1 file contains input overrides that allow minor changes to be made to the input data, prior to computation, without having to rerun the IDP and MIXER sections. The most common input override change is setting of start, restart, and end times for simulation runs. (3) In the SIMCOM file, the size of all dimensioned variables for each model application, as determined by IDP, is stored as common statements for input to the next section (MIXER).

The MIXER section combines SIMCOM with the FORTRAN source code of the model. Compilation and linkage-editing steps produce an executable load module that is tailored to each geographic area being modeled.

The computation section (SIM2D) executes the load module that was produced by MIXER and incorporates SIMINP and SIMPT1 data files created by IDP. Computed water elevations, transports, constituent concentrations, and other variables are stored at user-selected time intervals on two tape files. The restart tape (SIMRST) contains sufficient information to restart simulations at intermediate points so that costly computations do not have to be repeated in case of program or computer failures. The restart capability can be used also to segment long simulations into small, manageable lengths. The history tape (SIMHST) contains information at all locations in the model at sufficiently small time increments, usually 30 minutes, to define the time variation of computed variables. Computations done between the time intervals of SIMHST are lost. SIMHST is the source of all computed information used in the POST PROCESSOR section.

In the initial step (POSTGEN) of the POST PROCESSOR section, the SIMHST tape is read, and several specialized disk data files, each using only a small part of the total data available, are created. Each disk file is then used as input to specialized post-processing programs to produce maps and graphical displays of model results (fig. 6). The post-processor programs are frequently changed as new ways of viewing or applying the data are conceived. Separate programs of the POSTGEN type are often needed to create special data files from SIMHST for each new application.

MODEL DEVELOPMENT AND APPLICATION

Model development is a process by which a general estuarine simulation system is structured and adjusted to represent a particular estuary, embayment, or other coastal area. The objective of the process is to achieve as close agreement as possible and practicable between simulated and observed values of tidal stage, tidal currents, constituent distributions, and other measurable factors. The closer the agreement, the more confident model users can be that results of subsequent numerical experiments accurately reflect real conditions.

The development procedure is composed of two basic steps, calibration and verification (fig. 7). Both steps involve comparison of computed and observed data. The calibration step has a feedback loop that is not present in the verification step. Feedback allows adjustments to imprecisely known input data to improve the match between observed and simulated data. Verification is conducted for one or more data sets that were not used during calibration. During verification, further adjustments are not allowed. The degree of agreement achieved between observed and simulated data during the verification step is a measure of model accuracy and reliability.

The following sections describe how bottom configuration, boundary conditions, and initial conditions were determined and show results of calibration and verification comparisons for development of the Tampa Bay model.

Bottom Configuration

The area of Tampa Bay and the Gulf of Mexico chosen for application of SIMSYS2D is shown in figure 1. The total modeled area was 826 mi^2, approximately 45 percent of which was land that had altitudes higher than

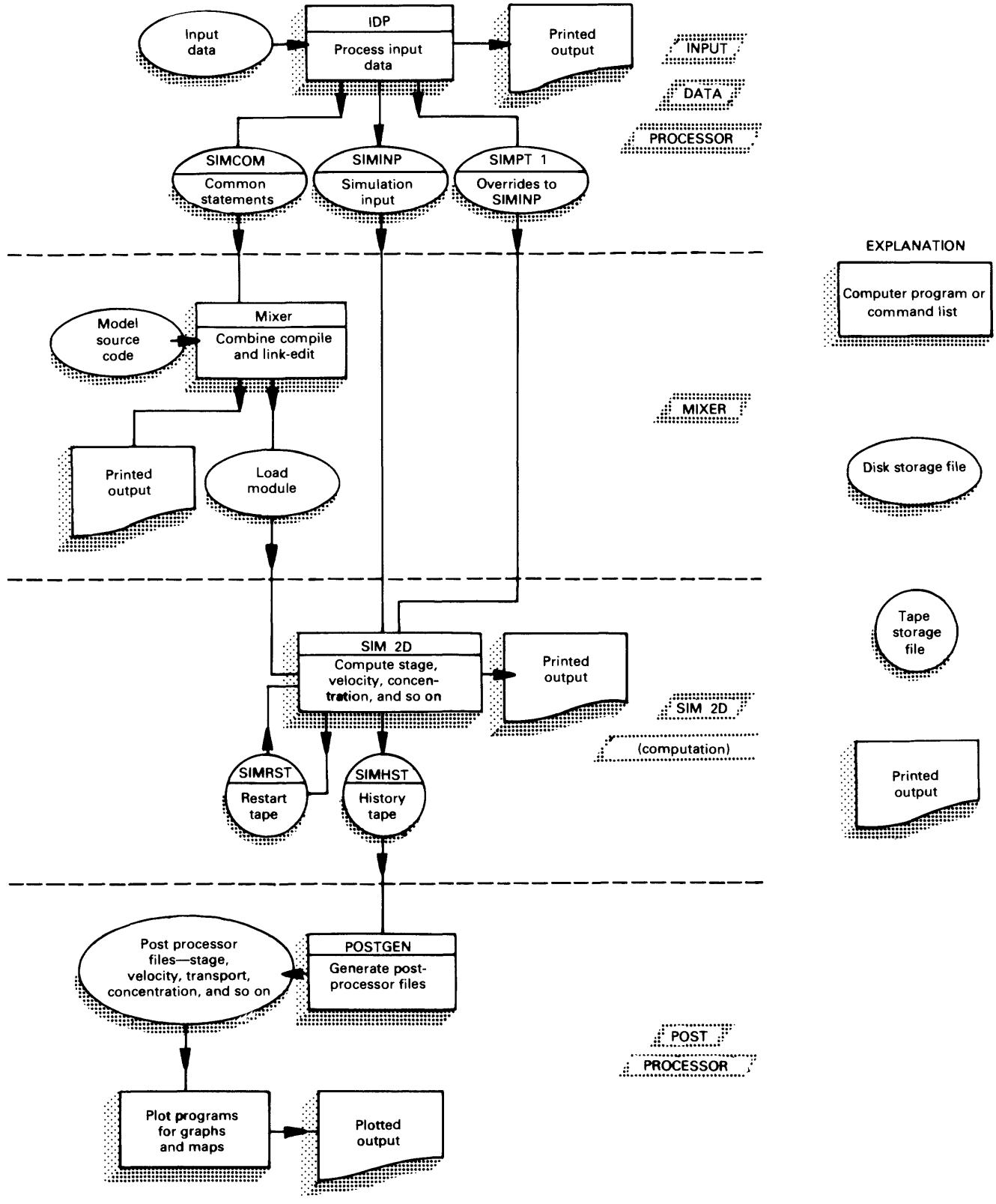

Figure 6. Relation of programs, files, input, and output for the simulation modeling system.

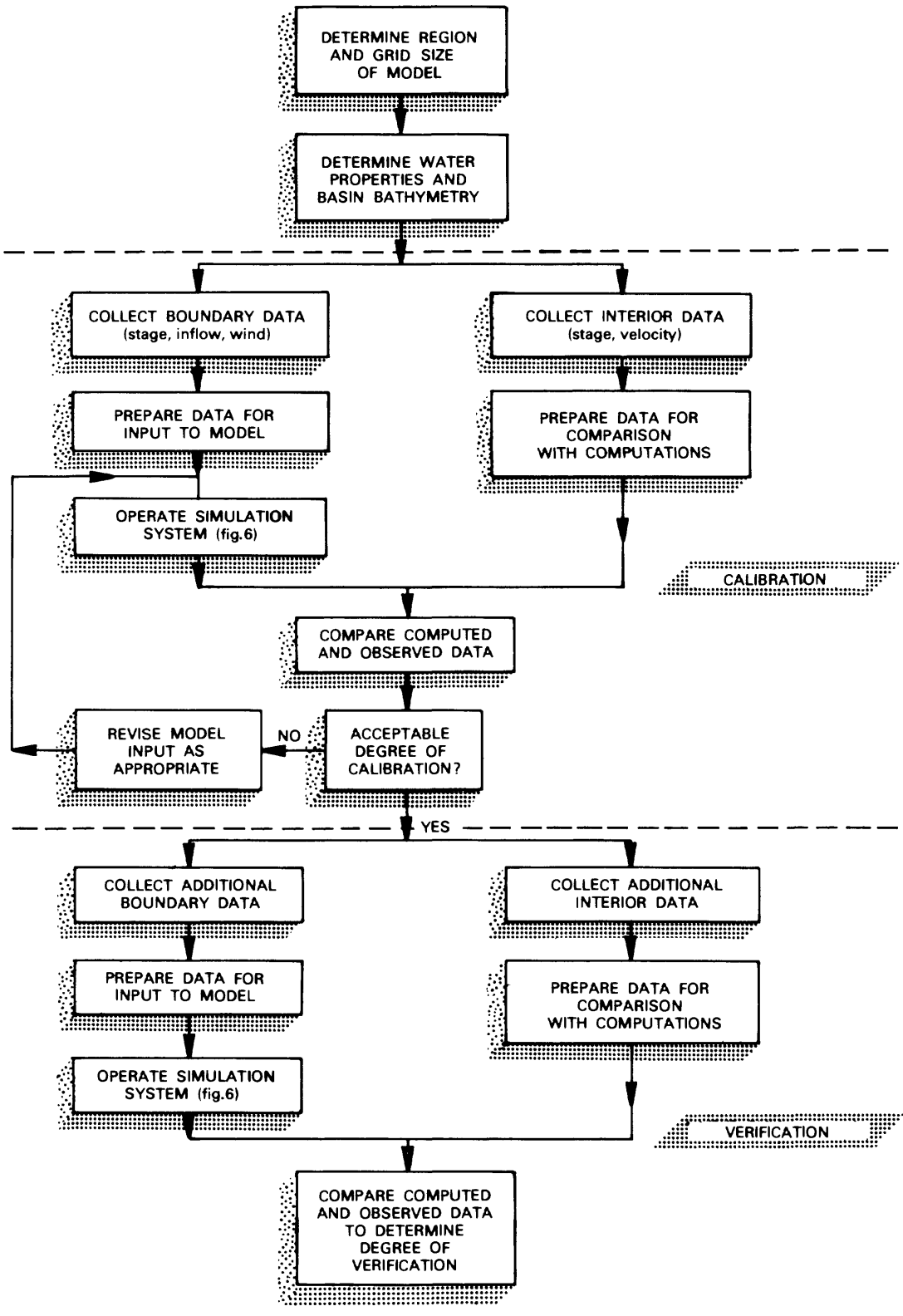

Figure 7. Calibration and verification steps in model development.

mean high water. The modeled area is defined by an 80 by 128 square grid system. Each cell in the system is 1,500 ft on a side, adequate to define most major physical features with little distortion. A time step of 5 minutes was used for each model run during this study.

The most important element in model development is the bottom configuration, as defined by water depth at each grid cell. These depths define bottom shape characteristics that largely control how water is numerically distributed by the model.

A combination of existing information and new data was employed to generate depths used in Tampa Bay model development. Detailed depth information was obtained from the NOS for surveys made from 1950 to 1958. Survey results were in the form of maps annotated with numbers representing the depth of water referenced to MLLW datum. The maps were compiled at scales of either 1:10,000 or 1:20,000. The density of coverage ranged from about 100 to 1,000 depth observations per square mile. For this study, all depths were adjusted to the NGVD of 1929.

Resurveys of selected areas were made by the U.S. Geological Survey in 1971 and 1973 by using automatic positioning equipment and a digital fathometer. The objectives were (1) to determine whether any significant, areally extensive bottom changes had occurred since the NOS surveys and (2) to define dredged channels and dredged material disposal sites constructed since the NOS surveys. Direct stereo-compilation of bottom configuration also was conducted wherever low-level aerial photography could sufficiently penetrate the water column to define bottom relief. A description of fathometric and photogrammetric approaches is given by Rosenshein and others (1977). No extensive nondredged bottom changes were detected.

Depth assignments were made by using a combination of automated and manual techniques. The automated procedure (Schaffranek and Baltzer, 1975) involved compilation, editing, combining, and gridding of data from the various sources. Thousands of quasi-random depth observations were fitted to a polynomial surface from which a representative depth for each cell was computed. The cell depths were then compared with bathymetric charts and manually revised if necessary. Revisions were sometimes needed near shorelines and channels and in areas of sparse data.

Land altitudes for cells that were higher than mean high water were assigned a default value of 3.0 ft. This value limited the model to investigation of tides that reached maximum altitudes of less than 3.0 ft. This limitation was not a constraint for this study.

Boundary Conditions

Boundaries of the Tampa Bay model include the bay bottom, the shorelines, tributary streams, a seaward boundary in the Gulf of Mexico, and the water surface. A description of the data used to describe conditions at each boundary follows.

Bottom Boundary

The bay bottom is treated as an impermeable, immovable boundary that causes resistance to free flow of water. Resistance increases as roughness of the bottom material increases. Values of the roughness coefficient, n in Manning's equation, were assigned to each cell of the model. A related open-channel flow equation by Chezy incorporates another bottom-roughness coefficient, C, that is actually used in model computations (see the sixth term in equations 2 and 3). The relation used to convert from Manning's n to Chezy's C is:

$$C=\frac{1.49}{n}H^{1/6} \tag{12}$$

where H is the water depth, in feet.

Manning's n is an empirical coefficient that cannot be measured directly. By varying the coefficient, model-computed tidal stage and current can be adjusted to closely match corresponding measured data.

Manning's n values used in simulation of other estuaries and bays were used to guide initial values used in this study even though n values are recognized as being somewhat dependent on the particular algorithm used in model computations. In a study of Jamaica Bay, N.Y., Leendertse (1972, p. 11) used n values that ranged from 0.026 to 0.034. For areas of corresponding depths in the St. Lawrence River, Prandle and Crookshank (1974, p. 523) used a Manning's n of 0.028. April and others (1975, p. 769) used n values that ranged from 0.010 to 0.018 for Mobile Bay, Ala. In a study of Masonborough Inlet, N.C., Masch and Brandes (1975, p. 230) used n values that ranged from 0.018 to 0.035 for depths from 4 to 30 ft. Beauchamp and Spaulding (1978, p. 525) used an n value of 0.028 for the Long Island Sound, Block Island Sound, Rhode Island Sound, and Buzzards Bay area of New England. Wang (1978, p. 505) used an n value of 0.025 for South Biscayne Bay, Fla.

An initial n value of 0.025 was chosen for this study on the basis of the most comparable conditions reported in the literature. Other n values, as low as 0.022, were used in the model calibration process. A uniform value of 0.0235 was chosen as providing the best fit to prototype data. Whenever water depth in any cell became less than 1 ft, however, the model automatically reassigned an n value of 0.040 to simulate the increased importance of bottom friction.

Shorelines and Tributary Streams

The shoreline is defined as a no-flow boundary except where tributary streams enter the bay. A flooding and

drying feature of the model simulates landward or seaward movement of the shoreline with changes in tidal stage. This feature is less significant in Tampa Bay when compared with other coastal plain estuaries that have extensive areas of tidal flats.

Freshwater inflow of streams tributary to Tampa Bay (fig. 1) was determined from data published by the U.S. Geological Survey (1977). The freshwater inflow used in the model (table 3) is the annual average inflow computed from long-term records at the most downstream gaging station on each river (U.S. Geological Survey, 1977). The inflow contribution from ungaged areas was approximated by a proportionate increase based on drainage area ratios. Inflow was entered at appropriate cells near the shoreline of the model.

Once-through, cooling-water systems of power-generating stations were handled in a similar way. Cooling-water intakes were simulated as negative discharges at cells close to the locations of intake structures. Cooling-water discharges were simulated as positive values at cells close to the discharge sites. A representative of the Tampa Electric Company (oral commun., 1975) indicated that typical cooling-water discharge rates for both the Big Bend and Gannon stations (fig. 1) were 1,960 ft^3/s. Information from a Florida Power Company representative (oral commun., 1975) indicated typical cooling-water discharge rates were 1,000 ft^3/s for both the Higgins and Weedon Island stations (fig. 1).

Seaward Boundary

Fluctuations in tidal stage, the primary force causing time-dependent water motion, were applied at the seaward boundary of the model. The model distributed water to and from sections of the estuary by solving equations 1, 2, and 3 for each designated time and space increment. At the seaward boundary, velocities were computed by using simplified linearized equations that did not require any information outside the boundary. This procedure produced less precise computations at and near the seaward boundary than at other locations.

Because of less precise velocity computations and increased susceptibility of the simplified equations to numerical instability, the seaward boundary had to be established some distance from areas where model results could be significant and where large depth changes could induce instability. Location of the seaward boundary approximately 4 mi offshore from Egmont Key accomplished these two objectives.

To generate offshore tidal conditions, a cross-spectral analysis technique described by Leendertse and Liu (1974) and used by Van der Ree and others (1978) was applied to transfer tidal-stage, time-series data for Fort De Soto (site 22, fig. 8) to the seaward boundary at location WC-154 (site 24, fig. 8). The technique required concurrent time-series data at each location to define cross-spectral relations. Once established, these relations could then be used to generate time-series data at site 24 for any period for which data were available at Fort De Soto.

Concurrent time-series data were available for the period January 25 to February 11, 1979, when offshore pressure recordings were obtained by Woodward-Clyde Consultants (1979) and when the Fort De Soto gage was in operation. A part of the concurrent data (fig. 9) shows significant amplitude and phase differences. The computed data at site 24, after cross-spectral adjustments were made to the Fort De Soto record, are shown in figure 10 and compared with measured data. The standard error between measured and computed data is about 0.1 ft.

The tide conditions that existed in the Gulf of Mexico during a period of intensive field measurements in Tampa Bay in 1972 were approximated by using cross-spectral relations. Computed results are shown in figure 11. Because additional information on tidal conditions in the Gulf of Mexico was not available, the computed tides at site 24 were applied along the entire seaward boundary

Table 3. Average annual discharge of streams tributary to Tampa Bay (U.S. Geological Survey, 1977)

Tampa Bay subarea	Stream	Average annual discharge (cubic feet per second)[1]
Hillsborough Bay	Hillsborough River	636
	Alafia River	459
	Total of several small streams	99
Old Tampa Bay	Total of several small streams	117
Middle Tampa Bay	Little Manatee River	240
Lower Tampa Bay	Manatee River	353
Total		1,904

[1]All values linearly adjusted to include effect of ungaged drainage area.

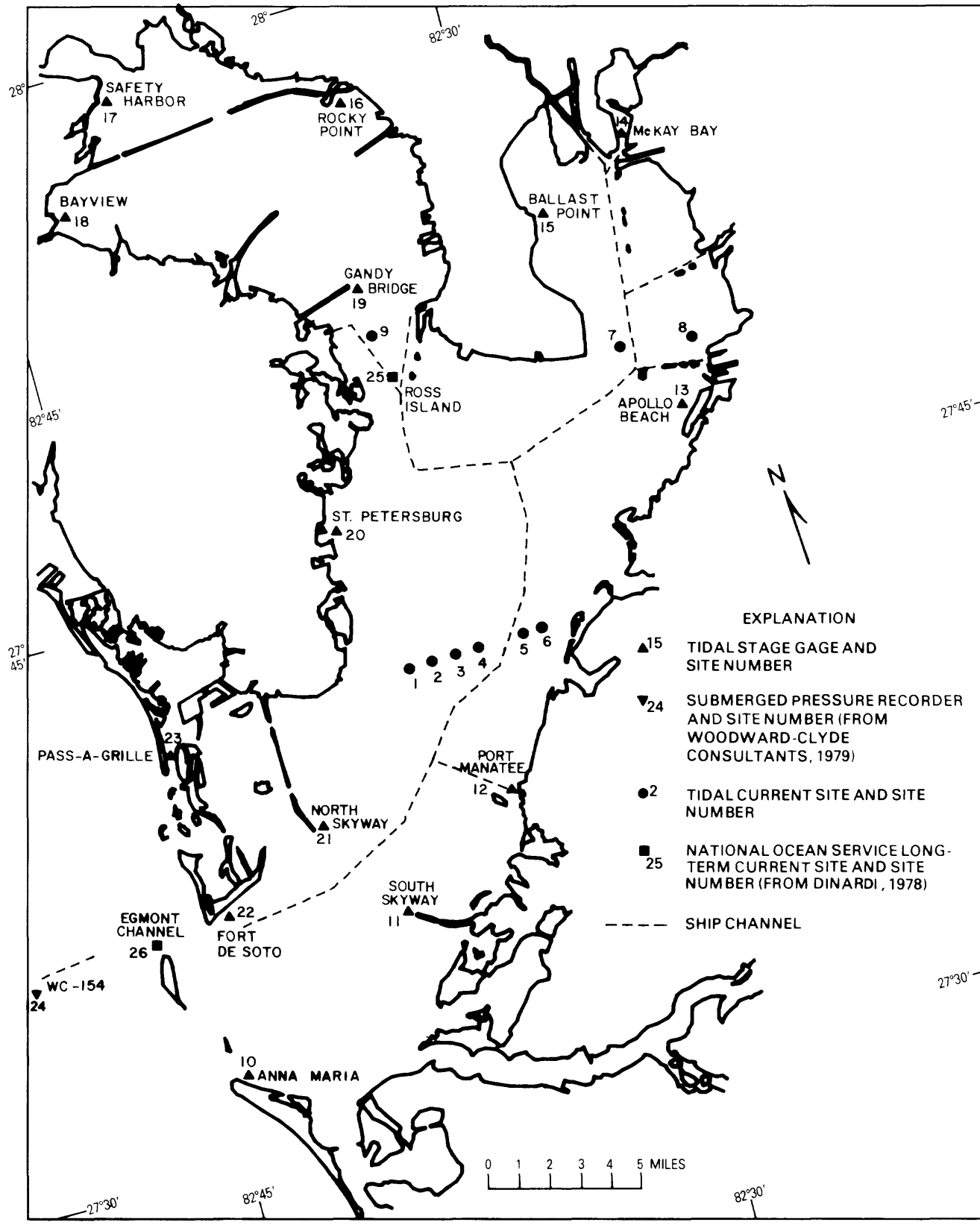

Figure 8. Location of tidal stage and tidal current measuring sites and submerged pressure recorder and long-term current sites in Tampa Bay.

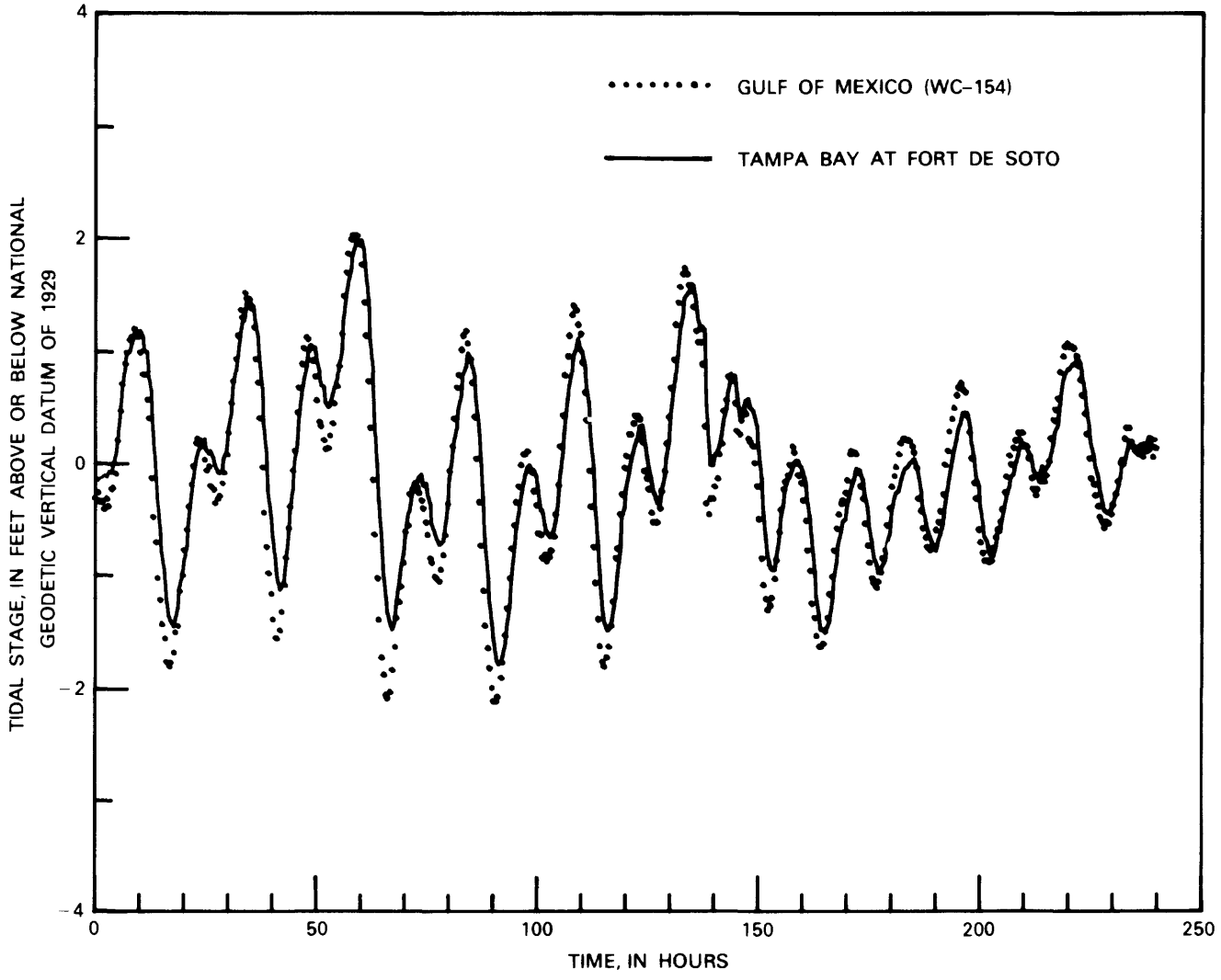

Figure 9. Comparison of observed tidal stage in the Gulf of Mexico and at Fort De Soto inside the mouth of Tampa Bay. Locations of sites are shown in figure 8.

for the model calibration and verification periods shown in figure 11.

Tide conditions during the calibration period were chiefly dirunal and had a tidal range of about 2.4 ft. The duration of rising tide was about 16 hours. The duration of falling tide was about 9 hours. The first verification period also had a predominantly diurnal tide that had a range of 3.6 ft. The second verification period had mixed tide characteristics and large semidiurnal inequalities. The diurnal tidal range was 3.0 ft. The three tides are representative of conditions in Tampa Bay.

Water-Surface Boundary

The water surface is treated as a vertically movable, impermeable boundary having wind-induced shearing stresses transmitted to the flow, depending on wind speed and direction. Wind-shear stress components at the air-water interface were computed by using equations 6 and 7 and were applied to spatially averaged wind fields determined from hourly observations of wind speed and direction made at several sites in the Tampa Bay area. The sites used for this purpose include the Tampa International Airport, MacDill Air Force Base, St. Petersburg-Clearwater International Airport, Sarasota-Bradenton Airport, and Albert Whitted Airfield (fig. 1).

The wind field was computed by averaging hourly orthogonal components from each of these five sites, in accordance with equations 13 and 14:

$$\overline{W}_x = \frac{1}{5}\sum_{i=1}^{5} W_i \cdot \sin\phi_i \qquad (13)$$

$$\overline{W}_y = \frac{1}{5}\sum_{i=1}^{5} W_i \cdot \cos\phi_i \qquad (14)$$

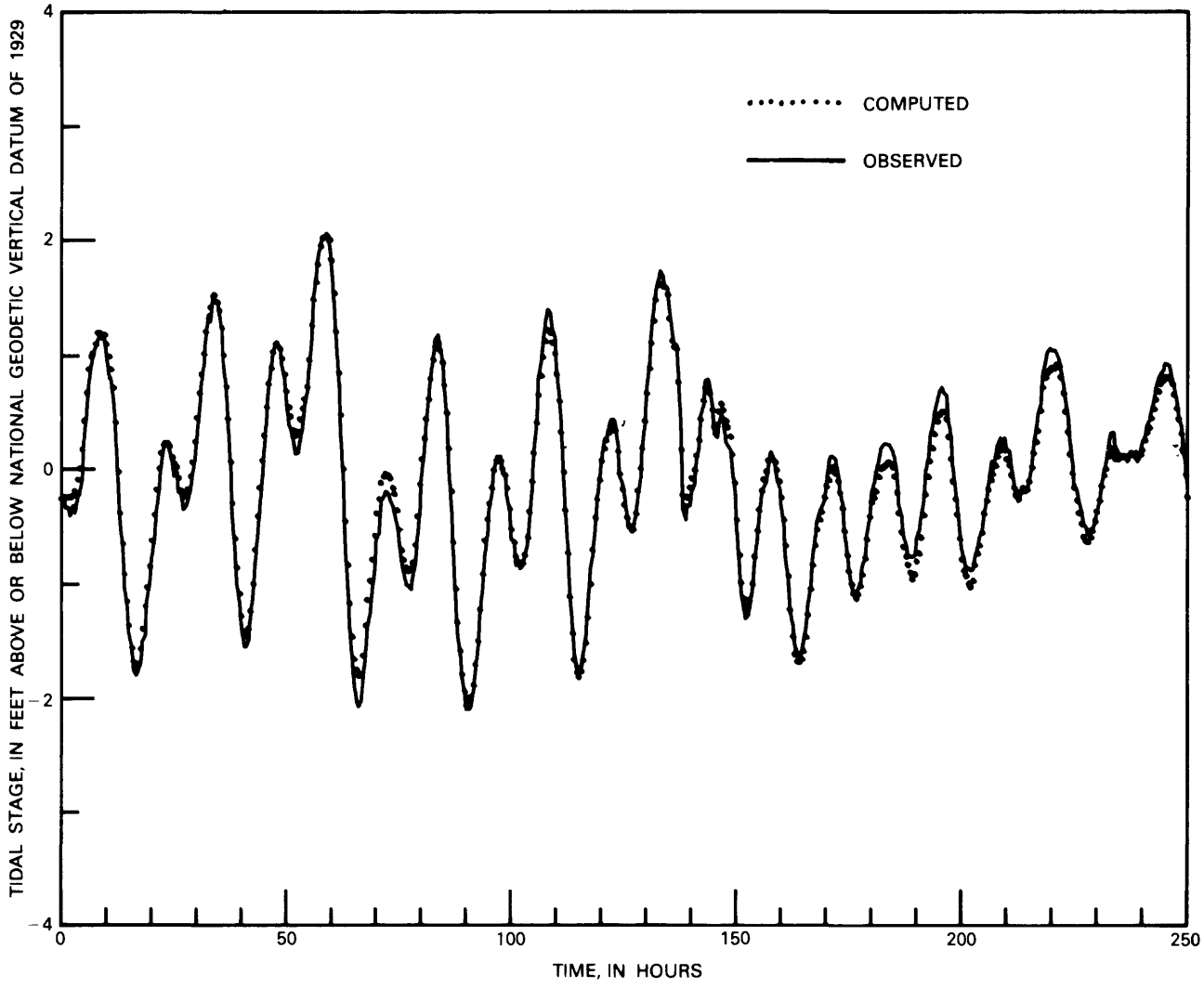

Figure 10. Comparison of observed tidal stage in the Gulf of Mexico with tidal stage computed by using cross-spectral procedure (described by Leendertse and Liu, 1974).

where

$\overline{W}_x = x$ component of spatially averaged wind speed, in miles per hour;

$\overline{W}_y = y$ component of spatially averaged wind speed, in miles per hour;

W_i = hourly wind speed, in miles per hour; and

ϕ_i = hourly wind direction, in degrees clockwise from north, that the wind is blowing from.

The results were reconstituted by using equations 15 and 16 to produce average hourly wind speed and direction over the study area:

$$\overline{W} = \left(\overline{W}_x^2 + \overline{W}_y^2\right)^{0.5} \quad (15)$$

$$\overline{\phi} = \arctan \frac{\overline{W}_x}{\overline{W}_y}, \quad (16)$$

where

$\overline{W}$ = spatially averaged wind speed, in miles per hour, and

$\overline{\phi}$ = spatially averaged wind direction, in degrees clockwise from north.

The computed wind field was assumed to be variable with time but spatially uniform over the modeled area. Because wind characteristics at the measuring locations were similar, no large error due to spatial averaging is expected. Wind speeds were generally within ±2 knots, and directions within ±30 degrees, of each other. Exceptions occurred primarily during rapid wind shifts associated with the passage of cold fronts. Wind speed and direction during calibration and verification periods are shown in figure 12.

Wind during the calibration period was initially light, about 5 knots from the east, became calm by the end of 20 hours, and picked up from the west during the last 2 hours of simulation. Wind speed during the first verification period averaged about 6 knots. The direction changed at a uniform rate in a clockwise manner starting from the east-southeast, through north, and around

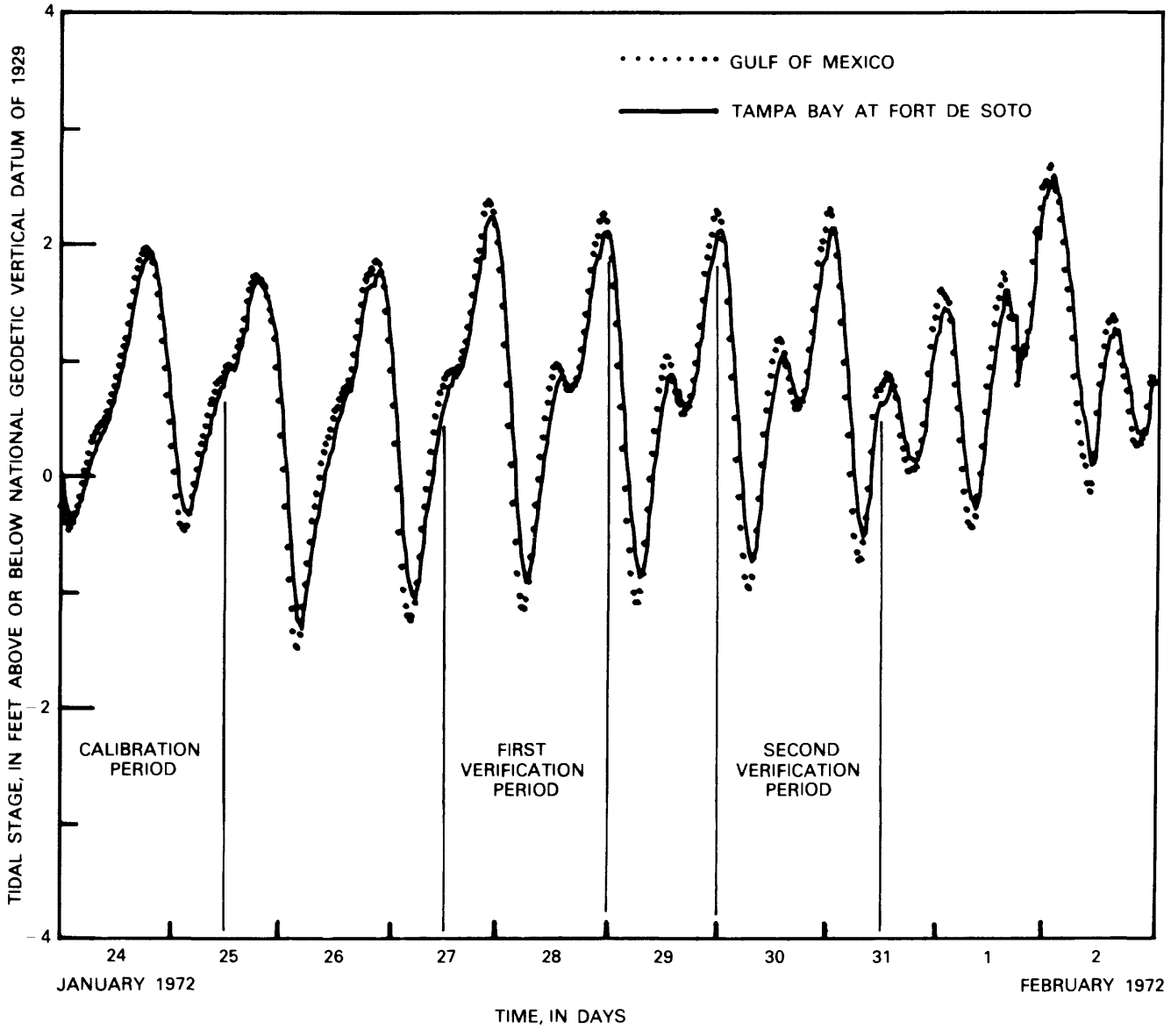

Figure 11. Comparison of computed tidal stage in the Gulf of Mexico with observed tides at Fort De Soto during model calibration and verification periods.

the points of the compass to reach north a second time. Wind during the second verification period began as calm, then averaged about 7 knots from the south-southwest for most of the period.

Initial Conditions

Establishing initial conditions is necessary to define three time-varying parameters—tidal stage, tidal current, and constituent concentration—when starting model computation. The following sections describe how these initial conditions are assigned and how they affect simulation results.

Tidal Stage and Tidal Current

A level water surface was assumed throughout the bay at the start of each model run at an altitude equal to the starting water level at the seaward boundary. Correspondingly, all tidal currents at the start of each model run were zero. The bay was motionless.

Operationally, about 12 hours of real time must be simulated before the effects of these assumed initial conditions disappear from the solution and before model computations accurately reflect real stage and current conditions. Circulation computations are more sensitive and require simulation of about 24 hours of real time before the effects of initial conditions disappear. Model computations during these periods are disregarded. If a model run is restarted to extend a previously simulated period, initial tidal stages and currents for each cell are read from a restart tape created by the prior run (see fig. 6).

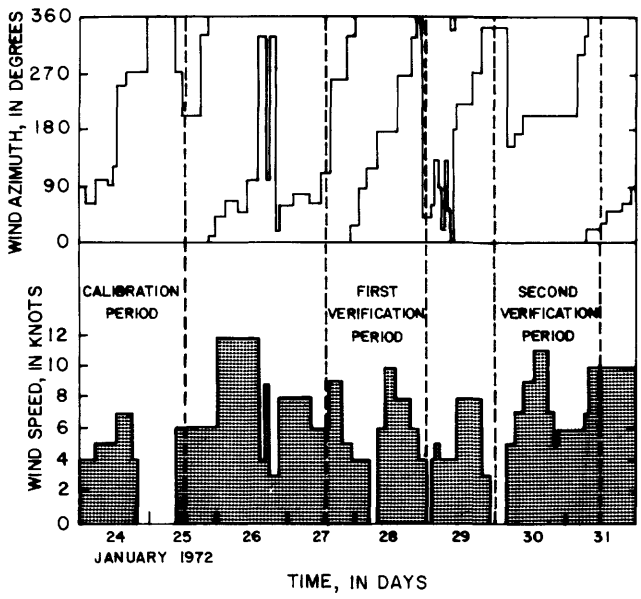

Figure 12. Wind speed and direction during calibration and verification periods.

Constituent Concentration

An initial concentration must be assigned to each cell for each constituent included in the computation. Assignments can be made in three ways: (1) a uniform concentration throughout the model can be generated by specifying a default value; (2) the default value can be changed at one or many cells by specifying values that override the default value; and (3) a complete array can be provided that defines the initial concentration at each cell.

A uniformly low initial background concentration is useful when simulating the spread of dye or other constituent injected at a point. Overrides can be used to advantage if one or more small subregions are known to have different concentrations than the rest of the simulated region. An array is normally provided if an accurate definition of constituent gradients is needed at the start of a model run.

Constituent concentrations at the seaward boundary of the model are computed from values at interior points during ebbflow. During floodflow, however, water having unassigned and uncomputed constituent concentrations can be brought from outside the modeled area. This water can cause rapid degeneration of computed concentrations near the seaward boundary. To avoid this, the model allows a gradual return of concentrations to an initially defined value. This procedure is approximate but allows reasonable computation of concentrations to continue at the seaward boundary through all phases of the tide. This procedure is considered to be more realistic than assignment of a constant concentration to all water crossing the seaward boundary during floodflows.

The initial concentration used for calibration of model dispersion was a constant, near-zero value for turbidity. Further description of turbidity plume simulation is given below in the section Calibration and Verification.

Calibration and Verification

Observations of tidal stage and tidal currents were made in 1972 for model calibration and verification. Table 4 shows starting and ending times for the calibration and verification periods and availability of field data for comparison with model computations. Tidal current data were not available for January 24 and 25, 1972; as a result, calibration was based on stage data only. Stage and current data were available for both verification periods.

Tidal Stage

Tidal stage data were measured at 14 locations (sites 10–23, fig. 8) from June 1971 to December 1973 (Goodwin and Michaelis, 1976). Table 5 gives the site number, the downstream order number, the complete station name, and the latitude-longitude position (progressing counterclockwise around the bay from the most southerly station) for tidal stage stations in Tampa Bay. Each of the 14 stations was equipped with digital recording instruments that measured water-level altitudes every 5 or 15 minutes, as controlled by crystal timers accurate to 5 s/mo. Gages were referenced to the NGVD of 1929 by spirit leveling to first-order benchmarks wherever possible. The latitude and longitude of gage WC-154 (site 24) also are given in table 5.

For the calibration period, the standard errors between computed and observed water levels at half-hour intervals during the last 24 hours of simulation ranged from

Table 4. Calibration and verification time periods and field data availability for tidal stage and current observations in Tampa Bay, 1972

Period	Start		End		Duration (hours)	Field data availability	
	Day	Hour	Day	Hour		Stage	Velocity
Calibration _____	1-24-72	0005	1-25-72	1200	36	Yes	No
First verification _	1-27-72	1205	1-28-72	2400	36	Yes	Yes
Second verification _	1-30-72	0005	1-31-72	1200	36	Yes	Yes

Table 5. Information summary for tidal stage stations in Tampa Bay

Site no. (see fig. 8)	USGS downstream order no.	Station identification[1]	North latitude	West longitude
10	02-3000.72	Tampa Bay at Anna Maria	27°32'03"	82°43'50"
11	02-3000.85	Tampa Bay near Terra Ceia (South Skyway)	27°35'30"	82°37'45"
12	02-3000.88	Tampa Bay near Piney Point (Port Manatee)	27°38'06"	82°33'32"
13	02-3005.60	Tampa Bay near Ruskin (Apollo Beach)	27°46'57"	82°25'53"
14	02-3017.61	McKay Bay at Tampa	27°54'54"	82°25'25"
15	02-3060.32	Hillsborough Bay at Ballast Point at Tampa	27°53'22"	82°28'47"
16	02-3061.00	Old Tampa Bay at Rocky Point at Tampa	27°57'59"	82°33'57"
17	02-3075.78	Old Tampa Bay at Safety Harbor	27°59'17"	82°41'07"
18	02-3077.69	Old Tampa Bay near Bayview	27°56'28"	82°43'15"
19	02-3079.30	Old Tampa Bay at Gandy Bridge near Tampa	27°52'46"	82°34'57"
20	02-3080.82	Tampa Bay at St. Petersburg	27°46'24"	82°37'25"
21	02-3084.26	Tampa Bay at Sunshine Skyway Bridge near St. Petersburg (North Skyway).	27°38'36"	82°40'12"
22	02-3086.00	Tampa Bay at Fort De Soto Park near Pass-a-Grille Beach	27°36'53"	82°43'33"
23	02-3086.50	Pass-a-Grille Channel near Pass-a-Grille Beach	27°41'30"	82°43'48"
24	–	Woodward-Clyde gage number 154 offshore of Egmort Key (WC-154)	27°36'12"	82°51'54"

[1]Underlined name is shown in fig. 8.

0.03 ft at South Skyway near the mouth of Tampa Bay, site 11, to 0.13 ft at Safety Harbor, site 17, and Bayview, site 18, in Old Tampa Bay (table 6). The average standard error for calibration was 0.07 ft. Graphical comparisons between observed and computed tidal-stage water levels for six stations from the mouth to the head of the bay are shown in figure 13. From the graphs it can be seen that about 12 hours of real time must be simulated before the effects of assumed initial conditions disappear and before model computations reflect real stage and current conditions.

The average standard error for both verification periods was 0.09 ft, and the range was from 0.04 to 0.15 ft (table 6). Graphical comparisons between observed and computed tidal stages for the first and second verification periods are shown in figures 14 and 15, respectively. Some difference between observed and computed stages is to be expected since all model adjustments were designed to make model computations match calibration-period field observations as closely as possible. Adjustments were not made for verification periods. That the standard errors are about the same for all three periods lends credibility to the model's capability to accurately simulate real conditions.

Tidal Current

Tidal currents were measured at sites 1–9 from January 25 to 31, 1972 (fig. 8 and table 7). Instruments used were

Table 6. Standard error of tidal stage in Tampa Bay for calibration and verification periods

Site no. (see fig. 8)	Station name	Standard error (feet)		
		Calibration	First verification	Second verification
10	Anna Maria	0.04	0.09	0.10
11	South Skyway	.03	.07	.08
12	Port Manatee	.04	.04	.04
15	Ballast Point	.06	.07	.11
16	Rocky Point	.11	.11	.07
17	Safety Harbor	.13	.15	.10
18	Bayview	.13	.15	.11
19	Gandy Bridge	.08	.13	.10
20	St. Petersburg	.05	.06	.09
21	North Skyway	.04	.06	.07
22	Fort De Soto	.04	.06	.07
	Average	.07	.09	.09

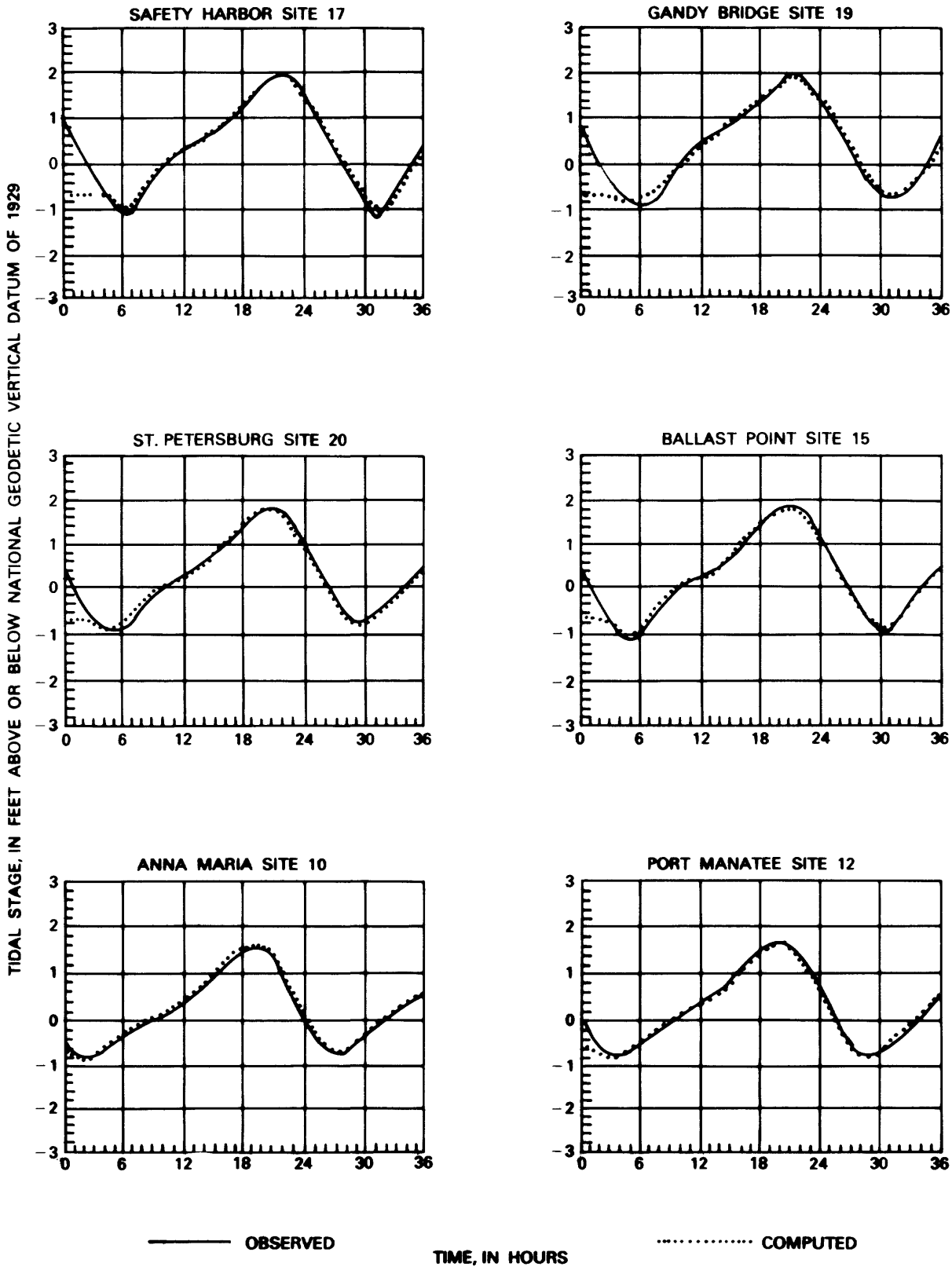

Figure 13. Observed and computed tidal stage at selected sites in Tampa Bay during calibration period.

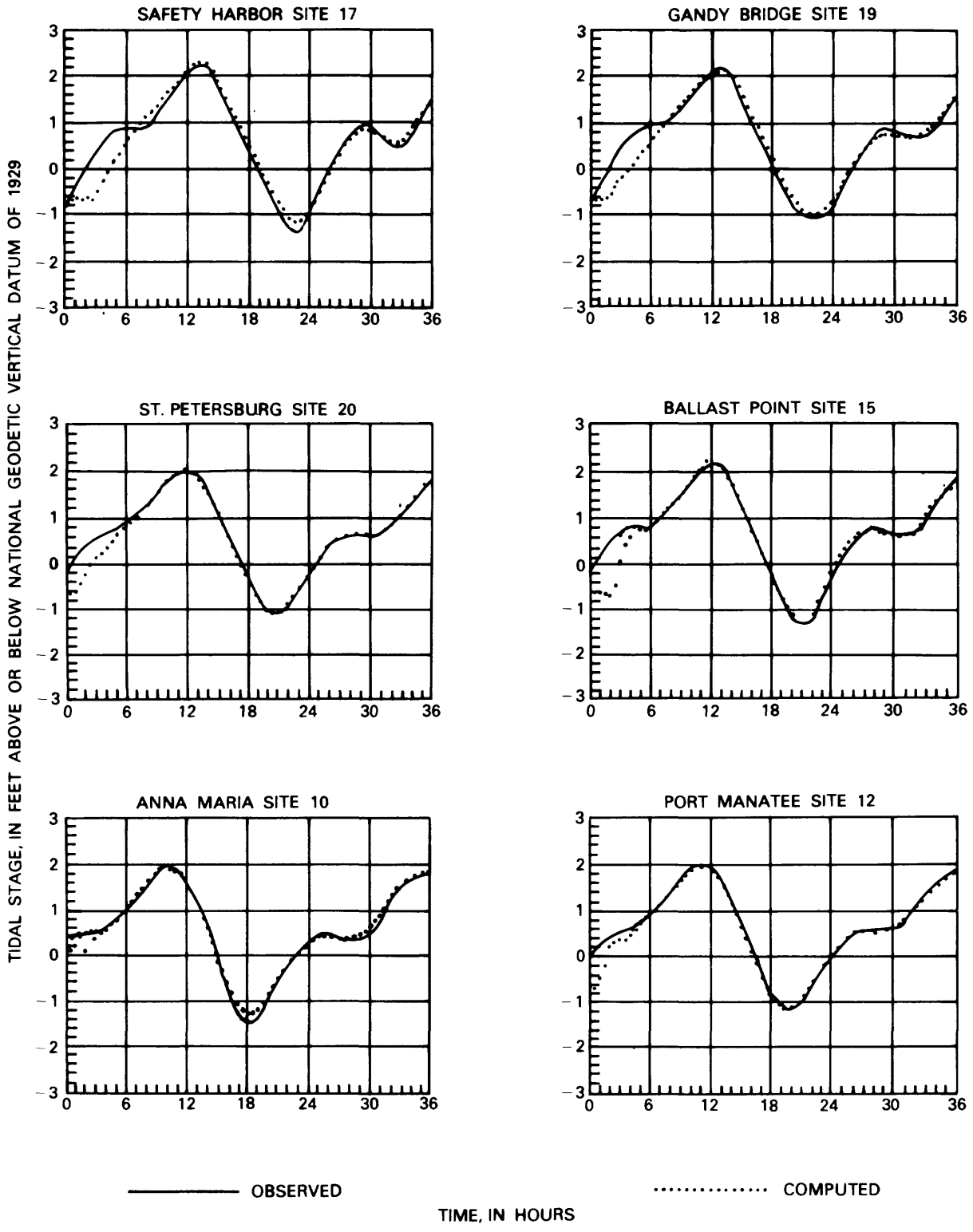

Figure 14. Observed and computed tidal stage at selected sites in Tampa Bay during first verification period.

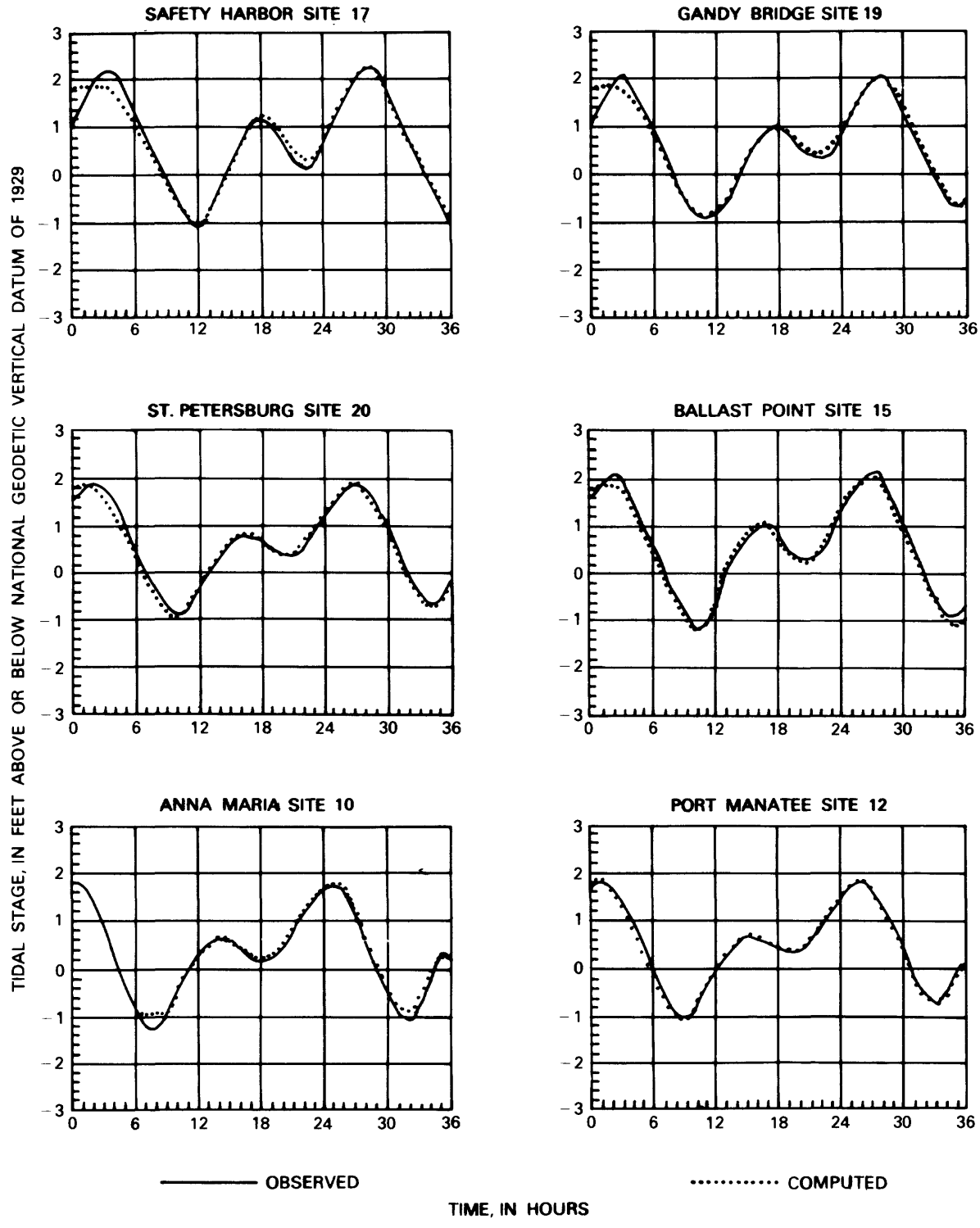

Figure 15. Observed and computed tidal stage at selected sites in Tampa Bay during second verification period.

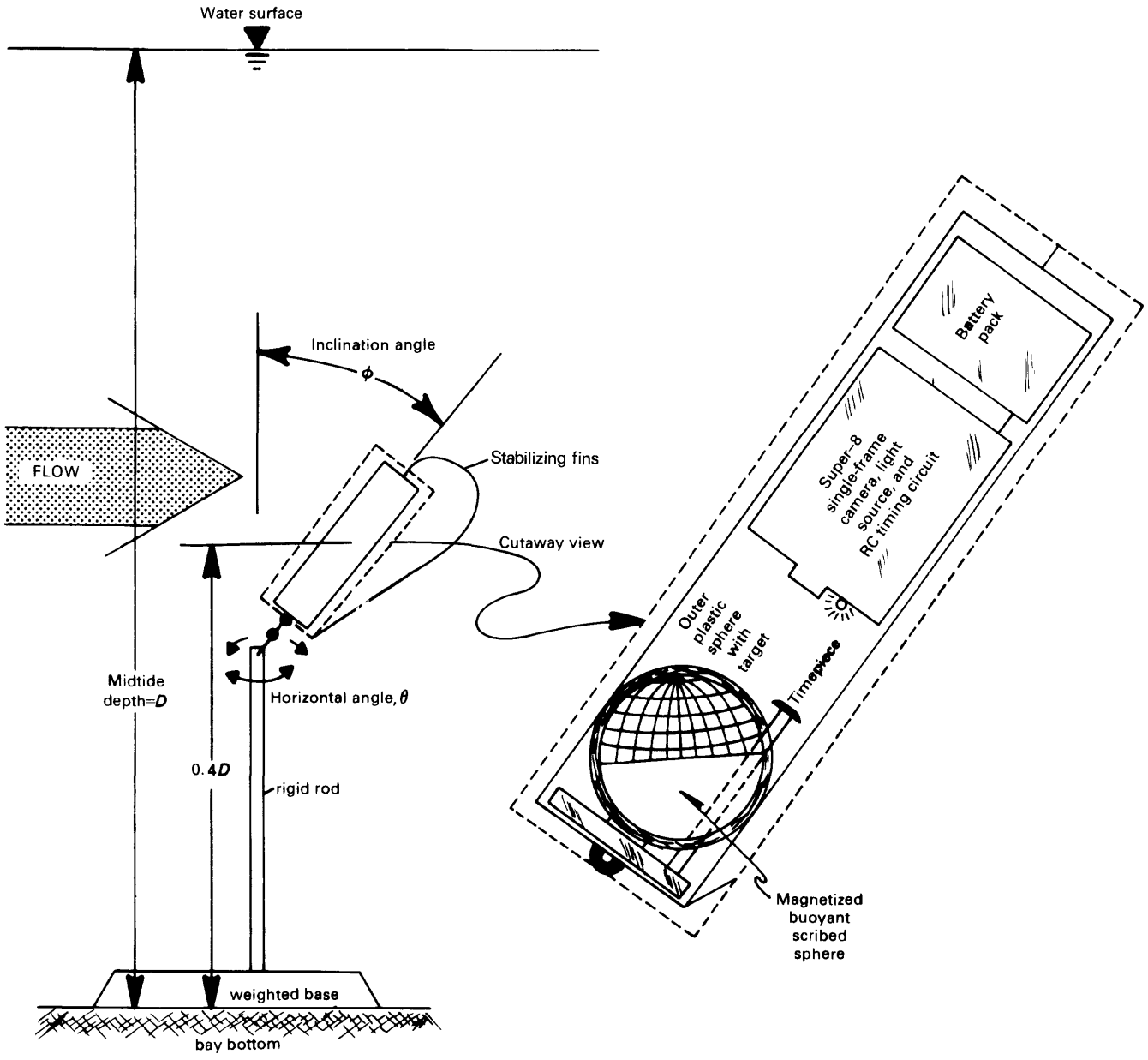

Figure 16. Inclinometer current-meter placement and operation.

Table 7. Location of tidal current measurement sites in Tampa Bay

Site no. (see fig. 8)	North latitude	West longitude
1	27°43′01″	82°36′04″
2	27°42′54″	82°35′18″
3	27°42′59″	82°34′25″
4	27°42′46″	82°33′40″
5	27°42′42″	82°32′28″
6	27°42′39″	82°31′45″
7	27°49′20″	82°26′57″
8	27°49′16″	82°25′44″
9	27°50′57″	82°34′47″
25 Ross Island	27°49′54″	82°34′12″
26 Egmont Channel	27°36′32″	82°46′06″

film-recording, inclinometer-type current meters (fig. 16 that had the capability to sense and record both speed and direction of flow.

The meters were placed to collect data that represented the average velocity in the vertical. The center of each meter was placed at approximately four-tenths of the mid-tide water depth from the bottom of the bay (fig. 16). Tidal current data collected by the NOS in 1963 (Dinardi, 1978) showed velocity profiles typical of vertically well-mixed, unstratified flow. Under such conditions, an average velocity can be adequately measured by strategic placement of one meter and by using the six-tenths-depth measurement technique of the U.S. Geological Survey (Buchanan and Somers, 1969, p. 32).

Errors in the measurement of tidal currents were due primarily to (1) a small amount of friction within the current meters and (2) the visual-manual data translation procedure needed to digitize the data. Visual interpretation errors between scribed lines on sequential frames of photographic film were approximately 1° for the inclination angle, ϕ. The error ranged from 1° to 9° for the horizontal angle, Θ, based on the range of ϕ, as follows:

Range of inclination angle (ϕ), in degrees	Translation error of horizontal angle (Θ), in degrees
0 to 10	9
11 to 20	3
21 to 90	1

Unavoidable friction errors were estimated to be equal to visual interpretation errors. As a result, errors for the inclination angle totaled 2° and ranged from 2° to 18° for the horizontal angle. Measured tidal current, therefore, had an overall error of about 0.1 ft/s at velocities of less than 0.5 ft/s and greater than 1.5 ft/s. Between these bounds, the error is about 0.03 ft/s.

Tidal current data collected over a 30-day time period at two sites by the NOS in 1963 (Dinardi, 1978) were sufficient to compute a long-term residual current. Locations of these sites, 25 and 26, are given in figure 8 and table 7. Errors associated with the residual currents at these sites are not known. According to Cheng and Gartner (1985), uncertainties exist when computing residual currents from tidal current measurements. Cheng and Gartner (1985) were able, however, to demonstrate close agreement between two independent methods for computation of residual currents in South San Francisco Bay. They concluded that satisfactory residual computations could be made from tidal current measurements.

Observed tidal current data were available at nine sites during the first verification period and at six sites during the second verification period. Tidal currents were not measured during the calibration period. Graphical comparisons between observed and computed tidal currents (both speed and direction) for selected sites are shown in figures 17 and 18, and computed standard errors are given in table 8. Standard errors for tidal current speed range from 0.08 to 0.17 ft/s, with an average of about 0.11 ft/s. Standard errors for direction range from 5° to 25°, with an average of about 14°. With a few exceptions, these comparisons are very good and provide additional assurance that the model simulates real conditions.

Measurement error for tidal current speed ranges from about 0.03 to 0.10 ft/s for the currents encountered. Measurement error, therefore, may account for half or more of the computed standard errors. The remaining error is attributed to local conditions that were not adequately represented by the 1,500-ft model grid.

Measurement error for tidal current direction ranged from an estimated 2° to 18°, depending on current speed; the lower the speed, the higher the direction error. Low current speed at sites 7 and 8 in Hillsborough Bay helps explain the high standard errors for direction at these sites (table 8). Direction errors also could have resulted from inability of the model grid size (1,500 ft) to adequately resolve details of many channels, islands, and submerged disposal areas. Computed currents in Hillsborough Bay are considered to be representative of real conditions but less accurate than in other areas of the bay.

Dispersion

Satellite imagery of a turbidity plume caused by dredging in Tampa Bay was used to calibrate dispersive characteristics of the model. Verification of model dispersive capabilities was not accomplished because only one plume was simulated.

The observed plume, reported by Goodwin and Michaelis (1984, p. 7), was created by a shell dredge on November 17, 1972 (fig. 19*A*). Scale distortion of the image is rectified and superimposed on the simulated plume in figure 19*B*. The barbell-shaped plume is unique to tidal waters and depends on the relative timing of turbidity generation and tidal phase. The ability to reasonably simulate the shape of the observed plume was considered to be a good test of the dispersive features of the model.

Costs of model operation precluded making a separate run devoted exclusively to plume analysis. Therefore, the plume was simulated during part of a model run designed primarily for tidal stage and tidal current verification. The simulated tidal range at St. Petersburg, near the plume, was 3.1 ft (fig. 14), and the actual range at St. Petersburg that produced the observed plume was approximately 1.9 ft (U.S. Department of Commerce, 1971, p. 129). Dispersion coefficients used in the model were computed by using equations 10 and 11, with $D_w = 50$ ft²/s and $d = 25$ (J. J. Leendertse, oral commun., 1980).

Tidal stage and tidal current (at the simulated dredge site) and the period of turbidity generation that were used to simulate the turbidity plume are shown in figure 20. Turbidity generation started at high slack tide and continued to about 1 hour after the next low slack tide. The series of six illustrations in figure 21 follows plume development at 1, 5, 9, 13, 17, and 23 hours after start of turbidity generation. Figure 21*A* shows a nearly circular plume at high slack tide. An elongated plume is shown during maximum ebbflow in figure 21*B*. Figure 21*C*, at low slack tide, shows maximum plume extent and the barbell shape. Figure 21*D–F* shows the plume at three succeeding times during floodflow, after turbidity generation had stopped.

A typical suspended solids discharge rate was used (Gren, 1976) to develop the simulated plume because the actual rate for the shell dredge was not known. Also, data

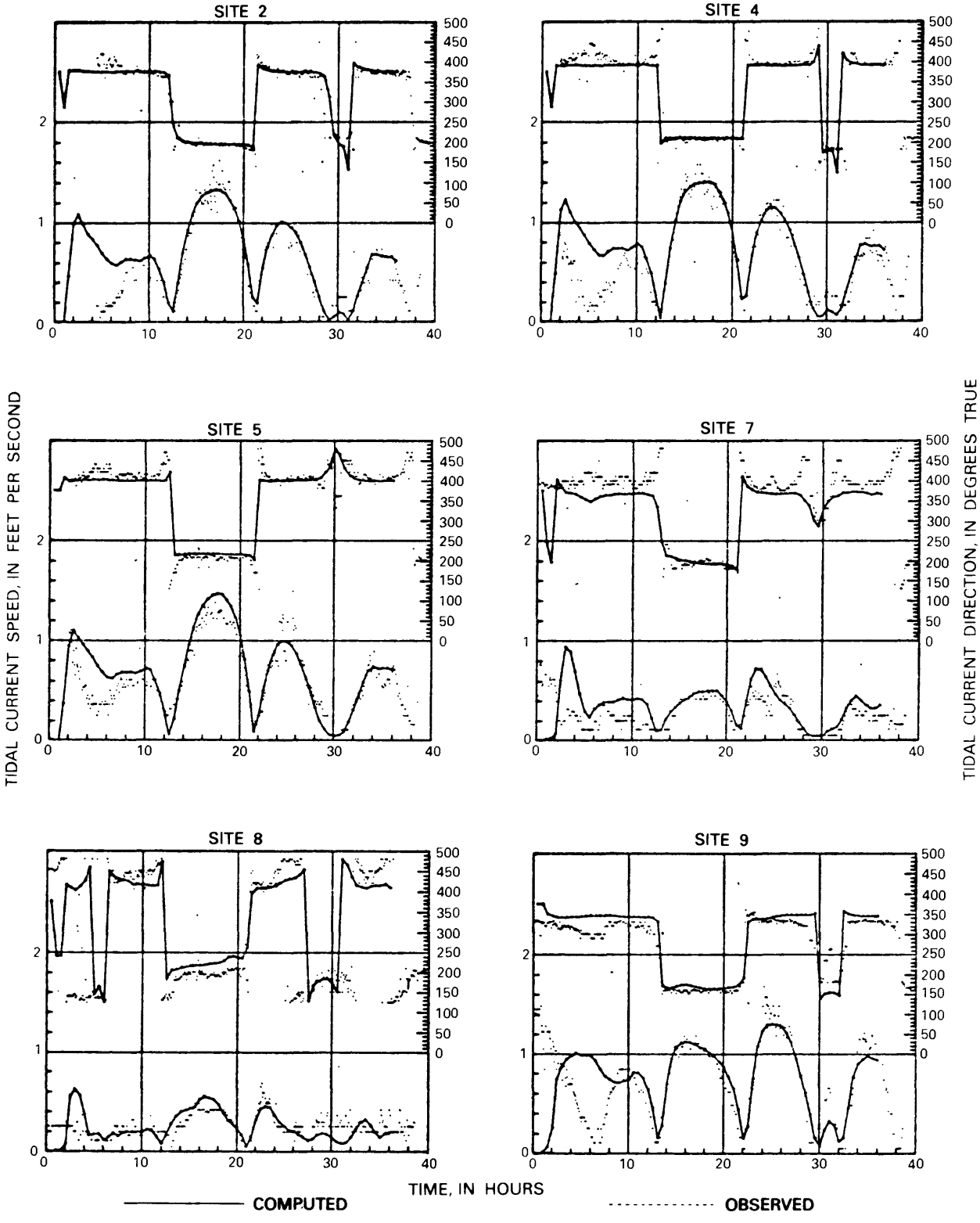

Figure 17. Observed and computed tidal current speed and direction at selected sites in Tampa Bay during first verification period.

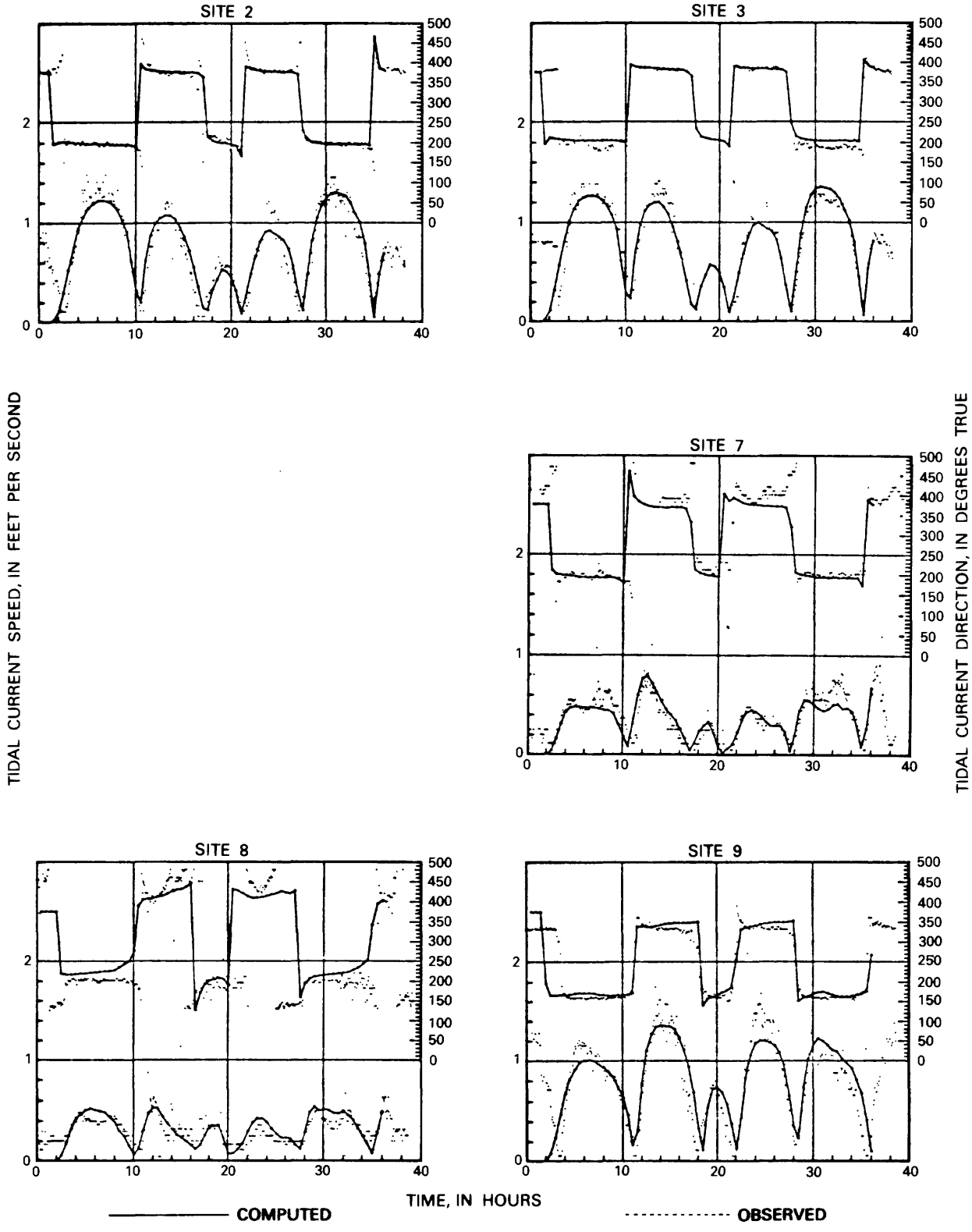

Figure 18. Observed and computed tidal current speed and direction at selected sites in Tampa Bay during second verification period.

Table 8. Standard error of tidal current speed and direction in Tampa Bay for verification periods

Site no. (see fig. 8)	Tidal current speed, standard error (feet per second)		Tidal current direction, standard error (degrees)	
	First verification	Second verification	First verification	Second verification
1	0.08	—	17	—
2	.09	0.12	5	8
3	.09	.12	8	10
4	.08	—	8	—
5	.12	—	9	—
6	.15	.16	16	16
7	.10	.10	17	17
8	.10	.08	25	22
9	.13	.17	14	13
Average	.10	.12	13	14

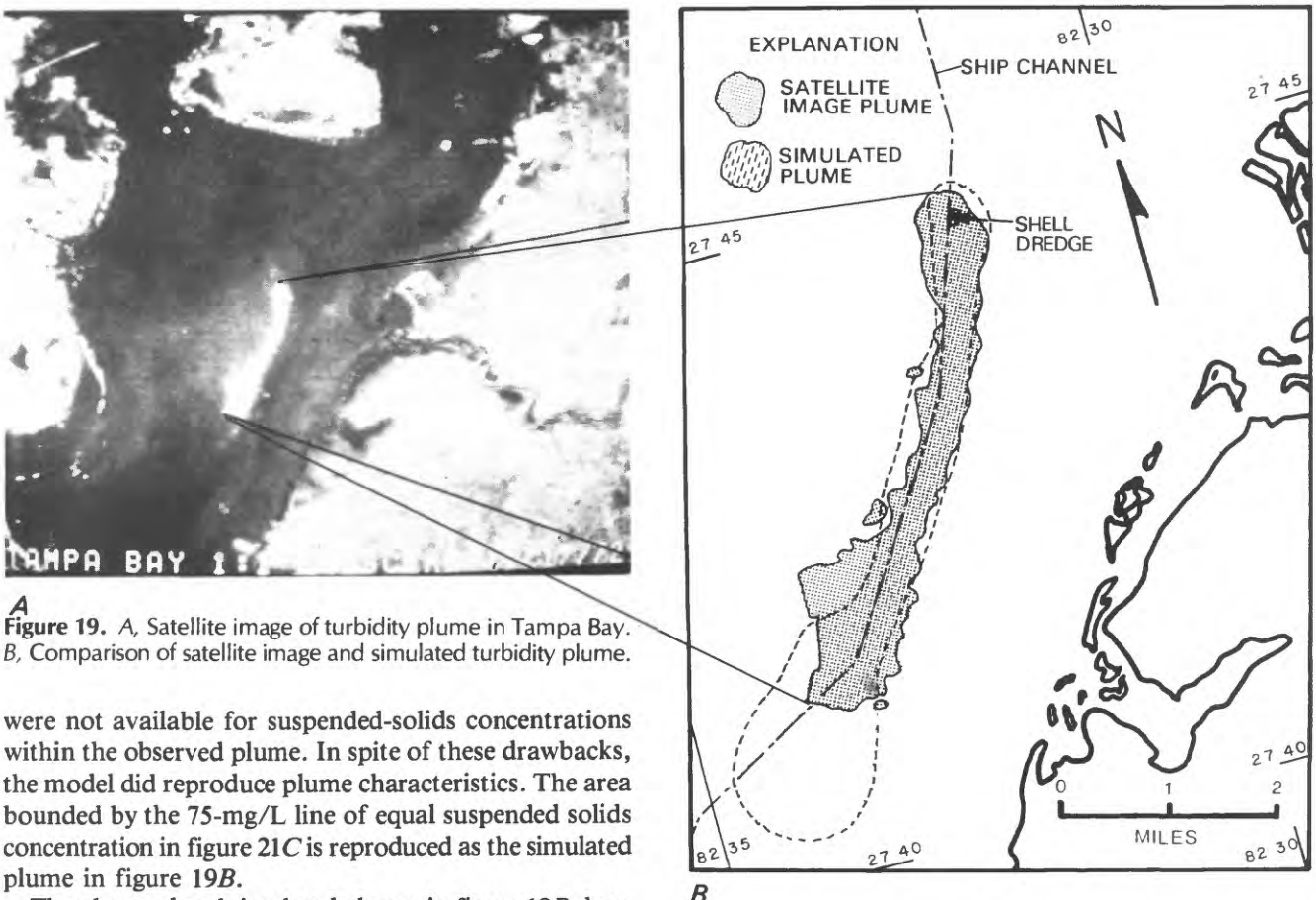

Figure 19. *A,* Satellite image of turbidity plume in Tampa Bay. *B,* Comparison of satellite image and simulated turbidity plume.

were not available for suspended-solids concentrations within the observed plume. In spite of these drawbacks, the model did reproduce plume characteristics. The area bounded by the 75-mg/L line of equal suspended solids concentration in figure 21*C* is reproduced as the simulated plume in figure 19*B*.

The observed and simulated plumes in figure 19*B* show nearly identical shape and orientation. The southern end of each plume has a large bulbous shape. The northern ends show less bulge because of limited dispersion time. A narrow section that follows the ship channel connects the northern and southern ends of each plume. The only significant difference between the observed and simulated plumes is their lengths. One factor causing the length difference is the inequality of tidal ranges (p. 28). Another factor affecting plume lengths is the difference between (1) vertically averaged tidal currents used in the simulation and (2) faster near-surface currents in the bay that carry suspended-sediment particles constituting the observed turbidity plume.

Simulated and observed plume lengths can be compared by adjusting results shown in figure 19*B* for the effects of different tidal ranges and different current speeds. The length of the simulated plume (measured from the shell dredge to the centroid of the southern end

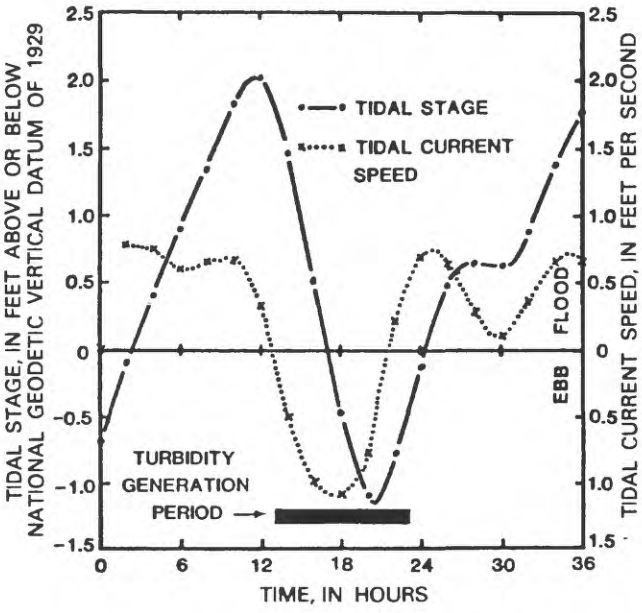

Figure 20. Tidal stage and tidal current used during turbidity plume simulation.

of the barbell) can be adjusted for tidal range differences by assuming a linear relation between plume length and tidal range. The simulated plume can be further adjusted by a proportionality factor relating vertically averaged tidal current speed to near-surface tidal current speed. The factor used was determined from velocity data presented by Dinardi (1978, p. 33) at two sites very close to the plume location. Surface waters in this area apparently move about 23 percent faster than the average speed in the water column. The following computation gives the adjusted simulated plume length:

$$\begin{pmatrix}\text{Simulated length (from fig. 19}B\text{)}\end{pmatrix} \times \frac{\text{Actual tidal range}}{\text{Simulated range}} \times \begin{pmatrix}\text{Speed correction factor}\end{pmatrix} = \begin{pmatrix}\text{Adjusted simulated length}\end{pmatrix} \quad (17)$$

$$5.2 \text{ mi} \times \frac{1.9}{3.1} \times 1.23 = 3.9 \text{ mi}$$

This compares very well with the length of the observed plume, 4.0 mi, as measured from figure 19*B*. The general agreement between observed and simulated turbidity plumes indicates that the dispersive features of the model adequately simulate actual conditions.

Application to 1880, 1972, and 1985 Levels of Development

The model, after calibration and verification, was applied to determine flow, circulation, and flushing characteristics of Tampa Bay for historical (1880), predredging (1972), and postdredging (1985) levels of development. The following sections define the bottom configurations, boundary conditions, and initial conditions used in each application.

Bottom Configurations

The bay shorelines and areas of bottom changes for 1880, 1972, and 1985 are shown in figures 3 and 4. In 1880, the bottom configuration was characterized by gradually varying depths in most parts of the bay. Notable exceptions occur at the northern end of Egmont Key and at the mouth of Old Tampa Bay. Several islands existed near the mouth of Tampa Bay and at other locations around the bay periphery. The 1972 bottom configuration was characterized by broad areas of slowly changing depths interrupted by extensive manmade linear features, channels and islands, aligned perpendicular and parallel to the major axis of the bay. In 1985, the bottom will have additional physical changes that will include large disposal islands in Hillsborough Bay and more extensive submerged mounds along a deepened and widened ship channel.

Boundary Conditions

Of the three types of tides that occur in Tampa Bay—diurnal, semidiurnal, and mixed (fig. 2)—the most prevalent is the mixed tide that has two unequal high tides and two unequal low tides during each cycle. Therefore, a mixed tide was chosen as the open-water boundary condition for model application. A mixed tide similar to that measured during the second verification period (fig. 11) was used as the repeating tide (fig. 22). To simplify analysis of results, the tidal period was adjusted to 24 hours (an even multiple of the time step), and small irregularities in the second verification tide were eliminated by assuring smooth first and second differences in tidal stage (table 9).

Because it was considered least likely to mask tidal flow, circulation, and flushing changes, a zero wind condition was used for all model applications. Changes in flow, circulation, and flushing due to wind were beyond the scope of this investigation.

Freshwater river inflow was held constant for each model application at the average annual discharges listed in table 3. Cooling water used by power-generating stations was treated as described under model development for 1972 and 1985 levels of development (p. 17). There were no power-generating stations on Tampa Bay in 1880.

Initial Conditions

Tidal currents throughout the modeled area were assumed to be zero at the start of each model application. Tidal stage throughout the modeled area was initially constant at the National Geodetic Vertical Datum of 1929.

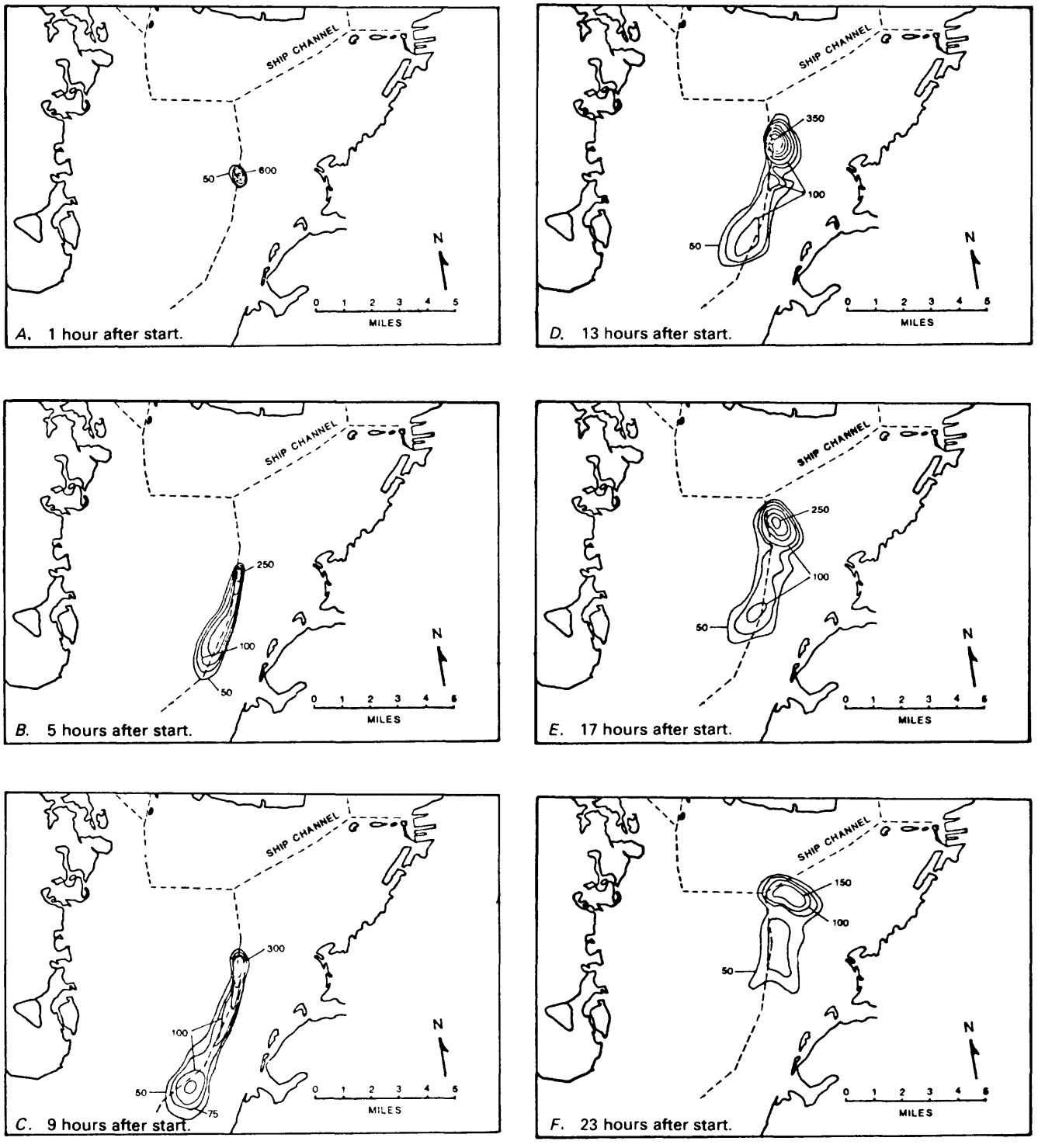

EXPLANATION

—*100*— Contours show lines of equal computed concentration of suspended solids, in milligrams per liter, with a simulated injection rate of 15 cubic feet of suspendable material per second (Gren, 1976). Contour interval 50 mg/L, with 75-mg/L contour added for clarity

Figure 21. Shape of simulated turbidity plume at selected times following start of turbidity generation.

Table 9. Stage, first difference, and second difference of repeating, 24-hour tide in Tampa Bay used as boundary condition for model application

[Stage values relative to National Geodetic Vertical Datum of 1929]

Time	Stage (feet)	First difference (feet)	Second difference (feet)	Time	Stage (feet)	First difference (feet)	Second difference (feet)
0000	0.00	0.23	−0.02	1200	1.67	0.13	−0.03
0030	.21	.21	− .03	1230	1.77	.10	− .03
0100	.39	.18	− .03	1300	1.84	.07	− .03
0130	.54	.15	− .03	1330	1.88	.04	− .05
0200	.66	.12	− .04	1400	1.87	− .01	− .08
0230	.74	.08	− .05	1430	1.78	− .09	− .08
0300	.77	.03	− .08	1500	1.61	− .17	− .08
0330	.72	− .05	− .05	1530	1.36	− .25	− .05
0400	.62	− .10	− .03	1600	1.06	− .30	− .03
0430	.49	− .13	.00	1630	.73	− .33	− .02
0500	.36	− .13	.03	1700	.38	− .35	− .02
0530	.26	− .10	.03	1730	.01	− .37	.00
0600	.19	− .07	.03	1800	− .36	− .37	.03
0630	.15	− .04	.04	1830	− .70	− .34	.06
0700	.15	.00	.05	1900	− .98	− .28	.07
0730	.20	.05	.04	1930	−1.19	− .21	.07
0800	.29	.09	.04	2000	−1.33	− .14	.08
0830	.42	.13	.03	2030	−1.39	− .06	.09
0900	.58	.16	.03	2100	−1.36	.03	.10
0930	.77	.19	.02	2130	−1.23	.13	.08
1000	.98	.21	0	2200	−1.02	.21	.06
1030	1.19	.21	− .02	2230	− .75	.27	.00
1100	1.38	.19	− .03	2300	− .48	.27	− .02
1130	1.54	.16	− .03	2330	− .23	.25	− .02

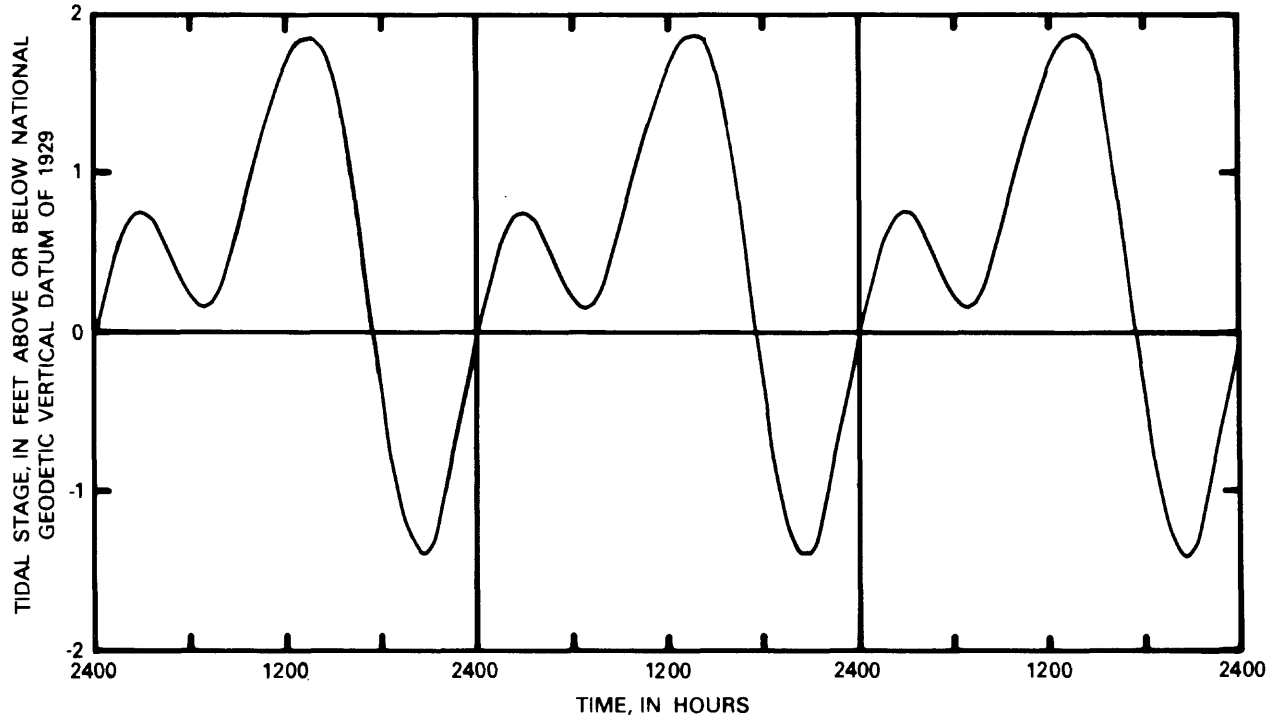

Figure 22. Repeating, 24-hour tide used as boundary condition for model application.

To help determine changes in the flushing rate of Tampa Bay between 1880, 1972, and 1985, a representative constituent distribution, measured during July 1975 and reported by Goetz and Goodwin (1980), was used. The distribution analysis (fig. 23) indicated that a primary source of phosphorus existed along the eastern shore of Hillsborough Bay in the vicinity of the Alafia River. Concentrations ranged from 1.5 to 2.5 mg/L in Hillsborough Bay, were nearly constant at 0.8 mg/L in Old Tampa Bay, and decreased to less than 0.2 mg/L at the entrance to Tampa Bay. Phosphorus concentrations throughout Tampa Bay were 10 to 100 times greater than that hypothesized as needed to maintain primary productivity (photosynthesis) in this area of Florida (U.S. Department of the Interior, 1969, p. 24). At these elevated concentrations, phosphorus is a conservative (nonreactive) substance and is useful as a tracer.

MODEL RESULTS AND ANALYSIS

The results of model computations presented in this section are largely dependent on using vector maps that visually represent water and constituent movement computed at each cell of the model. Vector transport symbols (representing the directional flux of material, either water or constituent passing through each model cell) are used for presentation and analysis of computed results. The flux of water, in cubic feet per second, is described in this report by the specific terms ebb, flood, and residual water transport. The flux of constituent, in pounds per second or pounds per day, is described in this report by the specific terms ebb, flood, and residual constituent transport.

Analysis of methods to discern differences in tidal flow, circulation, and flushing among the 1880, 1972, and 1985 levels of development is dependent on some concepts of vector arithmetic. The methods used are described in some detail in the following section.

Methods

Vector Computations

Addition and subtraction of vectors (fig. 24) are basic computations used to present and analyze flow, circulation, and flushing patterns. Figure 24*A* shows two directional-line segments, $\overline{A}$ and $\overline{B}$, that represent the magnitude (proportional to the line length) and direction of two vector quantities, such as water or constituent transport. Vector addition (fig. 24*B*) results in a third vector ($\overline{A} + \overline{B}$) defined by a line from the starting point of $\overline{A}$ to the ending point of $\overline{B}$. Vector subtraction (fig. 24*C*) also results in a third vector ($\overline{A} - \overline{B}$) defined by a line from the starting point of $\overline{A}$ to the ending point of $-\overline{B}$. Note that $-\overline{B}$ is the same magnitude but of opposite direction to $\overline{B}$.

Water and constituent transport during flood and ebb conditions at each cell in the model are computed as the average of six vectors at 5-minute intervals, as shown in figure 25*A*. Averaging avoided overemphasis of possible short-term, local oscillations. The direction of the summation vector defines the direction of the average vector. The magnitude of the average vector is one-sixth the summation vector.

Water circulation and constituent flushing patterns are composed of computed residual-transport vectors at each cell. The computation is shown schematically in figure 25*B*. For a repeating, 24-hour tide, such as given in figure 22, the summation of 288 5-minute transport vectors is actually computed at each grid location. Twenty-four 1-hour transport vectors are shown here for clarity. The lack of closure between the starting point of vector 1 and the ending point of vector 24 indicates a net or residual transport equal to the summation vector at that location. Magnitudes of residual-transport vectors are generally one to two orders of magnitude less than those of typical flood- or ebb-transport vectors at any location.

Transport-Change Maps

Transport-change maps are designed to answer the following questions: (1) How much and what parts of Tampa Bay have undergone significant transport changes between 1880 and 1972? and (2) How do these changes compare with those expected between 1972 and 1985? The symbol plotted at each cell location on a transport-change map represents a difference range (in percent) between transport vectors computed for two levels of development.

Percentage differences at each cell are computed as 100 times the magnitude of the difference vector ($\overline{A} - \overline{B}$) in figure 24*C*, divided by the magnitude of the vector associated with the earlier level of development ($\overline{B}$), or

$$\frac{|\overline{A} - \overline{B}|}{|\overline{B}|} \times 100 = \text{percent change in transport} \quad (18)$$

This technique recognizes that changes in transport direction are often as important as changes in transport magnitude. Directionality is inherently incorporated into the computation so the percentage change need not be associated with a positive or negative concept of directionality.

Longitudinal Summary

A longitudinal summary technique was developed to further evaluate the effect of changes indicated by the transport-change maps and to answer the following questions: (1) Has dredge-and-fill construction (channels, islands, causeways, and so forth) caused significant

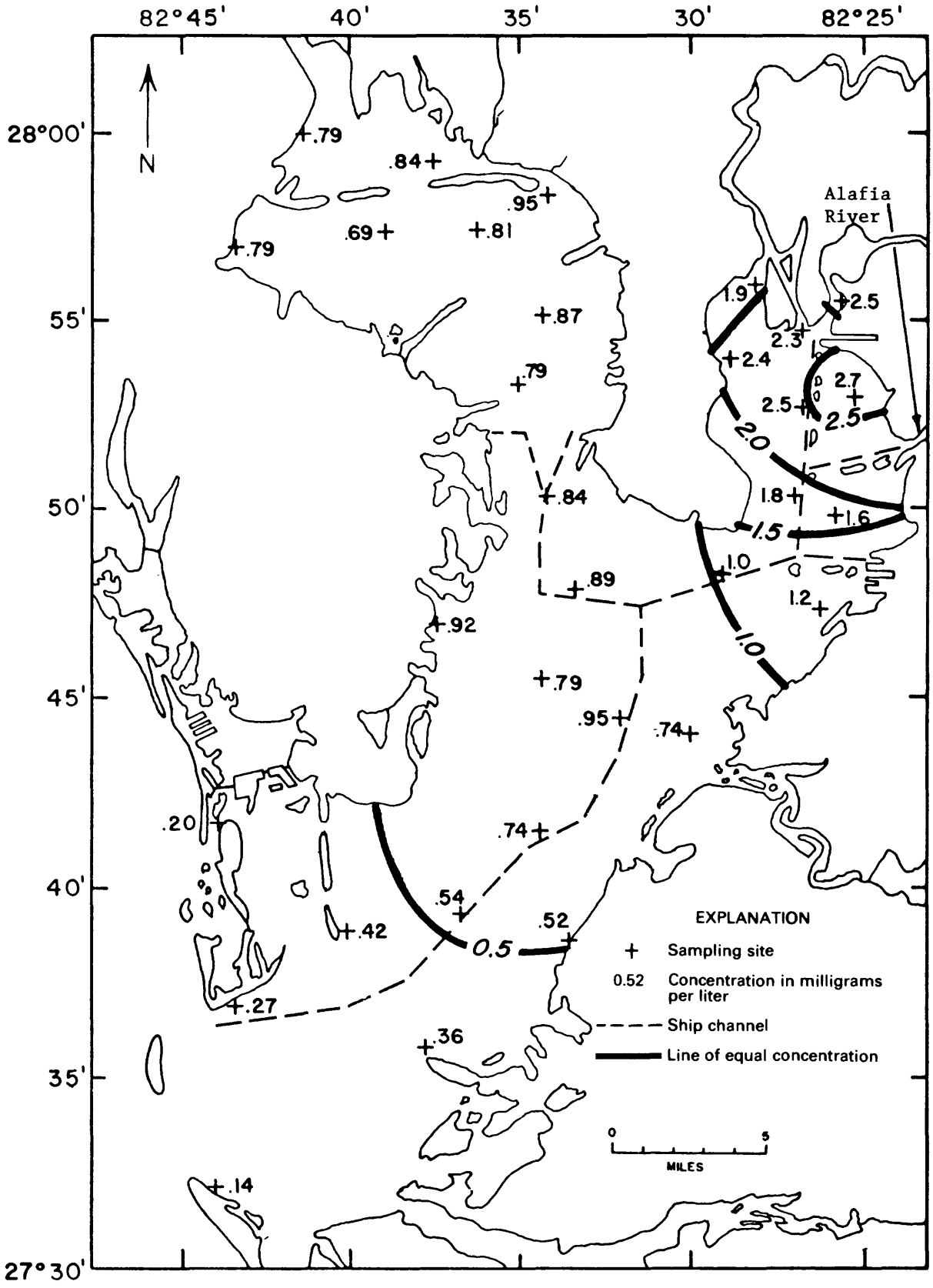

Figure 23. Phosphorus distribution in Tampa Bay, July 1975 (from Goetz and Goodwin, 1980).

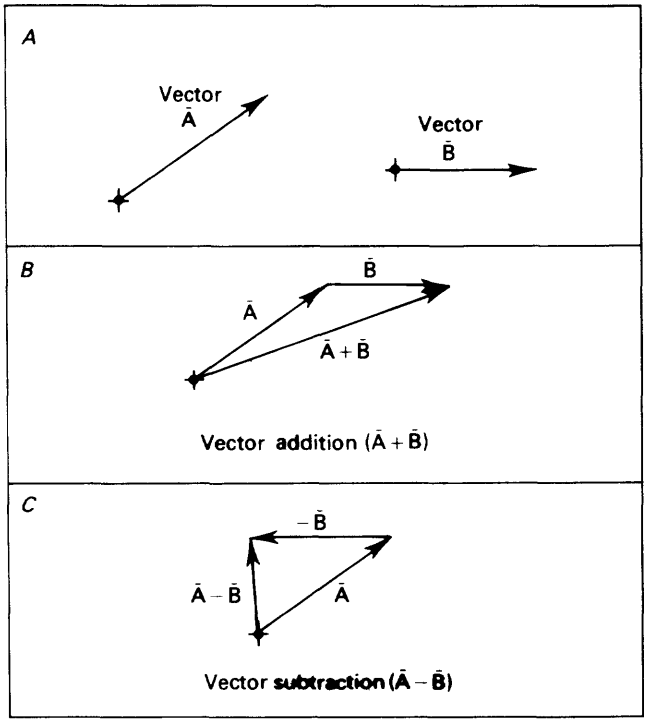

Figure 24. Computations for vector addition and subtraction. $\bar{A}$ and $\bar{B}$ represent the magnitude and direction of two vector quantities, such as water or constituent transport.

changes to the overall circulation and flushing characteristics of the bay? and (2) How large are the changes in various parts of the bay?

The technique summarizes computed transport along a series of cross sections within the bay. Each cross section extends from bank to bank and is approximately perpendicular to the predominant direction of tidal flow. The series of cross sections extends from the model boundary in the Gulf of Mexico to the head of Hillsborough and Old Tampa Bays along the longitudinal summary lines shown in figure 26. Information extracted from the model for each level of development for each cross section includes:

1. water and constituent transport during a typical floodtide,
2. water and constituent transport during a typical ebbtide,
3. landward-flowing residual water transport (defined as tide-induced circulation for purposes of this report),
4. net residual constituent transport (defined as total constituent flushing due to tide and streamflow effects), and
5. total mass of water and constituent landward of each cross section.

Items 1 and 2 are computed by summing the appropriate vector components normal to a cross section. Item 3 is computed by summing all landward-flowing, residual, water-transport vector components normal to a cross section. Gulfward-flowing vectors are disregarded. Item 4 is computed by summing all residual, constituent-transport vector components, both landward- and gulfward-flowing, normal to a cross section. Item 5 is self-explanatory.

Water Transport

Water transport is computed at water-depth locations of the finite-difference scheme (fig. 5) by using the cell dimension (1,500 ft), the depth value, and the four velocity and four water-level values on the sides and corners of the surrounding square. Transport, rather than velocity, was chosen as the unit to represent flow and circulation results in this study to avoid potentially misleading visual portrayals. The length of a transport vector is directly related to the quantity of water being moved, whereas large velocity vectors can be associated with little water transport.

Flood and Ebb Water Transport

Typical water-transport patterns during floodflow for 1880, 1972, and 1985 levels of development are shown in figures 27, 28, and 29, respectively. The transport-vector maps show many similarities, including flow concentrations at the mouth of Tampa Bay and Old Tampa Bay. Each map also confirms that regions of high transport are generally coincidental with deep, fast-flowing areas of the bay and that low transport regions are coincidental with shallow areas. For areas of similar depth, transport magnitudes generally decrease with distance from the Gulf of Mexico.

The magnitudes and directions of flood-transport vectors at 25 selected sites are listed in table 10. Locations of the sites are shown in figure 27, and reference dots are given in figures 28 and 29. From 1880 to 1985 levels of development, vector magnitudes were computed to decrease from about 105,000 ft^3/s to 97,000 ft^3/s at the mouth of Tampa Bay (site 1), from 37,000 ft^3/s to 29,000 ft^3/s in mid-Tampa Bay (site 9), from 7,000 ft^3/s to 4,000 ft^3/s in Old Tampa Bay (site 25), and from 2,000 ft^3/s to 1,000 ft^3/s in Hillsborough Bay (site 18).

At some sites, significant computed increases in transport magnitude or changes in direction among 1880, 1972, and 1985 levels of development are evident, such as at sites 5, 6, 16, 19, 20, and 22. Most sites, however, show little change in either magnitude or direction of flood-transport vectors.

Typical water-transport patterns during ebbflow for 1880, 1972, and 1985 levels of development are shown in figures 30, 31, and 32, respectively. Overall ebb-transport patterns, although opposite in direction, are similar to flood-transport patterns shown in figures 27, 28, and 29. Flow concentrations occur in the same general areas, and transport magnitudes are greatest near the mouth and least near the head of the bay.

One difference between flood and ebb transport is that maximum ebb transport is substantially greater than maximum flood transport throughout the bay. This difference

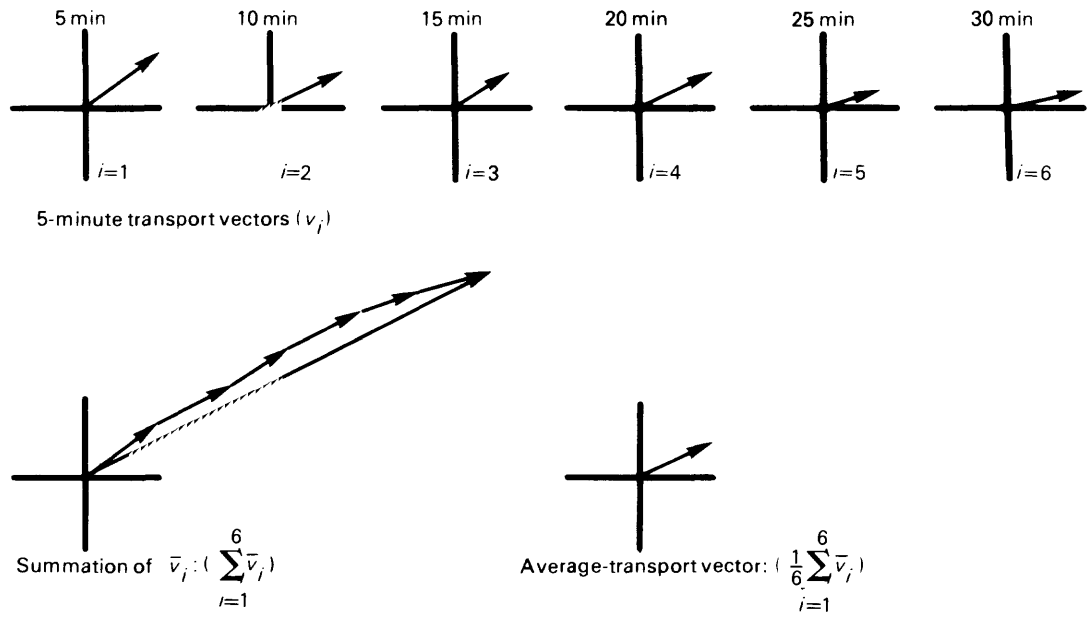

A. Computation for average transport vector for flood or ebb conditions.

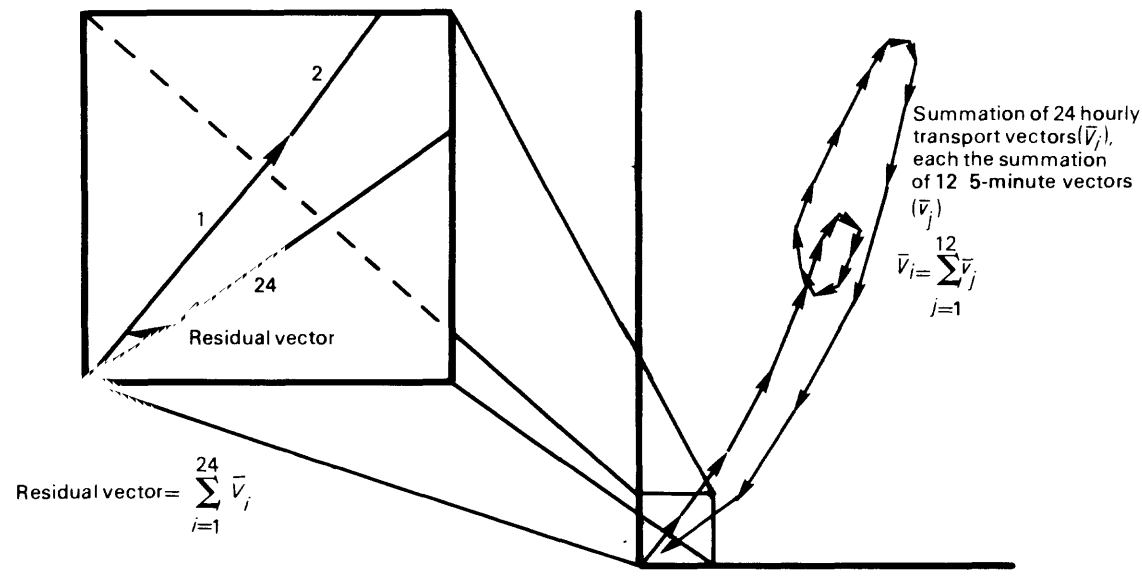

B. Computation for 24-hour residual-transport vector.

Figure 25. Computations for average flood- or ebb-transport vector and for residual-transport vector.

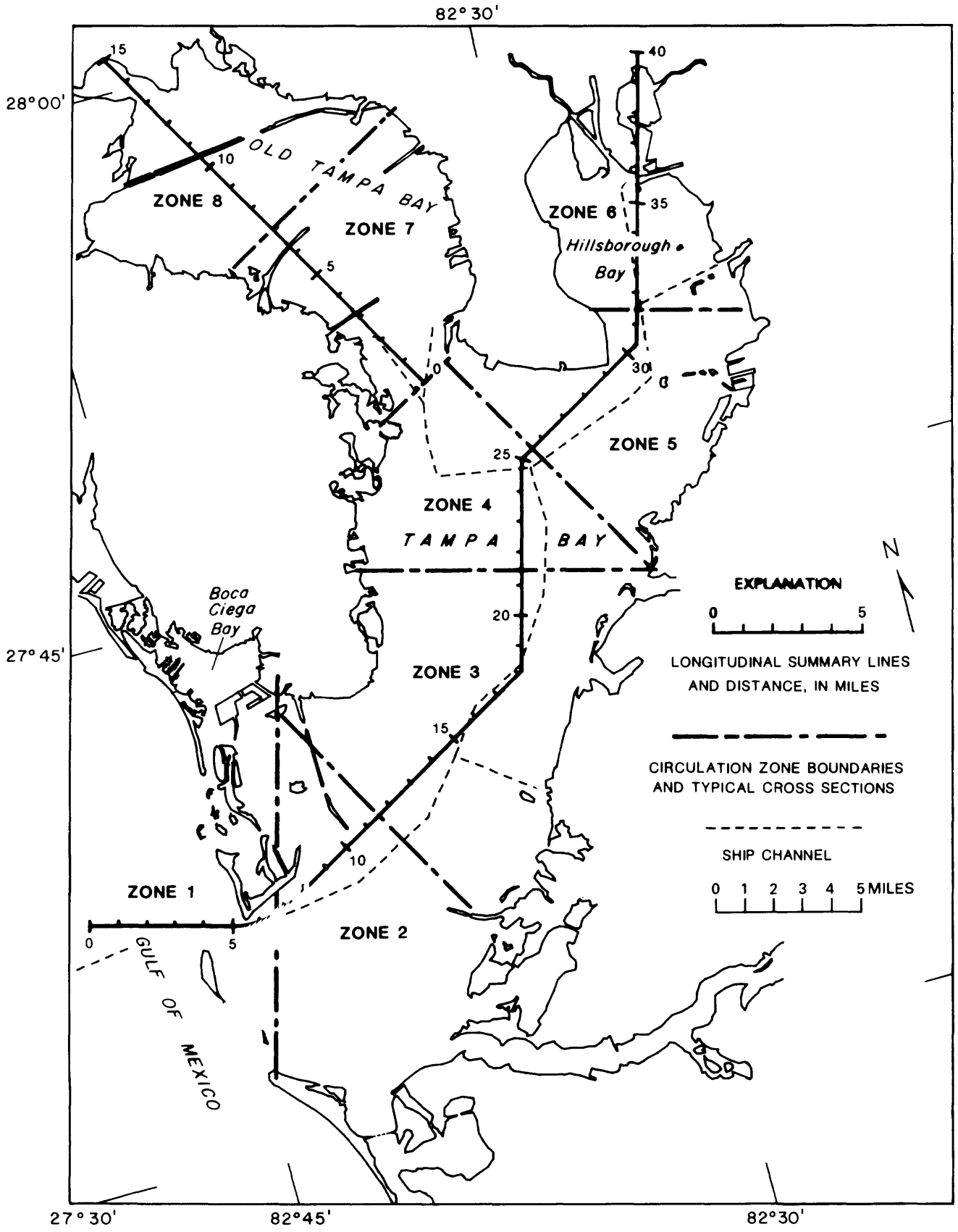

Figure 26. Longitudinal summary lines and circulation zones of Tampa Bay.

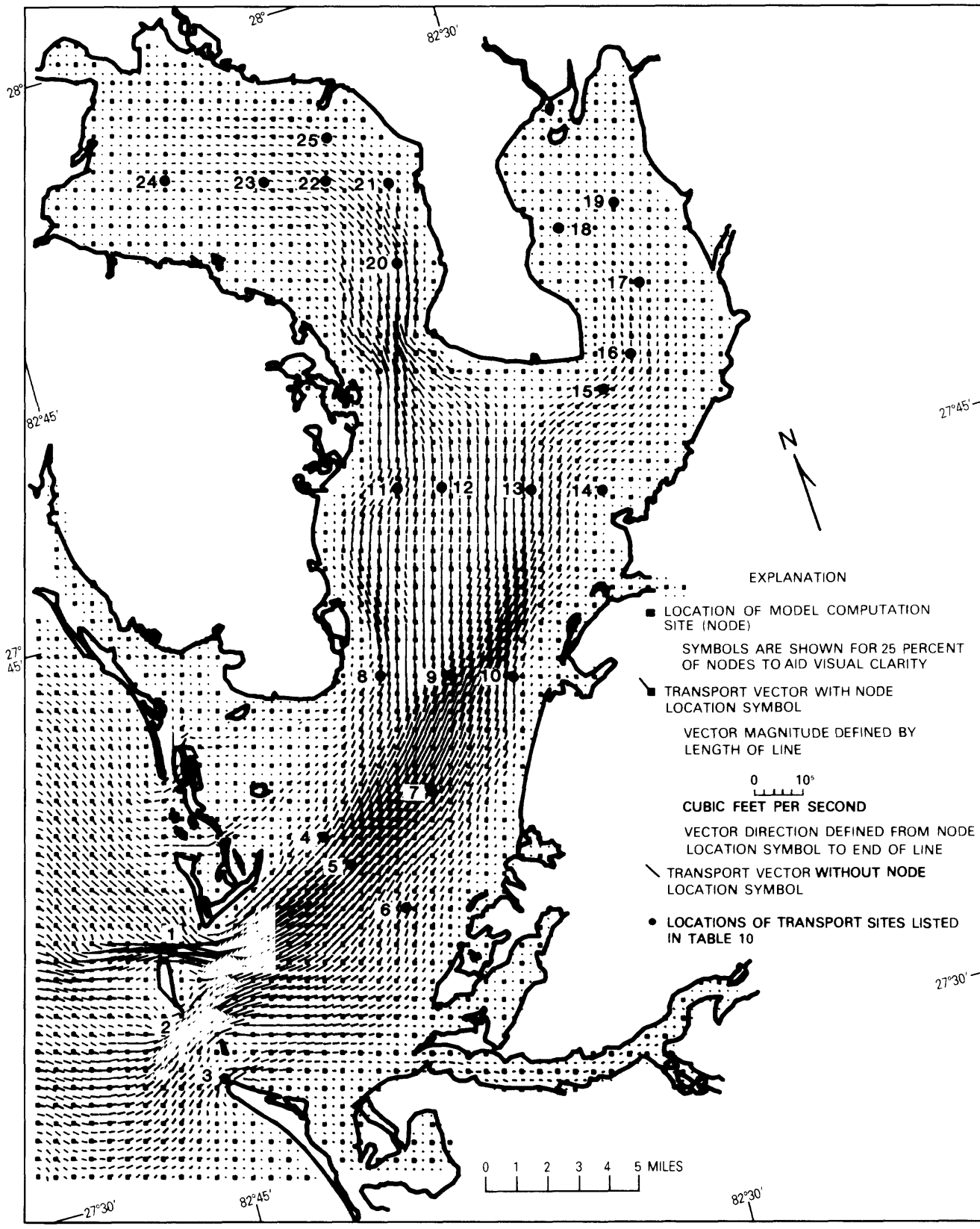

Figure 27. Water-transport pattern during typical floodtide in Tampa Bay for 1880 level of development. Numbers refer to sites listed in tables 10, 11, 13, 15, 16, and 18.

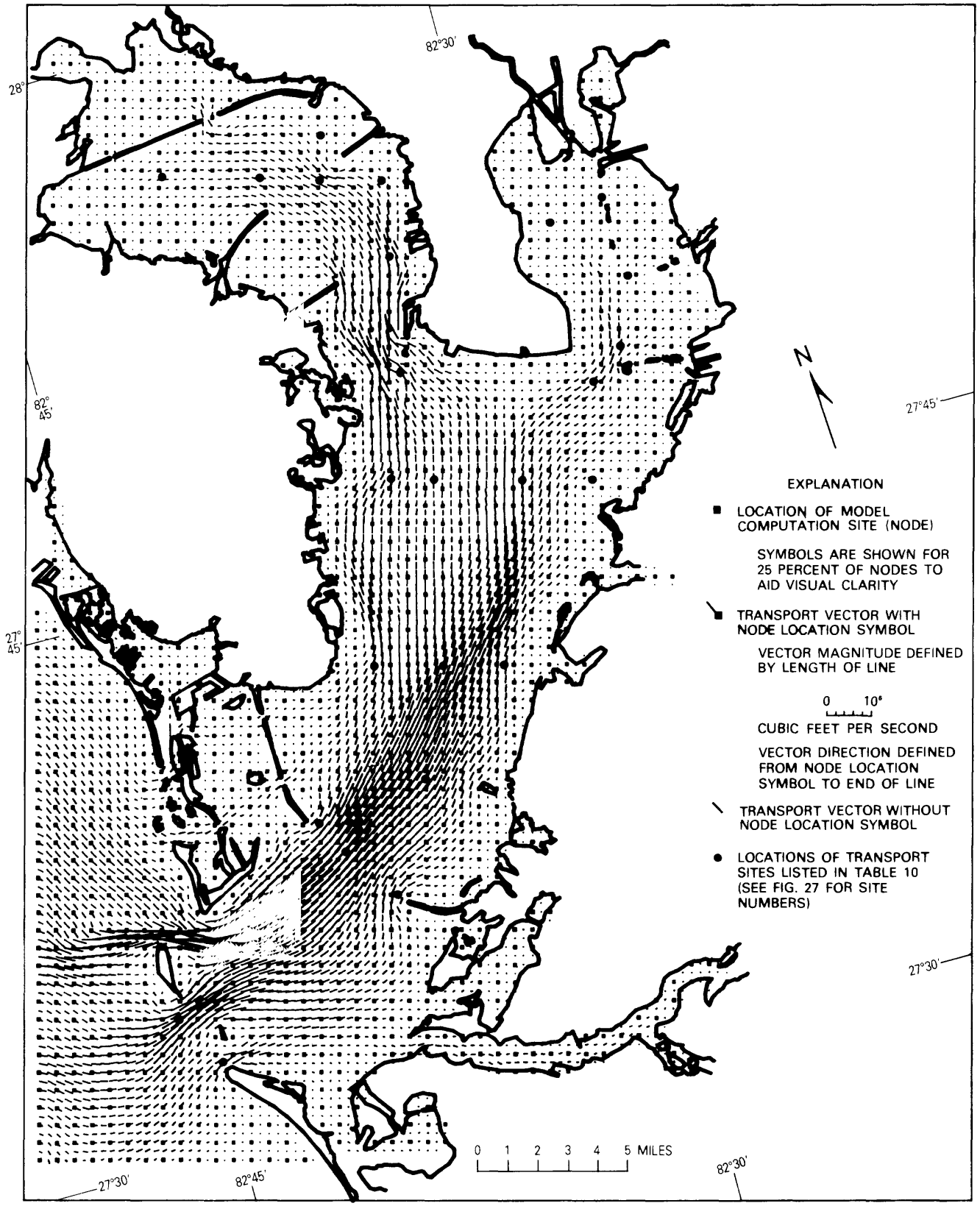

Figure 28. Water-transport pattern during typical floodtide in Tampa Bay for 1972 level of development.

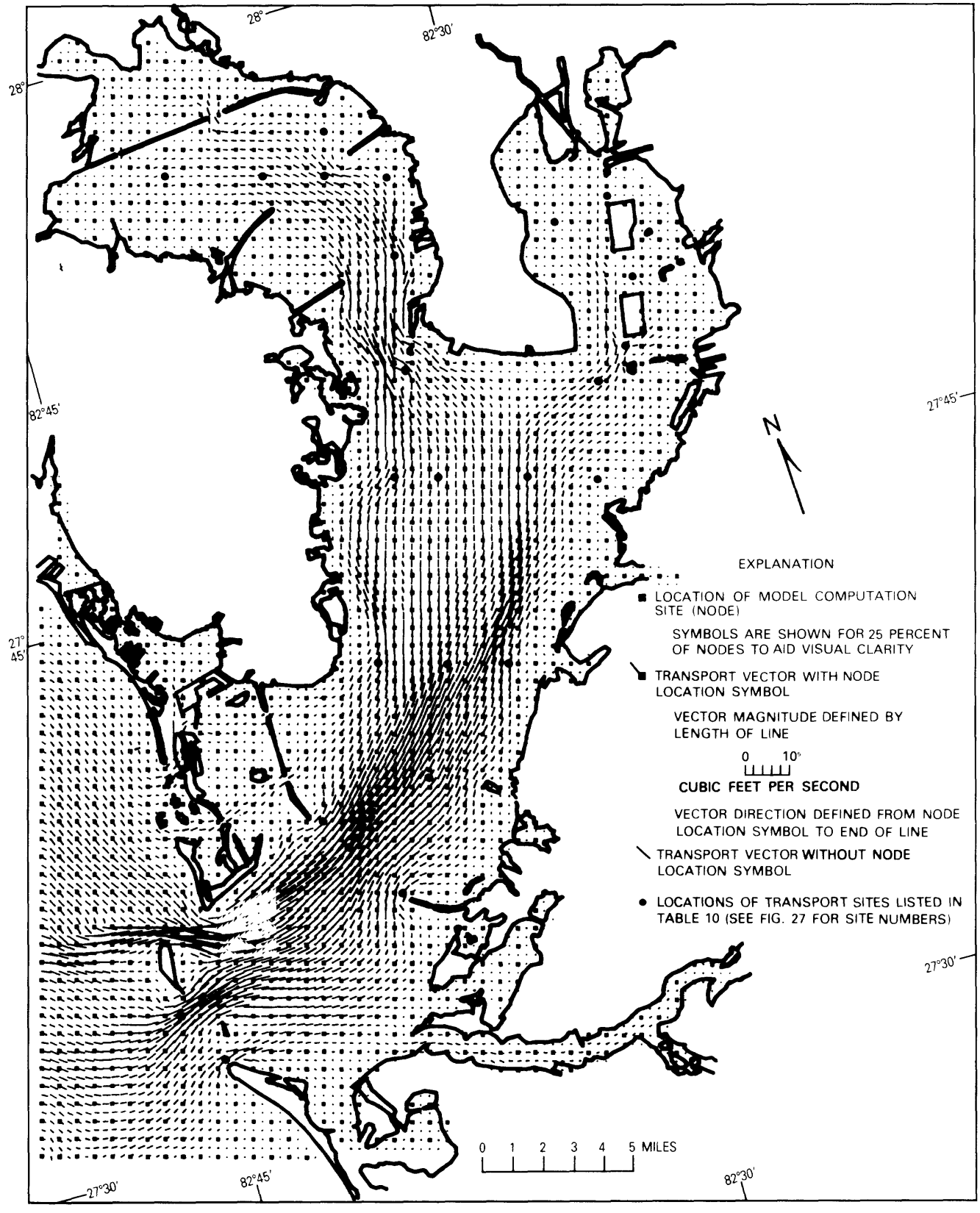

Figure 29. Water-transport pattern during typical floodtide in Tampa Bay for 1985 level of development.

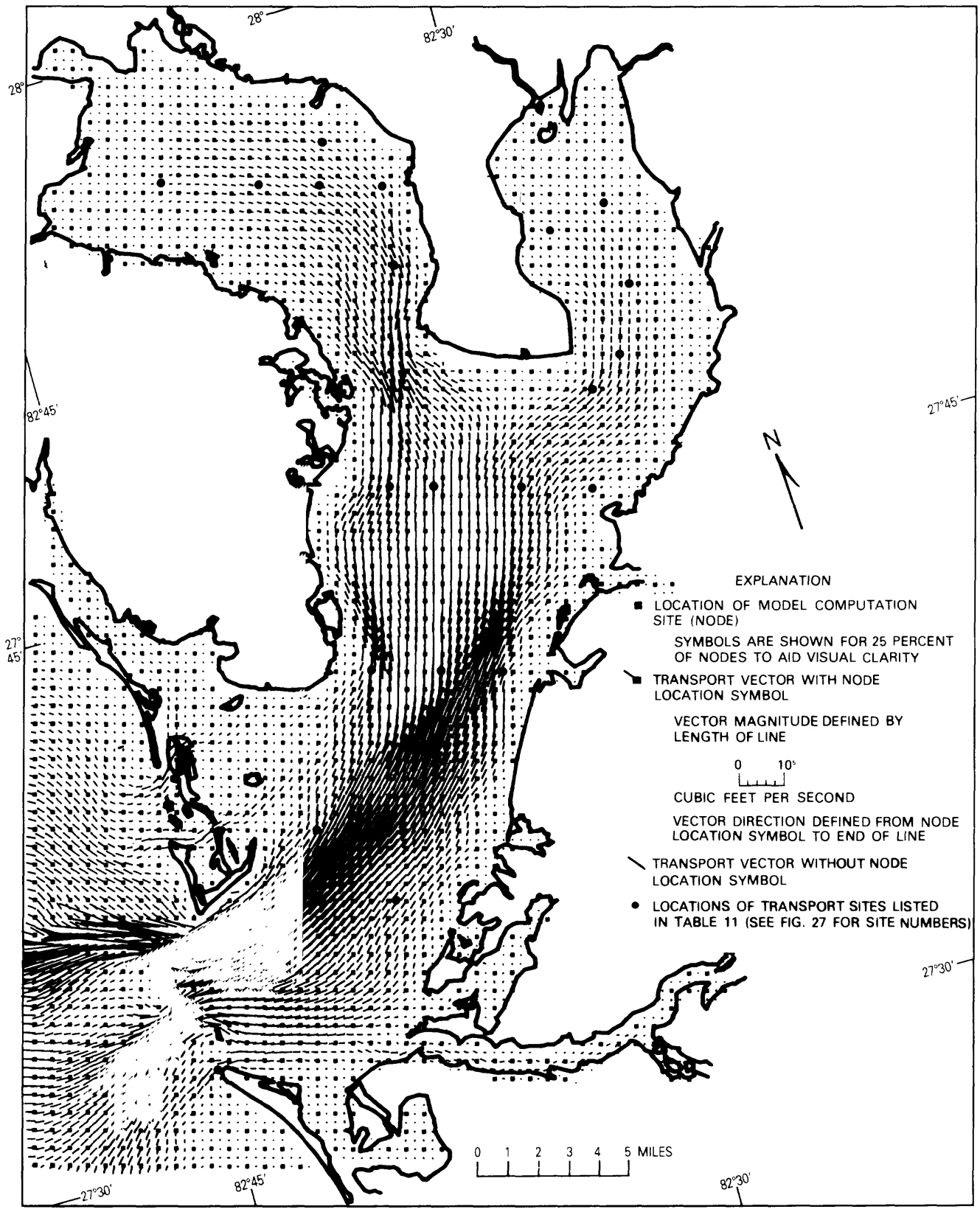

Figure 30. Water-transport pattern during typical ebbtide in Tampa Bay for 1880 level of development.

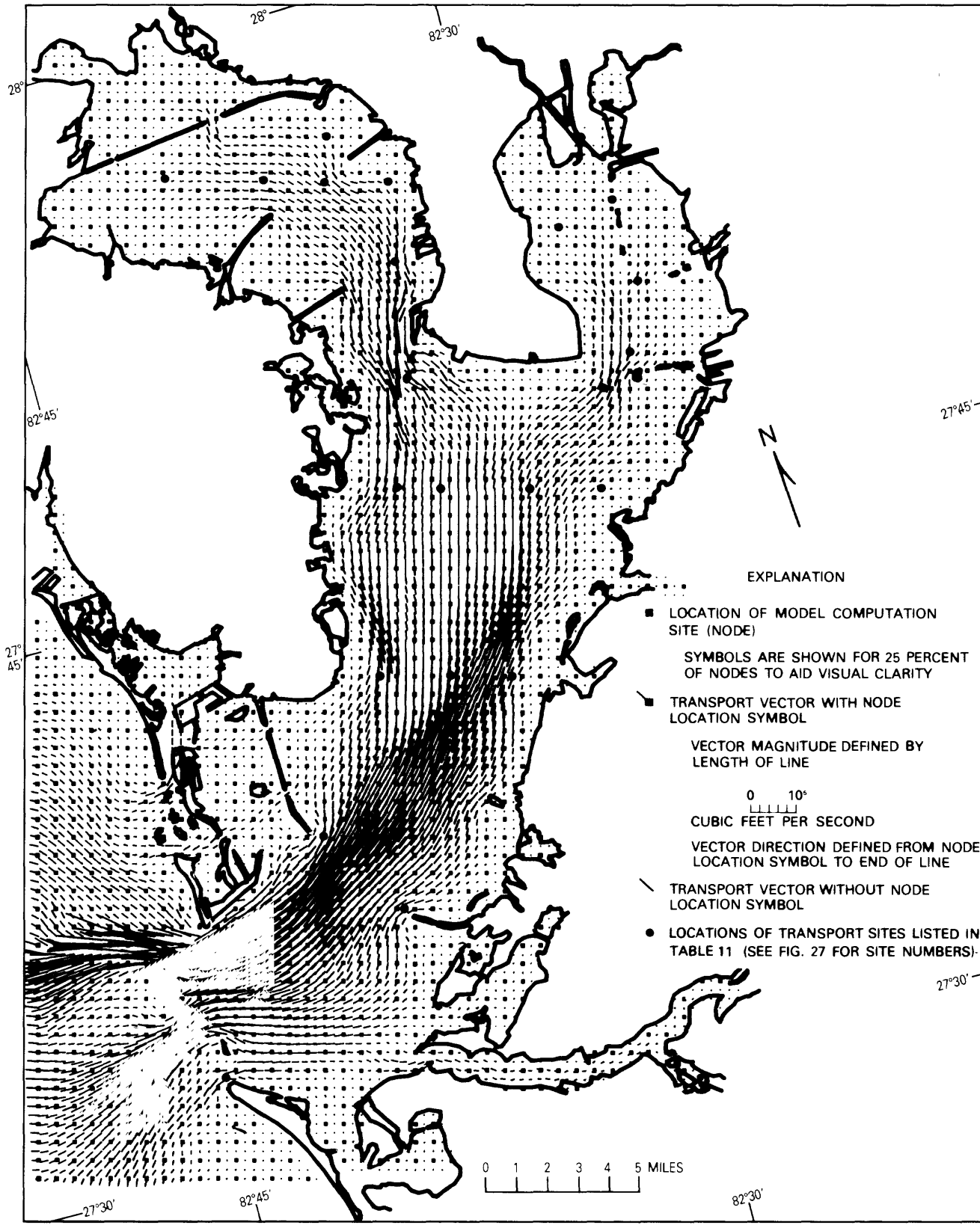

Figure 31. Water-transport pattern during typical ebbtide in Tampa Bay for 1972 level of development.

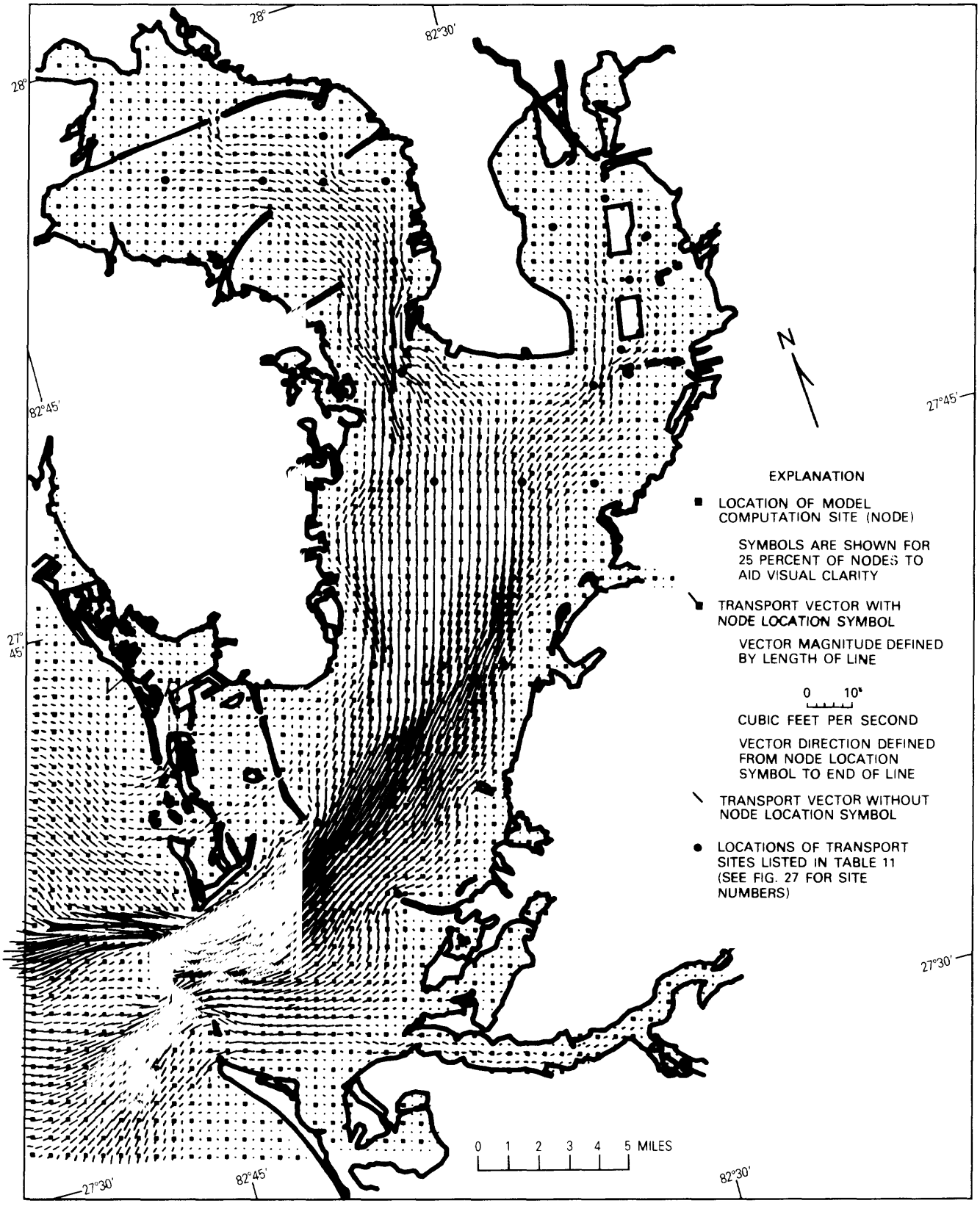

Figure 32. Water-transport pattern during typical ebbtide in Tampa Bay for 1985 level of development.

Table 10. Water transport and direction during typical floodtide at selected sites in Tampa Bay for 1880, 1972, and 1985 levels of development

Site no. (see fig. 27)	Transport (thousands of cubic feet per second)			Direction (degrees, clockwise from north)		
	1880	1972	1985	1880	1972	1985
1	105	101	97	114	114	115
2	71	68	67	69	69	70
3	36	33	33	65	65	65
4	24	28	28	49	48	47
5	58	63	65	51	48	48
6	14	11	12	45	85	85
7	42	37	22	44	41	42
8	25	24	25	31	32	31
9	37	35	29	28	28	32
10	22	21	22	29	30	31
11	23	20	20	39	38	38
12	15	14	13	16	14	15
13	20	21	23	19	17	15
14	6	5	5	59	59	59
15	15	16	15	62	55	55
16	10	17	16	24	39	54
17	6	6	4	6	31	355
18	2	1	1	337	346	349
19	4	1	2	348	348	31
20	26	31	30	359	356	356
21	8	6	6	348	337	337
22	14	19	19	313	316	316
23	7	10	10	298	285	285
24	2	4	4	251	280	280
25	7	4	4	305	348	348

is caused by the faster rate of water-level change for falling tide than for rising tide during the simulation (fig. 22). The faster rate is balanced by a shorter time of ebb-flow duration. Ebb-transport magnitudes and directions for 25 selected sites are given in table 11. From 1880 to 1985 levels of development, ebb-transport magnitudes were computed to decrease from 239,000 ft^3/s to about 223,000 ft^3/s at the entrance to Tampa Bay (site 1) and from 51,000 ft^3/s to 40,000 ft^3/s in mid-Tampa Bay (site 9). Ebb-transport magnitudes increased from 8,000 ft^3/s to 13,000 ft^3/s in Old Tampa Bay (site 23) and remained constant at 3,000 ft^3/s in Hillsborough Bay (site 18).

The most visible differences between flood- and ebb-transport patterns occur in localized areas that are alternately exposed to and then sheltered from tidal currents due to the presence of islands, causeways, shoals, or points of land. A good example is near the eastern shore of Egmont Key, at the mouth of Tampa Bay (fig. 1), where floodflows produce low transport magnitudes (see fig. 29) and ebbflows produce high transport magnitudes (see fig. 32). The sheltering effect is much more subtle in most other areas, particularly where natural or man-made shoals occur.

Flood and Ebb Water-Transport Differences For 1880, 1972, and 1985

Figure 33 shows computed flood water-transport differences for Tampa Bay between 1880 and 1972. Computed differences between 1972 and 1985 are shown in figure 34. Substantial flood-transport changes are shown in both figures, with more and larger changes indicated between 1880 and 1972 than between 1972 and 1985. The largest changes are the result of (1) shoreline changes in Boca Ciega and Hillsborough Bays (fig. 1), (2) construction of causeways for four major roadways, (3) ship-channel construction, and (4) construction of associated islands and submerged disposal areas. Channel and island construction between 1972 and 1985 has and will cause additional changes in Hillsborough Bay and along the ship channel from mid-Tampa Bay to the Gulf of Mexico.

Areas totaling about 218 mi^2 sustained flood-transport changes of greater than 10 percent between 1880 and

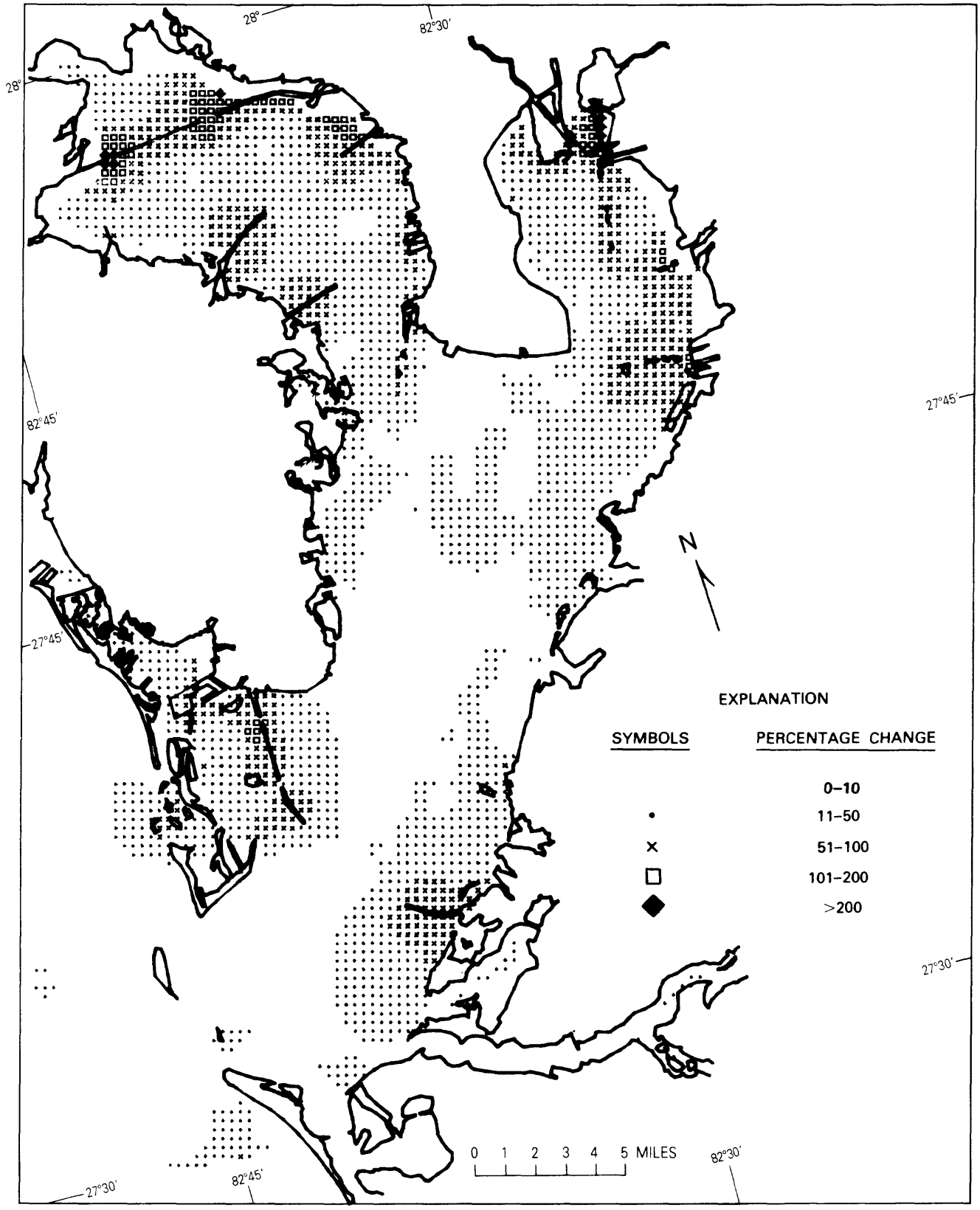

Figure 33. Changes in water transport in Tampa Bay for typical floodtide between 1880 and 1972 levels of development.

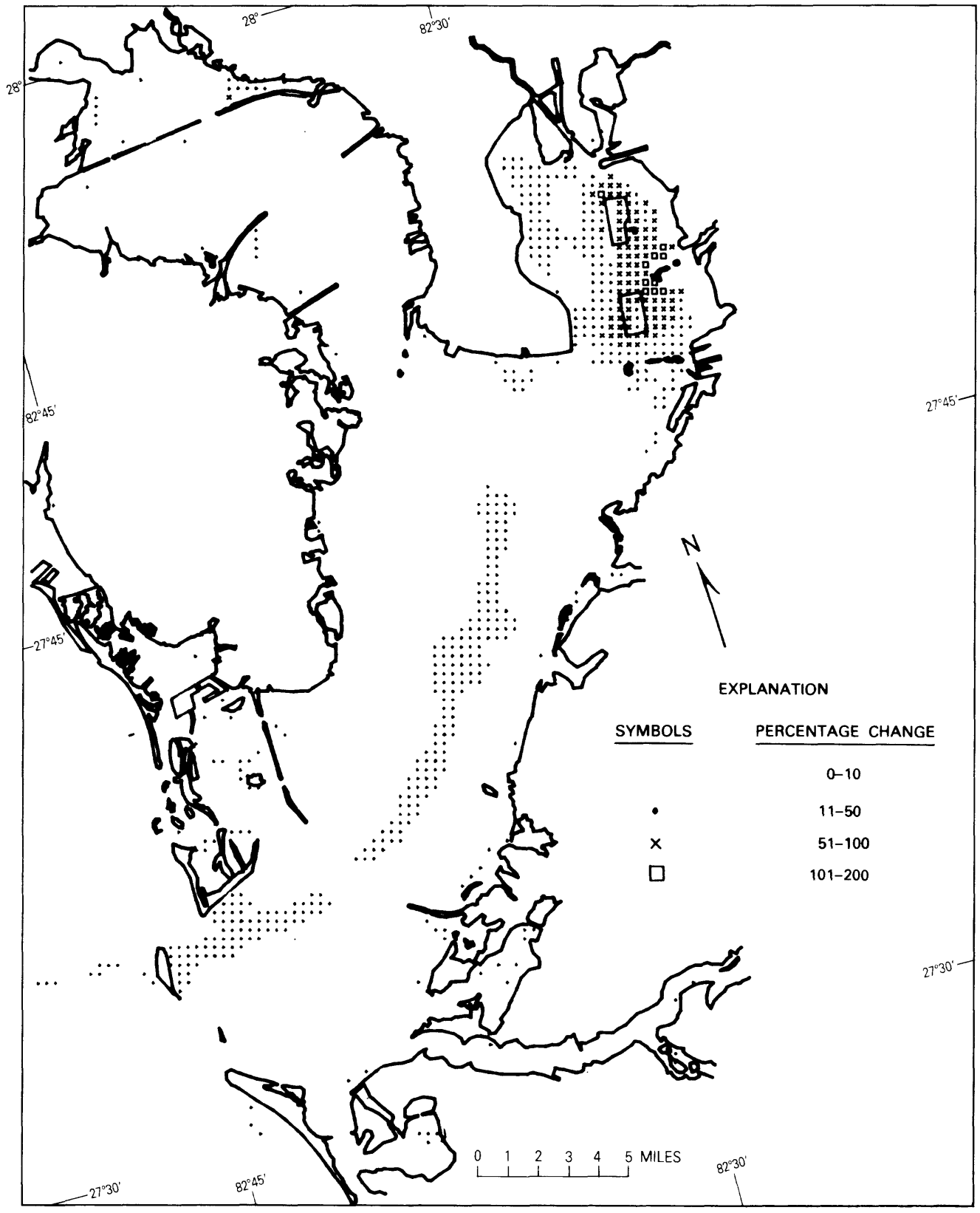

Figure 34. Changes in water transport in Tampa Bay for typical floodtide between 1972 and 1985 levels of development.

Table 11. Water transport and direction during typical ebbtide at selected sites in Tampa Bay for 1880, 1972, and 1985 levels of development

Site no. (see fig. 27)	Transport (thousands of cubic feet per second)			Direction (degrees, clockwise from north)		
	1880	1972	1985	1880	1972	1985
1	239	232	223	290	290	290
2	116	112	113	243	243	244
3	27	26	26	250	250	250
4	40	45	45	224	224	224
5	89	90	104	231	230	232
6	20	21	22	229	266	266
7	66	60	39	225	224	224
8	40	38	40	206	206	206
9	51	49	40	206	207	211
10	29	29	31	213	216	216
11	31	28	27	216	215	215
12	20	19	18	203	204	204
13	24	26	27	207	205	203
14	10	9	9	246	246	246
15	20	26	24	234	228	226
16	14	18	6	201	215	245
17	8	9	6	187	214	198
18	3	3	3	166	167	170
19	5	2	2	172	169	182
20	27	37	36	175	179	179
21	8	6	6	164	143	143
22	12	17	17	137	143	143
23	8	14	13	122	100	100
24	2	5	5	88	135	135
25	7	5	5	129	150	150

1972. Areas totaling about 53 mi² will sustain similar changes between 1972 and 1985. The following table gives a breakdown of percentage changes and size of affected areas. The computation of percentage change at each cell is defined earlier at equation 18.

Water transport, floodtide

Percentage change	Area of change, in square miles	
	1880 to 1972	1972 to 1985
0-10	244	393
11-50	160	40
51-100	51	8
101-200	6	1
>200	1	0

Figure 35 shows computed ebb water-transport differences between 1880 and 1972. Computed differences between 1972 and 1985 are shown in figure 36. Areas of ebb-transport change are substantial and similar to those computed for flood transport (see figs. 33 and 34). The largest changes are closest to channels, islands, causeways, and shoreline fills. Areas totaling about 188 mi² sustained ebb-transport changes of greater than 10 percent between 1880 and 1972. Areas totaling about 46 mi² will sustain similar changes between 1972 and 1985. Percentage changes and size of areas involved are given in the following table:

Water transport, ebbtide

Percentage change	Area of change, in square miles	
	1880 to 1972	1972 to 1985
0-10	274	400
11-50	130	38
51-100	53	7
101-200	5	1
>200	0	0

Figure 37 shows typical floodflow and ebbflow determined for each cross section along longitudinal summary lines (see fig. 26) for 1880, 1972, and 1985 levels of development. Progressive flow reduction throughout the bay over time is a reflection of reduced bay surface area

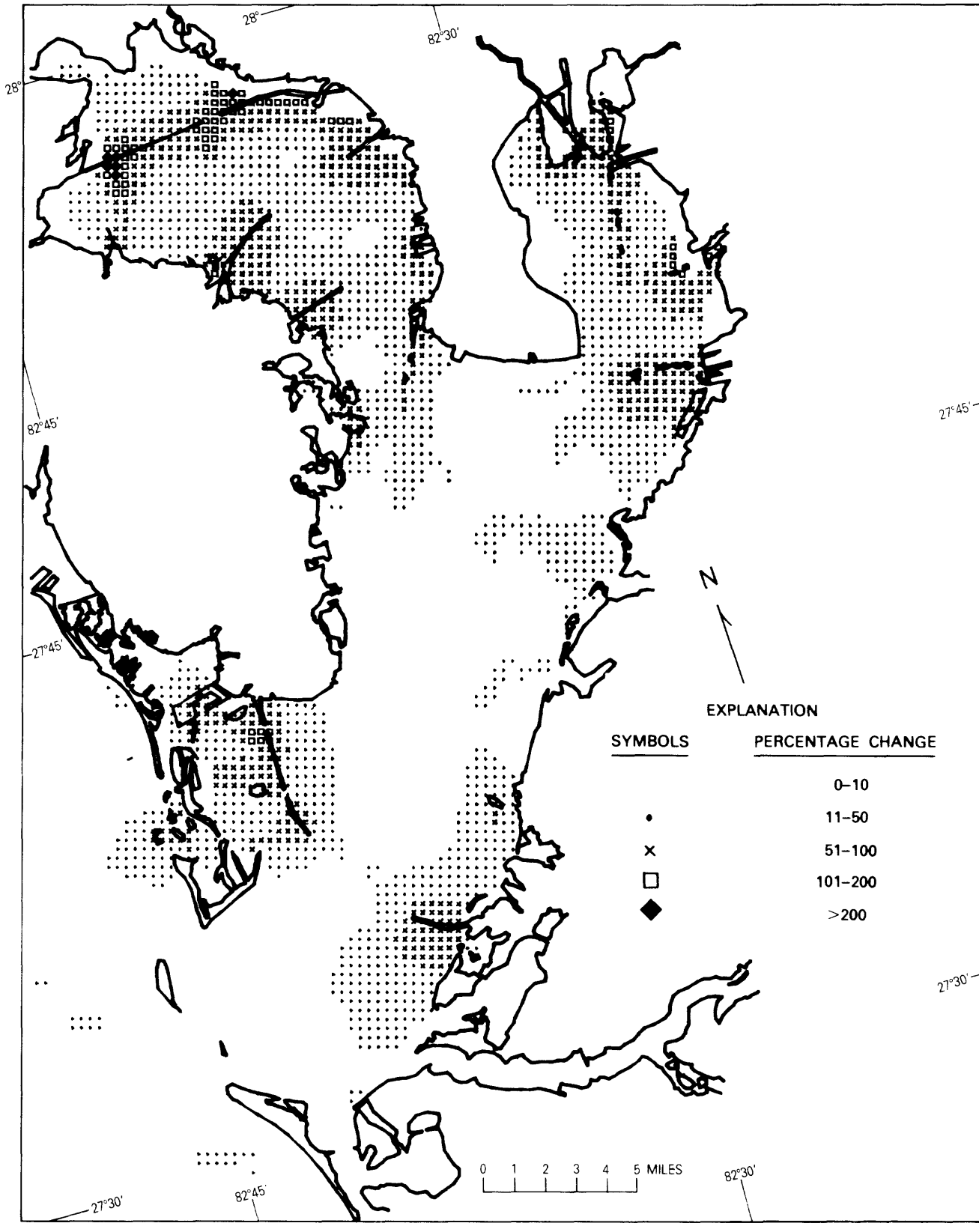

Figure 35. Changes in water transport in Tampa Bay for typical ebbtide between 1880 and 1972 levels of development.

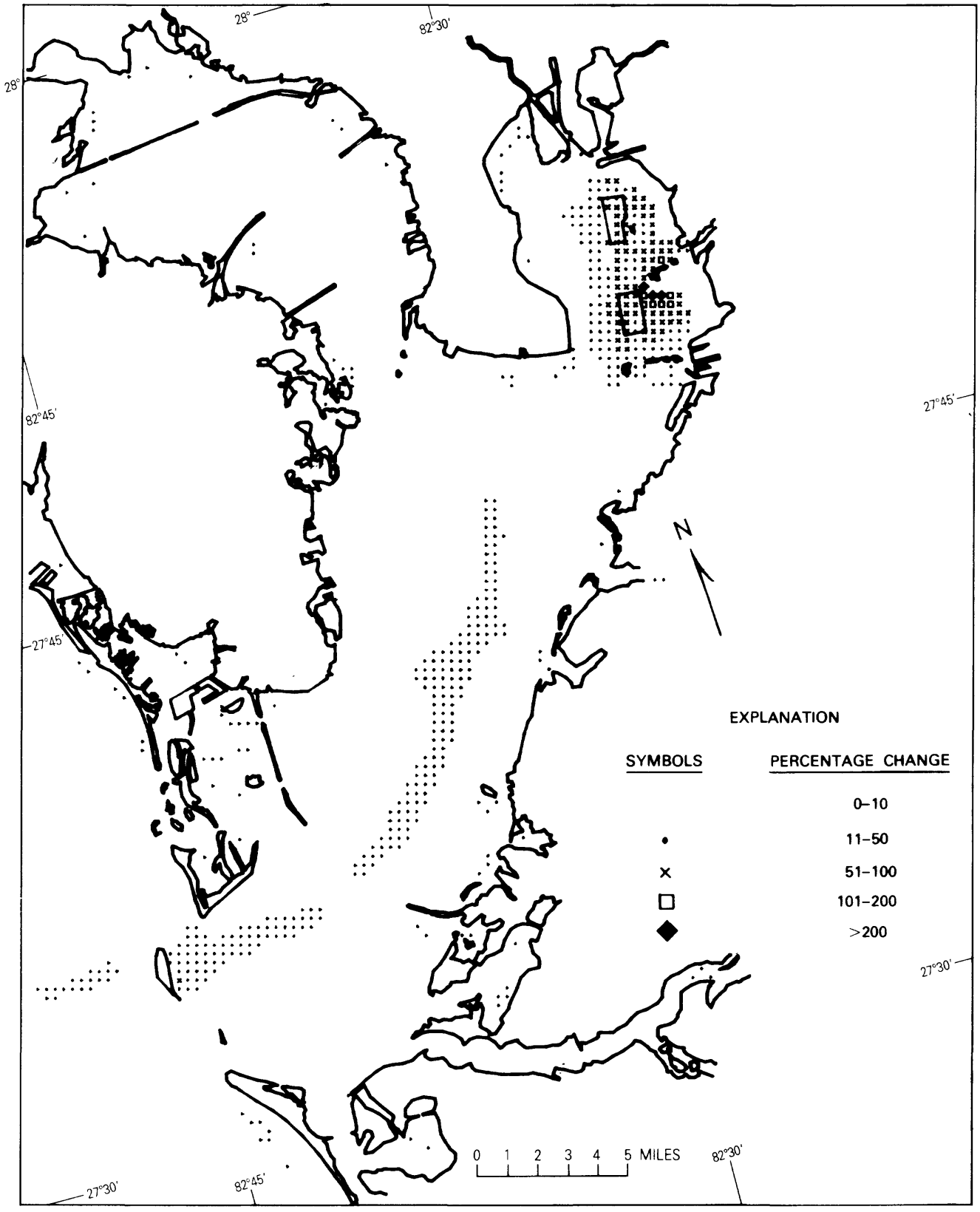

Figure 36. Changes in water transport in Tampa Bay for typical ebbtide between 1972 and 1985 levels of development.

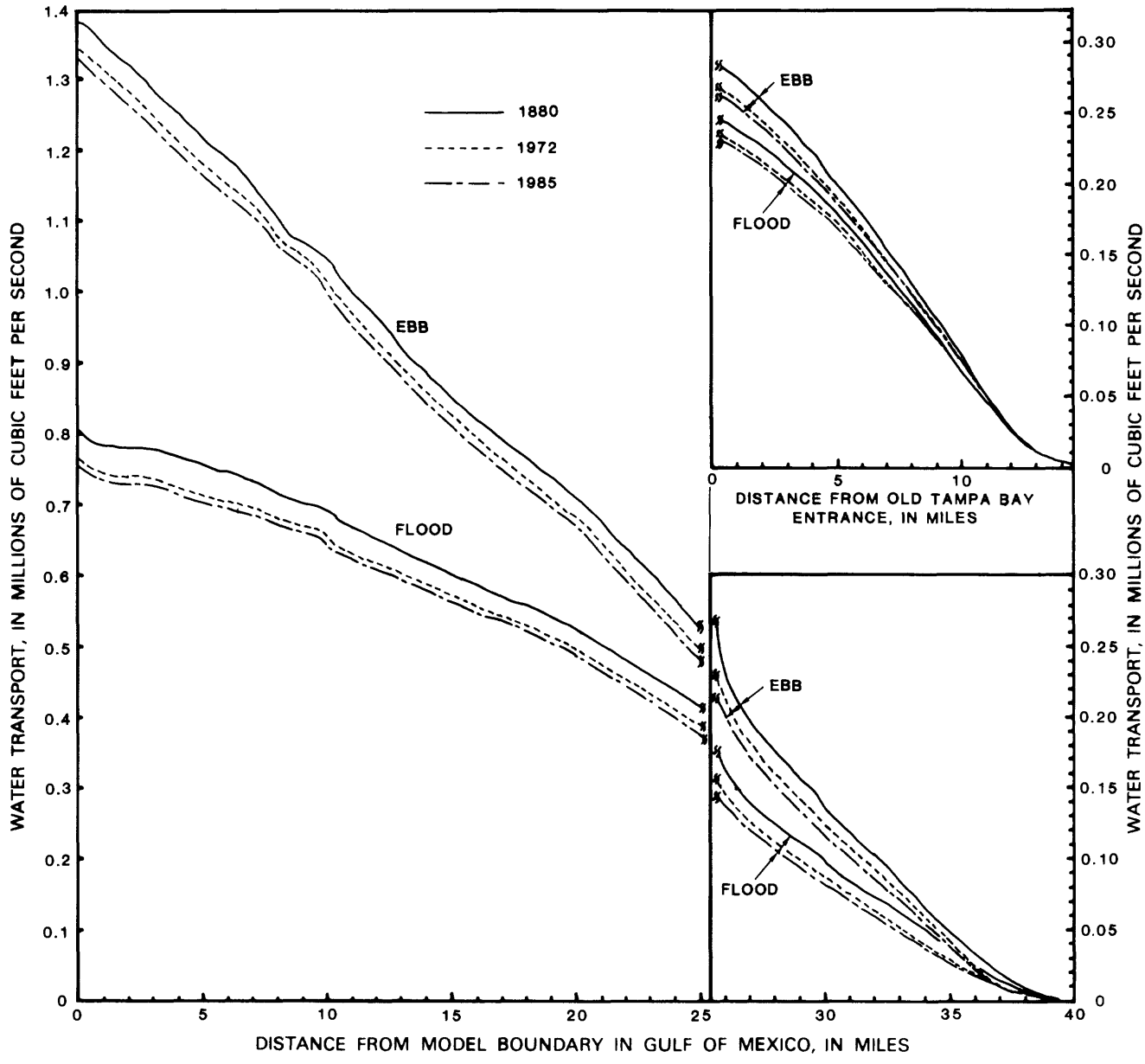

Figure 37. Water transport along longitudinal summary lines (see fig. 26) during typical floodtide and ebbtide in Tampa Bay for 1880, 1972, and 1985 levels of development.

and tidal prism (see table 2). Water-transport and percentage changes among levels of development are given in table 12 for the seaward end of each major bay subarea (see fig. 4). A comparison of table 2 and table 12 shows that the greatest changes in water transport occur between the times and in the areas that have the greatest change in surface area and tidal prism.

Small computed reductions in water transport (table 12) for Old Tampa Bay between 1972 and 1985 were unexpected because no physical changes were anticipated in that part of Tampa Bay. Apparently, a change in the distribution of tidal flow between Hillsborough and Old Tampa Bays, as a result of channel construction between 1972 and 1985, will slightly favor Hillsborough Bay and cause minor flow reductions into and out of Old Tampa Bay.

Residual Water Transport

Figures 38, 39, and 40, show computed residual water-transport (circulation) patterns for 1880, 1972, and 1985 levels of development, respectively. Each vector map shows a series of 20 or more circulatory features or gyres that range in diameter from about 1 to 6 mi. These features define tide-induced water circulation for a mixed tide in the absence of density stratification and wind effects.

Residual transport-vector magnitudes are several times greater near the entrance to Tampa Bay than at most loca-

Table 12. Flood and ebb water transport and percentage changes in Tampa Bay for 1880, 1972, and 1985 levels of development

Area	Water transport (cubic feet per second)			Percentage change		
	1880	1972	1985	1880 to 1972	1972 to 1985	1880 to 1985
During typical floodtide, computed at the seaward end						
Lower Tampa Bay	7.46×10^5	7.09×10^5	7.00×10^5	−5.0	−1.3	− 6.2
Middle Tampa Bay	5.72×10^5	5.45×10^5	5.39×10^5	−4.7	−1.1	− 5.8
Old Tampa Bay	2.43×10^5	2.32×10^5	2.30×10^5	−4.5	− .9	− 5.3
Hillsborough Bay	0.91×10^5	0.83×10^5	0.77×10^5	−8.8	−7.2	−15.4
During typical ebbtide, computed at the seaward end						
Lower Tampa Bay	11.94×10^5	11.55×10^5	11.35×10^5	−3.3	−1.7	− 4.9
Middle Tampa Bay	7.94×10^5	7.66×10^5	7.53×10^5	−3.5	−1.7	− 5.2
Old Tampa Bay	2.78×10^5	2.62×10^5	2.60×10^5	−5.8	− .8	− 6.5
Hillsborough Bay	1.28×10^5	1.18×10^5	1.10×10^5	−7.8	−6.8	−14.1

tions within the bay. At the scale of figures 38–40, circulation patterns near the entrance are not easily discerned. Entrance circulation patterns for 1880, 1972, and 1985 levels of development are very similar because few physical changes have been made in that area; figure 41 shows a representative residual pattern at an enlarged scale.

Computed residual water-transport magnitudes and directions are given in table 13 for 25 selected sites (see fig. 27 for site numbers). Residual magnitudes range from 19,300 ft^3/s in 1880 to 18,100 ft^3/s in 1985 at the entrance to Tampa Bay (site 1), from 1,200 ft^3/s in 1972 to 700 ft^3/s in 1985 at site 9 in mid-Tampa Bay, from 400 ft^3/s in 1880 to 1,200 ft^3/s in 1972 at site 23 in Old Tampa Bay, and from 400 ft^3/s in 1880 to 500 ft^3/s in 1985 at site 18 in Hillsborough Bay. By comparing tables 10, 11, and 13, the degree of residual-vector variability among levels of development can be seen to be much greater than the corresponding variability in either flood or ebb vectors for many sites. The sensitivity of residual transport to physical changes in the bay is greater than the sensitivity of flood or ebb transport to the same changes.

Circulation at the entrance to Tampa Bay is dominated by (1) large gulfward-flowing vectors in the deep channel north of Egmont Key (site 1, fig. 41 and table 13), (2) small bayward-flowing vectors at other locations at the entrance (sites 2 and 3, fig. 41 and table 13), (3) intense, small-diameter gyres up to 4 mi bayward from Egmont Key, and (4) significant south-to-north residual transport about 1–2 mi bayward of the entrance.

Gyres and residual-transport features near the entrance to Tampa Bay adjoin other less intense gyres within the bay (see figs. 38–41). Each gyre or residual-transport feature adjoins other features in a progressive series to the head of Hillsborough and Old Tampa Bays. Some gyres mesh like a pair of interlocking gears and enhance residual-transport magnitudes where they join. Other pairs of gyres seem to rotate in directions opposite to each other and to partially or wholly cancel residual transport where the pairs join.

In spite of the large local variability in computed residual water transport, the overall pattern of circulation for each of the three levels of development is similar. Major gyres that existed in 1880 can be identified in the 1972 and 1985 maps. Detectable changes include deflection or skewing of gyres, strengthening or weakening of residual-transport vectors, and addition of new gyres associated primarily with causeways, islands, and channels.

Sufficient tidal current data have been collected by the NOS at two sites in Tampa Bay, Ross Island and Egmont Channel (sites 25 and 26, fig. 8 and table 7), to determine long-term residual currents for comparison with model results. The comparison is given in the following table:

Location	Residual current	
	Measurements	Model
Ross Island	0.12 ft/s (C. R. Muirhead, written commun., 1983) in flood direction (358°) (from Dinardi, 1978, p. 34).	0.09 ft/s at 306° clockwise from north.
Egmont Channel	0.29 ft/s in ebb direction (289°) (from Dinardi, 1978, p. 30).	0.27 ft/s at 284° clockwise from north.

At Egmont Channel, the comparison is very good. The residual current speeds determined by both measurements and the model are within 10 percent, and residual current directions coincide within 5°. At the Ross Island site, the comparison is not as good as at Egmont Channel but is sufficient to indicate a fair level of agreement between measurements and model values, particularly in a region

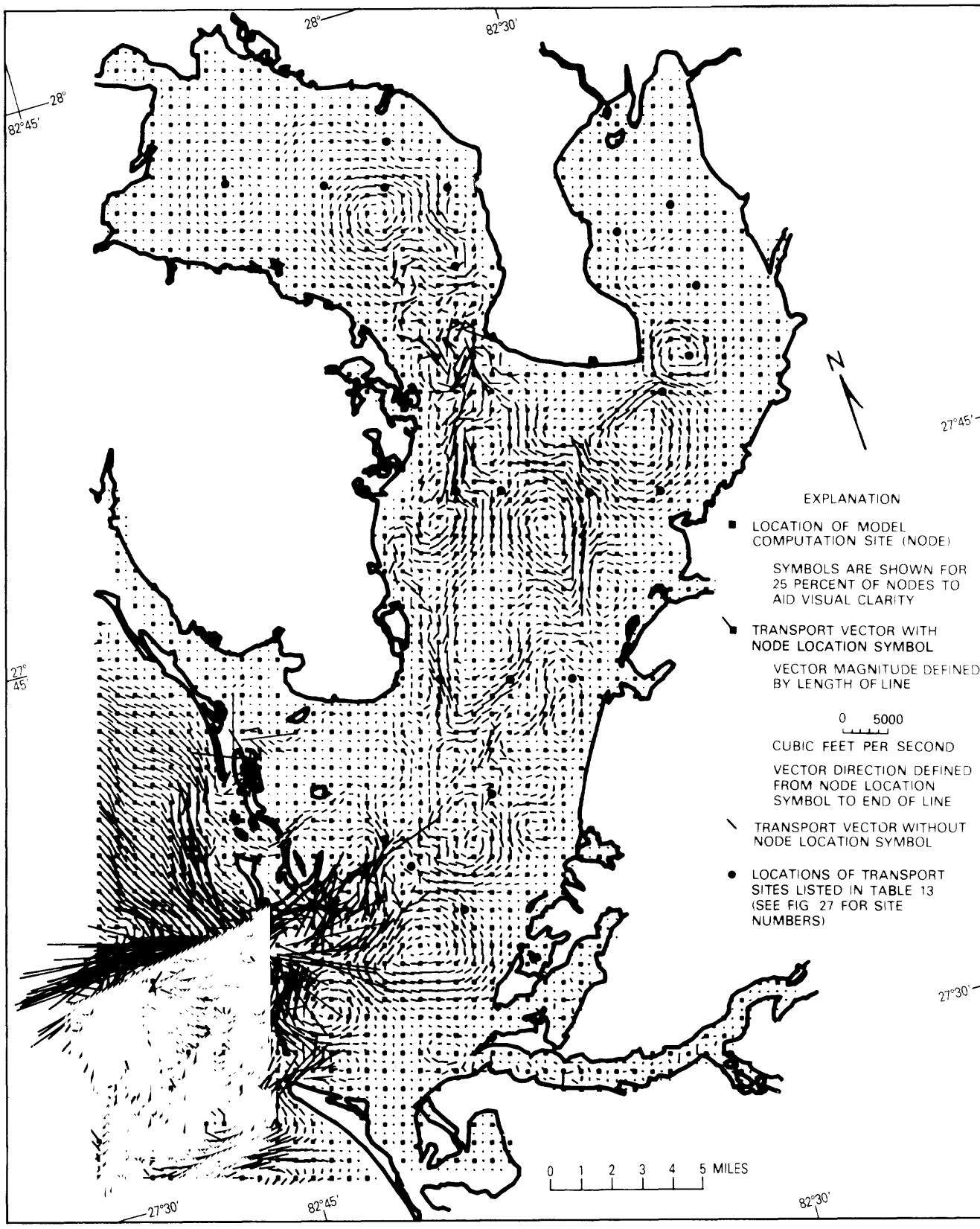

Figure 38. Residual water-transport pattern in Tampa Bay for 1880 level of development.

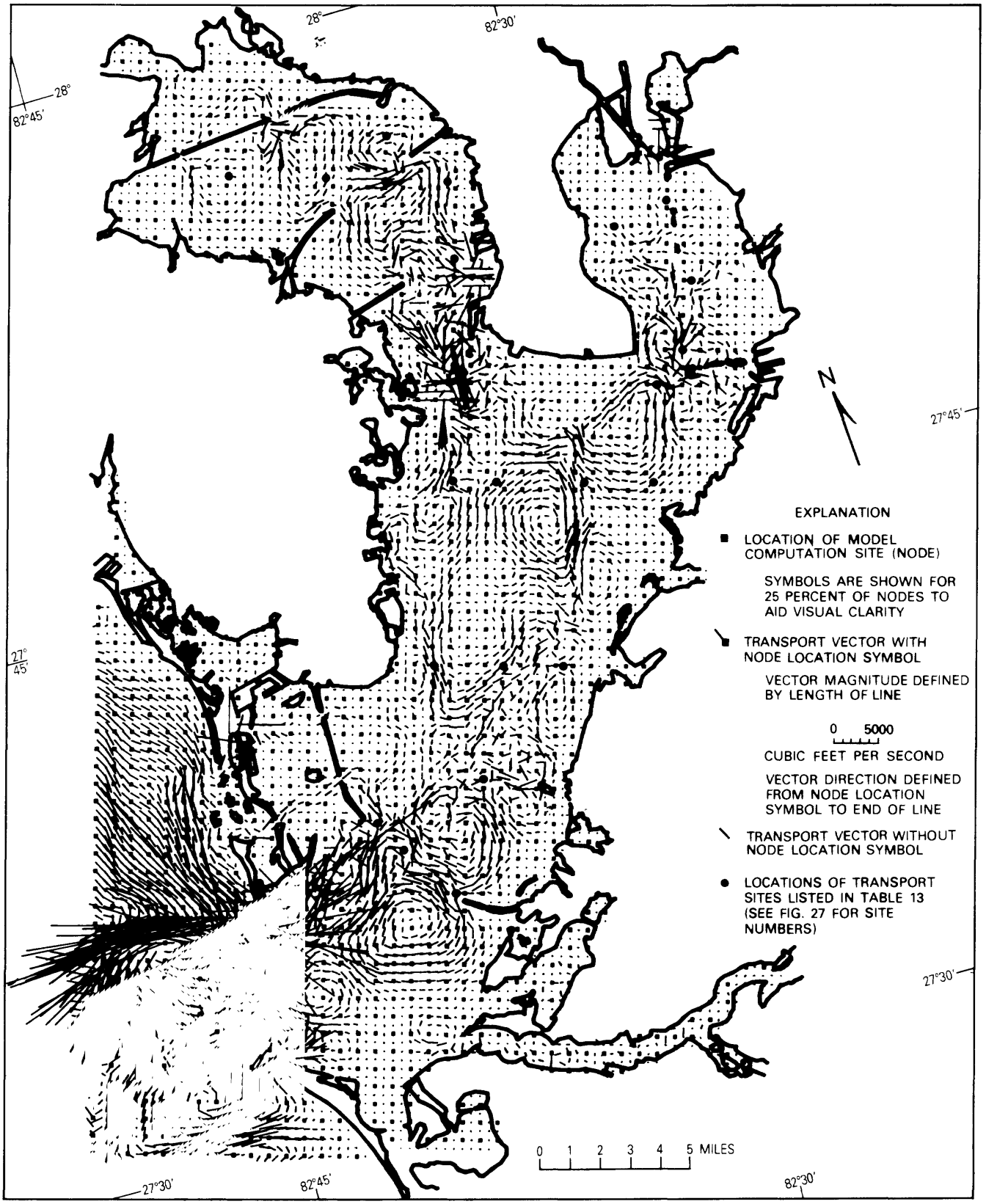

Figure 39. Residual water-transport pattern in Tampa Bay for 1972 level of development.

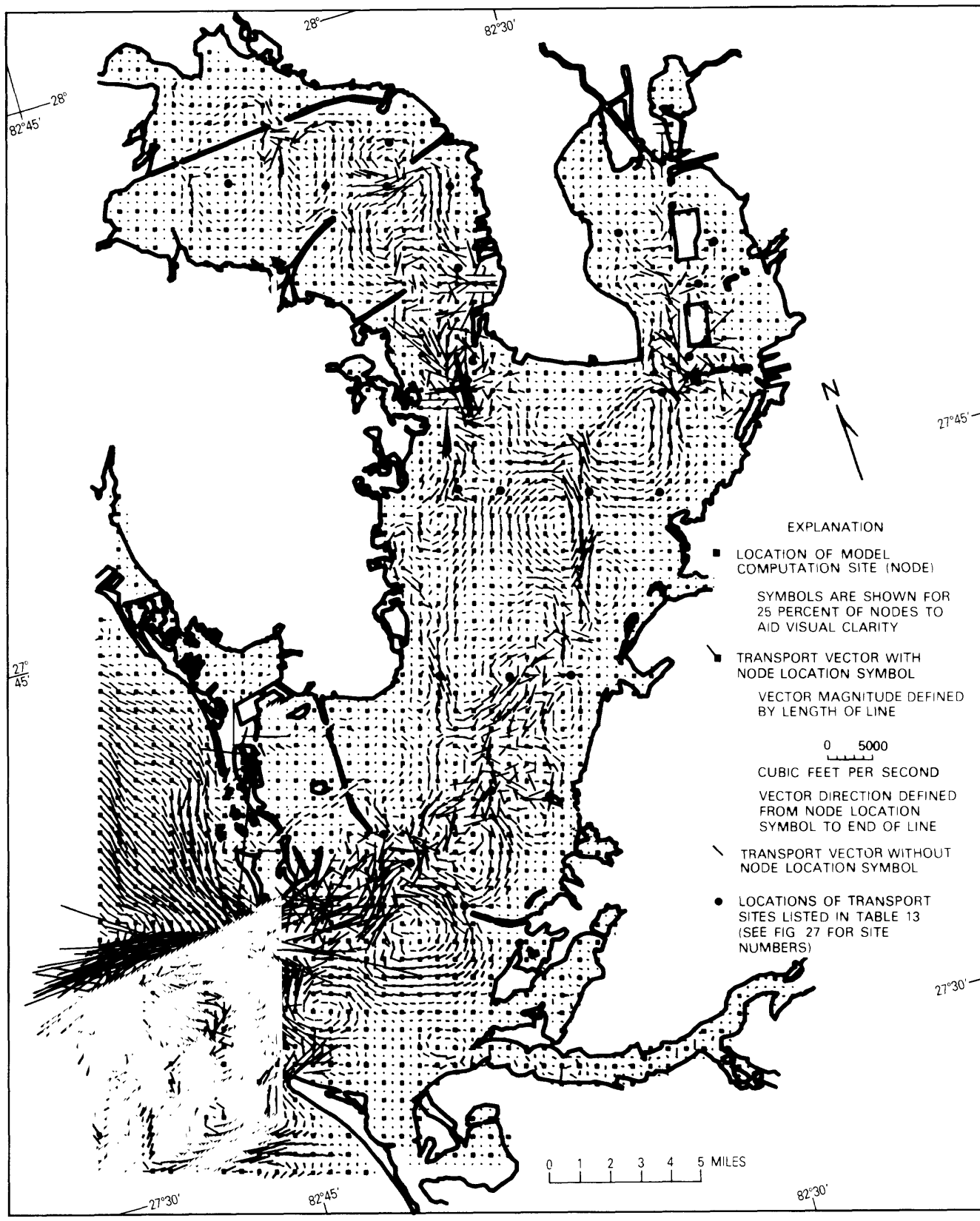

Figure 40. Residual water-transport pattern in Tampa Bay for 1985 level of development.

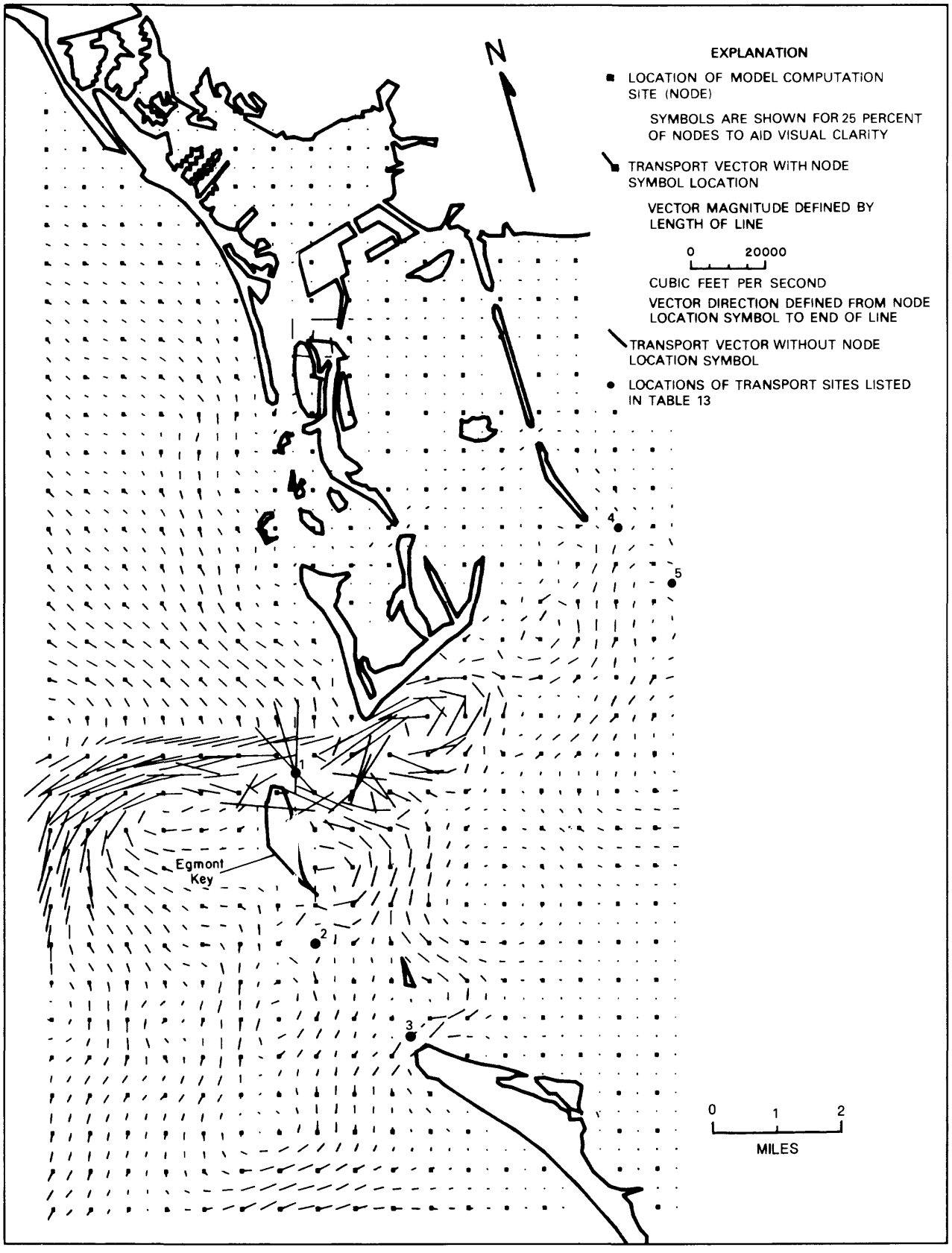

Figure 41. Representative residual water-transport pattern at the entrance to Tampa Bay for 1972 level of development.

Table 13. Residual water transport and direction at selected sites in Tampa Bay for 1880, 1972, and 1985 levels of development

Site no. (see fig. 27)	Transport (thousands of cubic feet per second)			Direction (degrees, clockwise from north)		
	1880	1972	1985	1880	1972	1985
1	19.3	18.5	18.1	285	284	282
2	4.2	4.2	3.6	119	118	130
3	5.1	5.0	4.7	59	59	59
4	1.3	1.0	1.0	207	195	193
5	.8	1.4	2.4	353	309	291
6	.3	1.6	1.6	319	267	267
7	1.3	1.4	1.6	224	260	227
8	2.1	2.0	1.9	176	174	174
9	1.1	1.2	.7	67	59	212
10	.5	1.0	.9	310	290	289
11	1.5	1.5	1.4	199	208	206
12	.6	.6	.5	196	240	230
13	1.3	1.6	1.6	345	356	4
14	.8	.8	.8	263	260	259
15	1.2	1.2	1.3	148	166	167
16	.3	3.5	7.1	76	58	58
17	.1	.3	1.0	12	222	283
18	.4	.4	.5	187	171	175
19	.1	.3	.6	290	152	79
20	.9	1.5	1.4	67	192	193
21	.5	.9	.9	37	30	30
22	1.1	2.3	2.3	292	283	283
23	.4	1.2	1.1	178	79	79
24	.3	1.2	1.2	210	189	189
25	.4	.8	.8	278	87	87

of very complex, computed residual transport (see fig. 39).

Comparison of residual currents at these two sites is not sufficient to judge the model's ability to accurately simulate residual currents throughout the modeled area. Results of the comparisons, although encouraging, may be spurious for several reasons:

1. The accuracy of residual currents computed from measurements is not known.
2. Residual currents computed throughout the bay are on the same order as reported standard errors between observed and computed tidal currents (table 8); this similarity indicates the probability of high percentage errors associated with residual currents at the Egmont Channel and Ross Island sites.
3. Two sites do not adequately represent the range of conditions within the modeled area.

Although these shortcomings are recognized, residual computations are considered useful and instructive, particularly for assessing relative changes caused by physical modification to Tampa Bay. Computed changes in residual water and constituent transports probably are more reliable than the residual transport values themselves.

Residual Water-Transport Differences For 1880, 1972, and 1985

Areas of change in residual water transport between 1880 and 1972 levels of development are shown in figure 42. Areas of change between 1972 and 1985 levels of development are shown in figure 43. Computed changes from 1880 to 1972 are extensive, occur throughout the bay, and extend into the nearshore region of the Gulf of Mexico. The largest changes are associated with causeway construction in Old Tampa Bay; ship-channel and port-facility construction at the mouth of Old Tampa Bay; residential, commercial, port-facility, and ship-channel construction in and at the mouth of Hillsborough Bay; causeway, port-facility, and ship-channel construction in lower Tampa Bay; and residential and causeway construction in Boca Ciega Bay.

All residual-transport changes from 1972 to 1985 are due to ship-channel construction and associated submergent and emergent dredged material disposal sites.

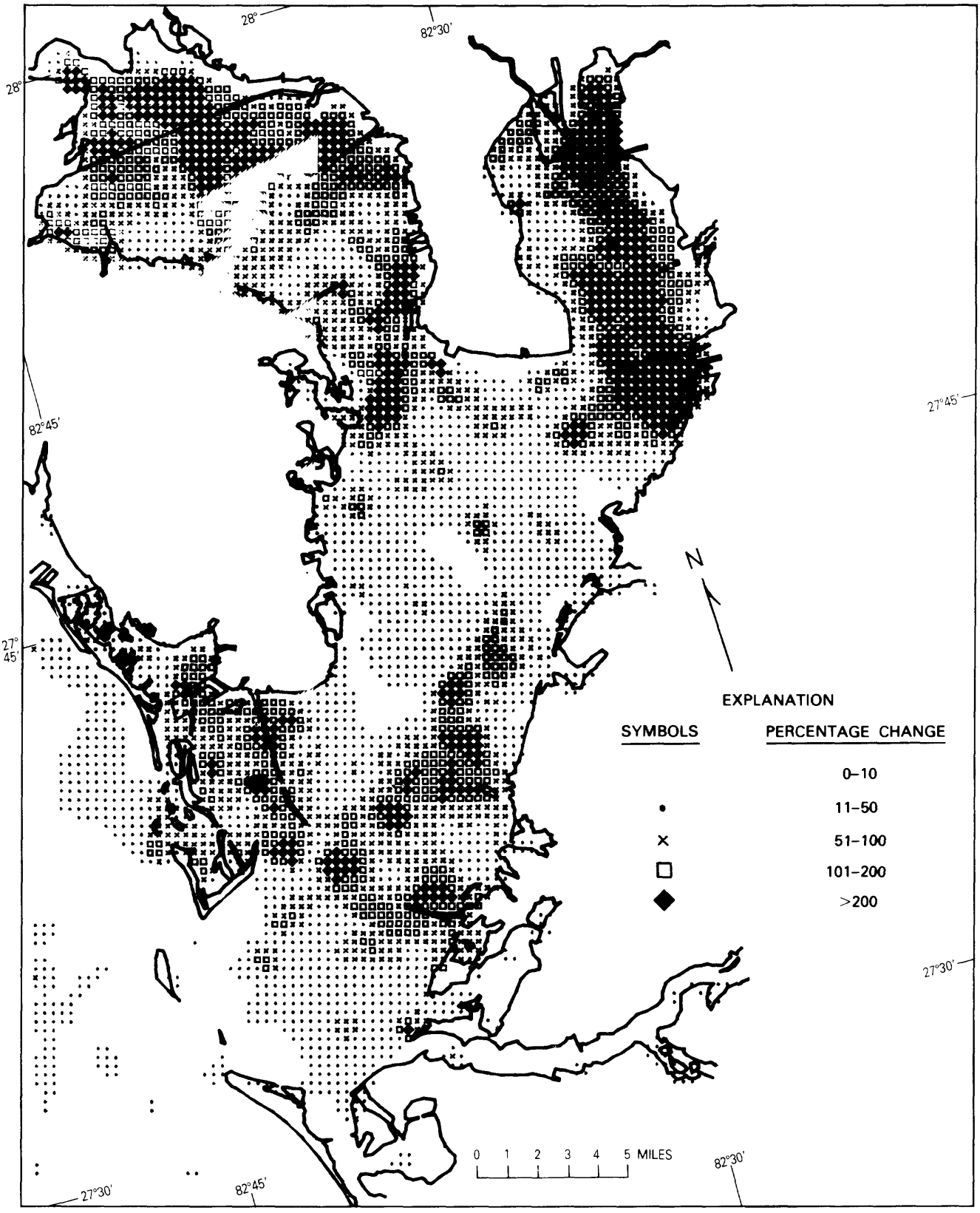

Figure 42. Changes in residual water transport in Tampa Bay between 1880 and 1972 levels of development.

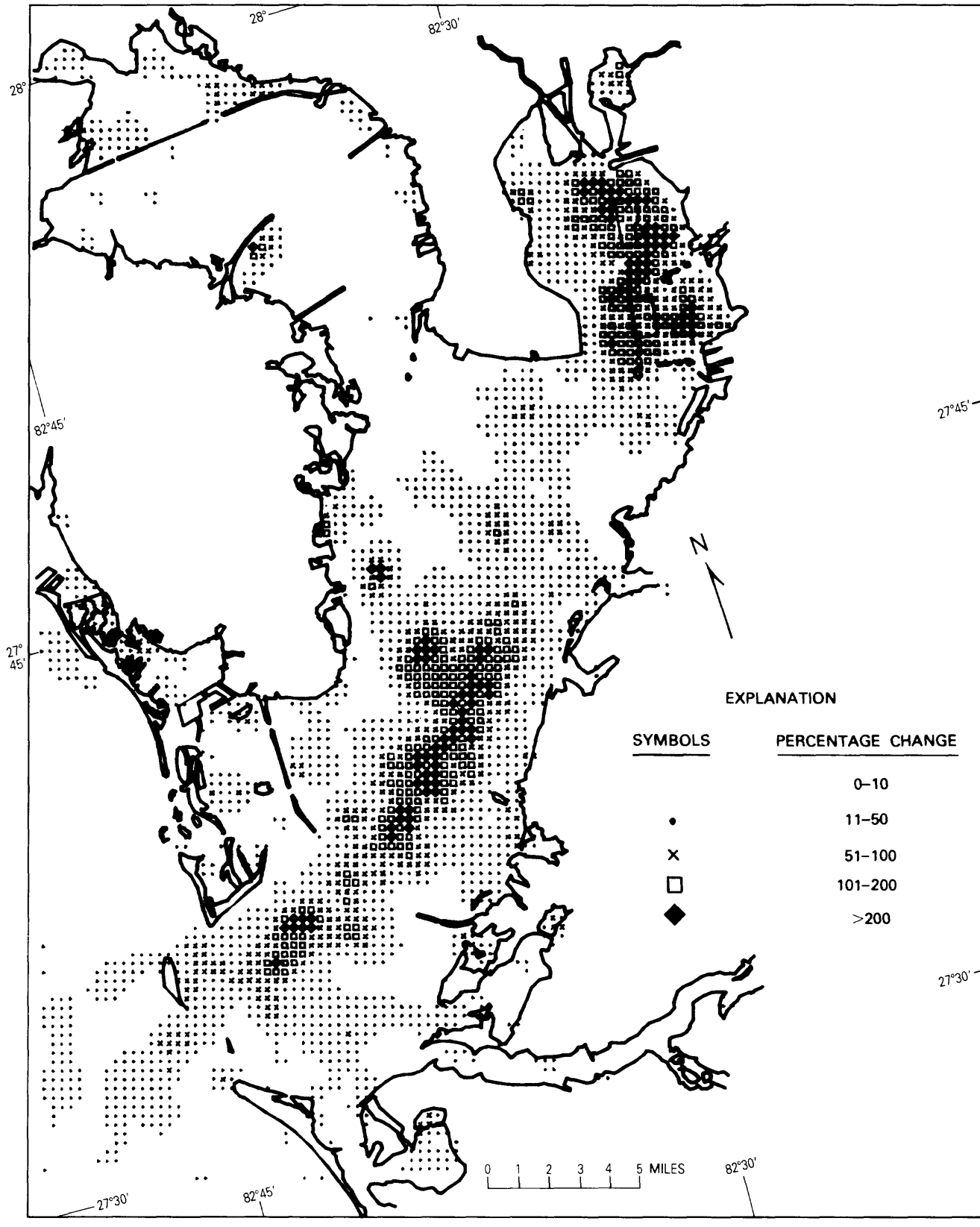

Figure 43. Changes in residual water transport in Tampa Bay between 1972 and 1985 levels of development.

Areas of major change are in Hillsborough Bay and near the boundary between middle and lower Tampa Bay. Some change also occurred offshore of the Tampa Bay entrance.

Computed residual transport changed little in Old Tampa Bay from 1972 to 1985. Although no physical changes were made in Old Tampa Bay during that period, a small difference in the distribution of tidal flow between Hillsborough and Old Tampa Bays may have resulted in a small change in residual transport.

Areas totaling about 306 mi^2 sustained computed residual water-transport changes greater than 10 percent between 1880 and 1972. Areas totaling about 183 mi^2 sustained similar changes between 1972 and 1985. The following table gives a breakdown of percentage changes and affected areas.

Residual water transport

Percentage change	Area of change, in square miles	
	1880 to 1972	1972 to 1985
0–10	157	263
11–50	139	125
51–100	71	30
101–200	59	21
>200	37	7

The areal extent of changes in residual water transport is one measure of the effects of physical change on water motion in a bay. Areal changes, however, are static in nature and do not provide information on how the dynamics of water motion are impacted, particularly the dynamics of circulatory features such as gyres. Standard methods for comparing gyre intensity do not exist. Therefore, a technique was developed to provide a measure of change in circulation characteristics in Tampa Bay.

Gyres are tide-induced features that are caused by interaction between tidal water motion and bottom configuration. Without the tide, there could be no incoming residual-transport vectors. All vectors would be outgoing, and the vector sum normal to each bay cross section would be equal to the total inflow from streams. A feature of tide-induced water transport is that some areas of the bay show residual incoming flows. To satisfy continuity, these areas are balanced by outgoing flow in other areas. Both conceptually and by computation, the sum of all incoming and outgoing residual-flow vectors along a particular cross section also equals the total freshwater stream inflow landward of the cross section.

Tide-induced circulation, as defined in the section on the longitudinal summary method (see p. 37), is used as a measure of circulatory intensity. The units of tide-induced circulation are the same as for streamflow, so direct comparisons can be made between tide- and streamflow-induced residual flows.

Figure 44 shows circulation, as the sum of incoming tide-induced residual transport, plotted against distance along the longitudinal summary lines (see fig. 26) for each level of development. Tributary streamflow also is shown. Circulation ranges from about 60,000 ft^3/s in the Gulf of Mexico to zero at the heads of Hillsborough and Old Tampa Bays for all three levels of development. Except in Hillsborough Bay, tide-induced circulation is consistently greater than the average inflow from streams.

On the basis of figure 44, Tampa Bay was divided into eight zones, each of which has significantly different circulation characteristics. The zones are shown in figure 26 and listed in table 14. The computed average tide-induced circulation in each zone for each level of development also is given in table 14, with the percentage increase or decrease between 1880 and 1972, between 1972 and 1985, and between 1880 and 1985.

The progression from the Gulf of Mexico to the head of Hillsborough and Old Tampa Bays consists of three sequences of high-circulation, transition, and low-circulation zones. The first sequence (zones 1, 2, and 3) defines circulation characteristics within the lower half of the bay system. Zone 1 has high circulation. Zone 3 has low circulation, about an order of magnitude less than zone 1. Zone 2 serves as a transition between zones 1 and 3.

The second sequence (zones 4, 5, and 6) depicts circulation characteristics in the northeastern part of the bay system, including Hillsborough Bay. Again, zone 4 has high circulation, zone 6 has low circulation, and zone 5 is a transition between them. Although not as obvious, the third sequence (zones 4, 7, and 8) in the northwestern part of the bay system, including Old Tampa Bay, also shows the same general pattern of high, transitional, and low circulation.

Computed tide-induced circulation in zone 1 averaged about 45,500 ft^3/s for 1880 level of development (table 14), by far the greatest of any area in the bay. About 3.93×10^9 ft^3 of water was tidally interchanged in this zone every day, or about 11 percent of the total water volume in the zone. Circulation throughout zone 1 was greatest for 1880 conditions. Circulation was reduced by about 1,600 ft^3/s for 1972 conditions and by another 2,800 ft^3/s for 1985 conditions. These reductions indicate that cumulative physical changes reduced circulation or tidal interchange of water between the Gulf of Mexico and the entrance of Tampa Bay by about 10 percent.

Circulation reduction in zone 1 is not considered a significant factor influencing overall flushing and constituent interchange rates of Tampa Bay. Circulation magnitudes are so high at the bay mouth, in comparison with other areas (fig. 44), that small reductions do not have a limiting effect. High circulation and mixing in zone 1 are the likely causes for low gradients of specific conductance reported by Goetz and Goodwin (1980, p. 23).

Zone 2 had an average circulation of about 10,400 ft^3/s for 1880 level of development. Zone 2 is characterized by large variations in circulation that are apparently

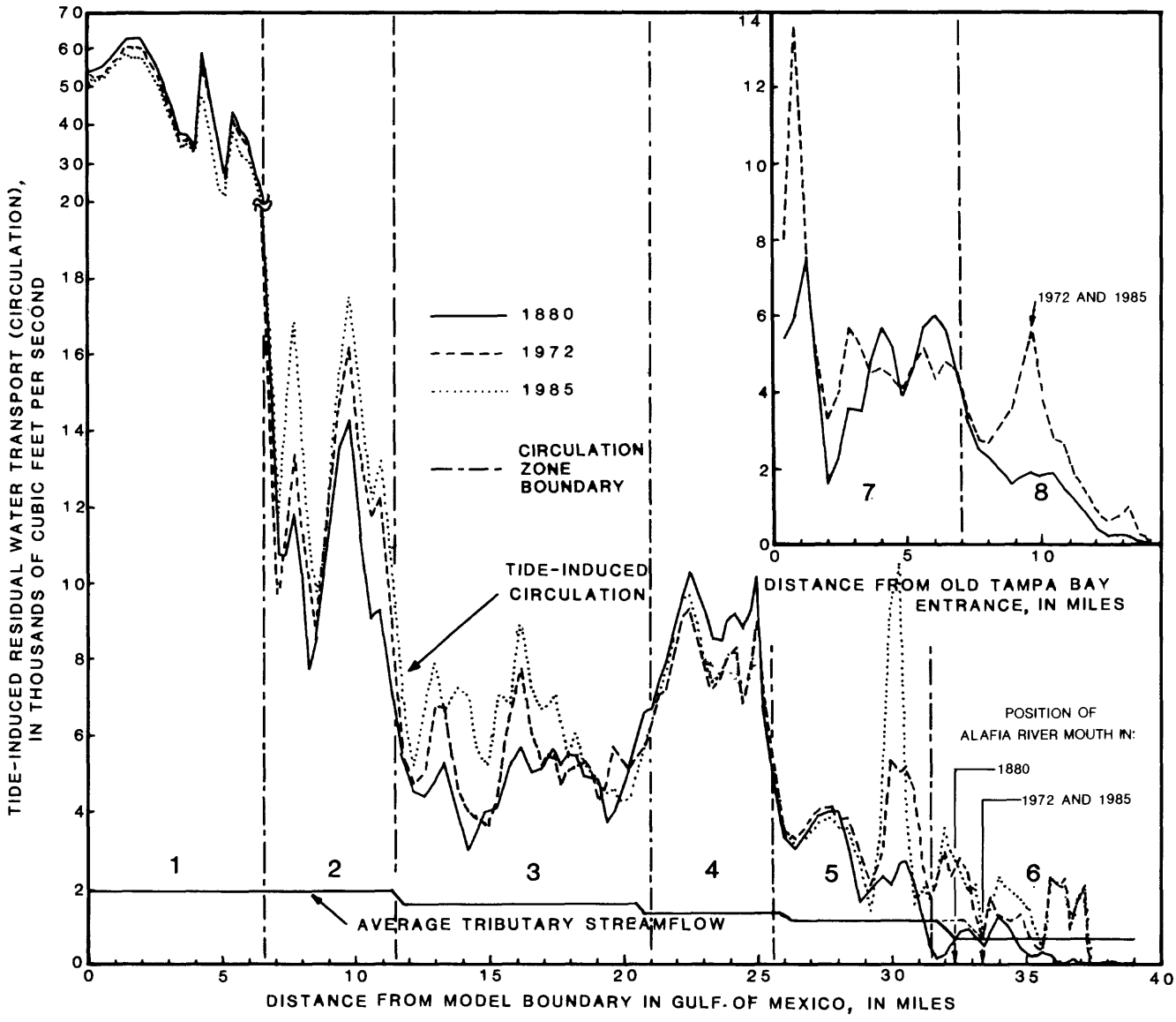

Figure 44. Average tributary streamflow and tide-induced circulation in Tampa Bay along longitudinal summary lines (see fig. 26) for 1880, 1972, and 1985 levels of development.

Table 14. Average tide-induced circulation and percentage changes for each circulation zone in Tampa Bay for 1880, 1972, and 1985 levels of development

Circulation zone (see fig. 26)	Distance along longitudinal summary line (miles) (see fig. 26)	Average circulation (cubic feet per second)			Percentage change		
		1880	1972	1985	1880 to 1972	1972 to 1985	1880 to 1985
1	0 to 6.5	45,500	43,900	41,100	− 3.5	− 6.4	− 9.7
2	6.5 to 11.5	10,400	11,800	13,400	+ 13.5	+13.6	+ 28.8
3	11.5 to 21.5	4,900	5,200	6,300	+ 6.1	+21.2	+ 28.6
4	21.5 to 25.5	8,600	7,900	7,800	− 8.1	− 1.3	− 9.3
5	25.5 to 31.5	2,700	3,600	3,700	+ 33.3	+ 2.8	+ 37.0
6	31.5 to 39.0	400	1,300	1,500	+225	+15.4	+275
7[1]	0 to 7.0	4,800	5,500	5,500	+ 14.6	0	+ 14.6
8[1]	7.0 to 14.0	1,400	2,500	2,500	+ 78.6	0	+ 78.6

[1]Old Tampa Bay.

caused by gyres that have little interaction. In 1880, an average of about 0.90×10^9 ft^3 of water was tidally interchanged in zone 2 each day, or about 5 percent of the volume of water in the zone. Average circulation throughout zone 2 was least for 1880 level of development, with an increase of about 1,400 ft^3/s for 1972 conditions and another increase of 1,600 ft^3/s for 1985 conditions. Physical changes in and near zone 2 caused an increase of nearly 30 percent in computed average circulation from 1880 to 1985.

Zone 3 is a 10-mi-long region of low circulation between regions of high circulation. In 1880, zone 3 had an average circulation of about 4,900 ft^3/s, about half of the average circulation in adjacent zones 2 and 4 (table 14). The minimum computed circulation in 1880 within zone 3 was very low, only about 3,000 ft^3/s (see mi 14.2, fig. 44), about double the tributary streamflow at that point. In 1880, an average of about 0.42×10^9 ft^3 of water was tidally interchanged in zone 3 each day, or about 1 percent of the volume of water in the zone.

This region of low circulation is interpreted as a natural constriction to the interchange of water and constituents between adjacent zones. Limited circulation is the likely cause of the steep specific-conductance gradients reported in zone 3 by Goetz and Goodwin (1980, p. 23).

Physical changes in zone 3 between 1880 and 1972 resulted in an average circulation increase of about 300 ft^3/s. An additional increase of about 1,100 ft^3/s occurred between 1972 and 1985. Cumulative physical changes in zone 3 have reduced its natural constrictive effect and increased circulation by about 30 percent. Long-term results of increased circulation in this area could be (1) more rapid flushing of waterborne constituents that have their primary source north of zone 3 and (2) more rapid intrusion into the bay of constituents that have their source south of zone 3.

Zone 4 is a 4-mi-long region of greater average circulation than that in adjacent zones 3, 5, and 7. Average circulation in 1880 was computed to be about 8,600 ft^3/s. About 0.74×10^9 ft^3 of water was tidally interchanged in zone 4 each day, or about 5 percent of the water volume in the zone. Zone 4 functions for Hillsborough and Old Tampa Bays in the same way that zone 1 functions at the entrance to Tampa Bay. Rather than constrict water and constituent interchange, as zone 3 does, zones 1 and 4 provide rapid, large-scale mixing. This mixing contributes to rapid removal of constituents that have their source in the north and to rapid intrusion of constituents that have their source in the south.

Physical changes in zone 4 between 1880 and 1972 caused a reduction in average circulation of about 700 ft^3/s (table 14). An additional reduction of about 100 ft^3/s occurred between 1972 and 1985. The cumulative circulation reduction of 9 percent in zone 4, accompanied by a 30-percent cumulative circulation increase in zone 3, largely erased the contrast between these zones from 1880 to 1985.

Zone 5, leading into Hillsborough Bay, was characterized in 1880 by a gradually reducing circulation that provided a transition to the very low circulation levels in zone 6. The increase in circulation (see mi 30, fig. 44) in 1972 and 1985 was caused by the combination of powerplant cooling-water flow, dredging of channels, and construction of spoil islands at the mouth of Hillsborough Bay.

Average circulation in 1880 was computed to be about 2,700 ft^3/s in zone 5. About 0.23×10^9 ft^3 of water was tidally interchanged each day, or about 1 percent of the total water volume in zone 5. Largely as a result of the powerplant cooling-water discharge and channel construction, the average circulation in the zone rose to about 3,600 ft^3/s in 1972 and about 3,700 ft^3/s in 1985, a cumulative circulation increase of 37 percent.

Zone 6 at the head of Hillsborough Bay has the least circulation of any zone in Tampa Bay. Circulation in 1880 averaged about 400 ft^3/s, less than the average discharge of the Hillsborough River, 636 ft^3/s. Tidal water interchange each day was about 0.035×10^9 ft^3, or only 0.4 percent of the water volume in zone 6. A powerplant cooling-water discharge (see mi 36, fig. 44) and extensive dredging and filling throughout the zone caused an increase in average circulation of about 900 ft^3/s by 1972 and another 200-ft^3/s increase by 1985. This is a cumulative circulation increase of 275 percent, the largest of any zone in the bay. Even with this large increase, however, zone 6 has and will continue to have the poorest circulation of any zone in Tampa Bay.

Zone 7, the lower half of Old Tampa Bay, is a transition zone between higher (zone 4) and lower (zone 8) average circulation. Because physical changes are not expected in Old Tampa Bay between 1972 and 1985, one line is used in figure 44 to represent both 1972 and 1985 conditions. The circulation increase at mi 3 (fig. 44) is attributed to cooling-water discharge from a powerplant.

In 1880, circulation in zone 7 was about 4,800 ft^3/s. About 0.42×10^9 ft^3, or nearly 4 percent of the water volume, was tidally interchanged each day. Physical changes between 1880 and 1972 caused an average circulation increase of about 700 ft^3/s, or about 15 percent.

In 1880, circulation in zone 8 was about 1,400 ft^3/s. About 0.21×10^9 ft^3, less than 1 percent of the water volume, was tidally interchanged each day. Physical changes in zone 8 between 1880 and 1972 caused an average circulation increase of about 1,100 ft^3/s, or about 79 percent. The increase in circulation at mi 9.5 (fig. 44) is due to effects of the Courtney Campbell Causeway (fig. 1). The circulation increase at mi 13 (fig. 44) is attributed to cooling-water discharge from a powerplant. Changes in circulation in zones 7 and 8 between 1972 and 1985 are computed to be minor because no physical changes are expected.

Constituent Transport

The patterns of flood, ebb, and residual constituent transport are developed in the model and presented in

this report in a manner analogous to that used for water transport. A hypothetical constituent is used that has an initial concentration distribution closely matching that measured for phosphorus in July 1975 (fig. 23). Constituent transport and flushing results presented in this report are applicable for this distribution only. Comparison of results for 1880, 1972, and 1985 levels of development, however, provides a means for assessing constituent-transport changes due to physical changes in Tampa Bay.

Flood and Ebb Constituent Transport

Constituent-transport patterns during floodflow for 1880, 1972, and 1985 levels of development are shown in figures 45, 46, and 47, respectively. These maps show many similarities, including low constituent transport near the bay mouth, where concentrations are low, and high constituent transport in the upper parts of the bay, where concentrations are high. The magnitudes and directions of constituent-transport vectors at 25 selected sites during floodtide are listed in table 15. The sites are the same as those chosen for water transport (see fig. 27). Vector magnitudes through each 1,500-ft cell were nearly constant at about 0.6 lb/s at the entrance to Tampa Bay (site 1) for each level of development, varied from about 1.0 lb/s in 1880 to 0.8 lb/s in 1985 in mid-Tampa Bay (site 9), varied from about 0.5 lb/s in 1880 to 0.7 lb/s in 1985 in Old Tampa Bay (site 23), and were nearly constant at 0.2 lb/s in Hillsborough Bay (site 18).

Notable differences in constituent-transport magnitude or direction at some sites for 1880, 1972, and 1985 levels of development are evident. Sites 6, 7, 16, 19, 24, and 25, for example, show changes due to construction of causeways, islands, channels, or submerged disposal areas.

Constituent-transport patterns during ebbflow for 1880, 1972, and 1985 levels of development are shown in figures 48, 49, and 50, respectively. Ebb patterns, although opposite in direction, are similar to the flood patterns shown in figures 45–47. High constituent transport occurs in the upper parts of the bay, and low constituent transport occurs near the mouth.

Table 15. Constituent transport and direction during typical floodtide at selected sites in Tampa Bay for 1880, 1972, and 1985 levels of development

Site no. (see fig. 27)	Transport (pounds per second)			Direction (degrees, clockwise from north)		
	1880	1972	1985	1880	1972	1985
1	0.626	0.611	0.598	115	115	116
2	.406	.382	.375	69	69	70
3	.152	.143	.143	65	64	64
4	.298	.346	.355	49	48	48
5	.576	.631	.692	51	48	48
6	.205	.161	.163	45	85	85
7	.688	.595	.377	44	41	42
8	.554	.525	.538	31	31	31
9	.972	.928	.767	28	28	32
10	.688	.650	.679	29	30	31
11	.939	.834	.818	39	38	38
12	.708	.670	.648	16	14	14
13	1.10	1.17	1.24	19	17	15
14	.439	.395	.373	59	59	59
15	1.28	1.47	1.36	62	55	55
16	1.08	1.71	1.63	24	39	54
17	.842	.761	.542	6	31	355
18	.238	.161	.170	336	345	348
19	.582	.163	.320	348	346	30
20	1.81	2.13	2.09	359	356	356
21	.723	.571	.562	347	337	337
22	1.16	1.74	1.71	313	316	316
23	.496	.681	.670	298	285	286
24	.139	.207	.203	251	280	280
25	.688	.368	.364	304	348	348

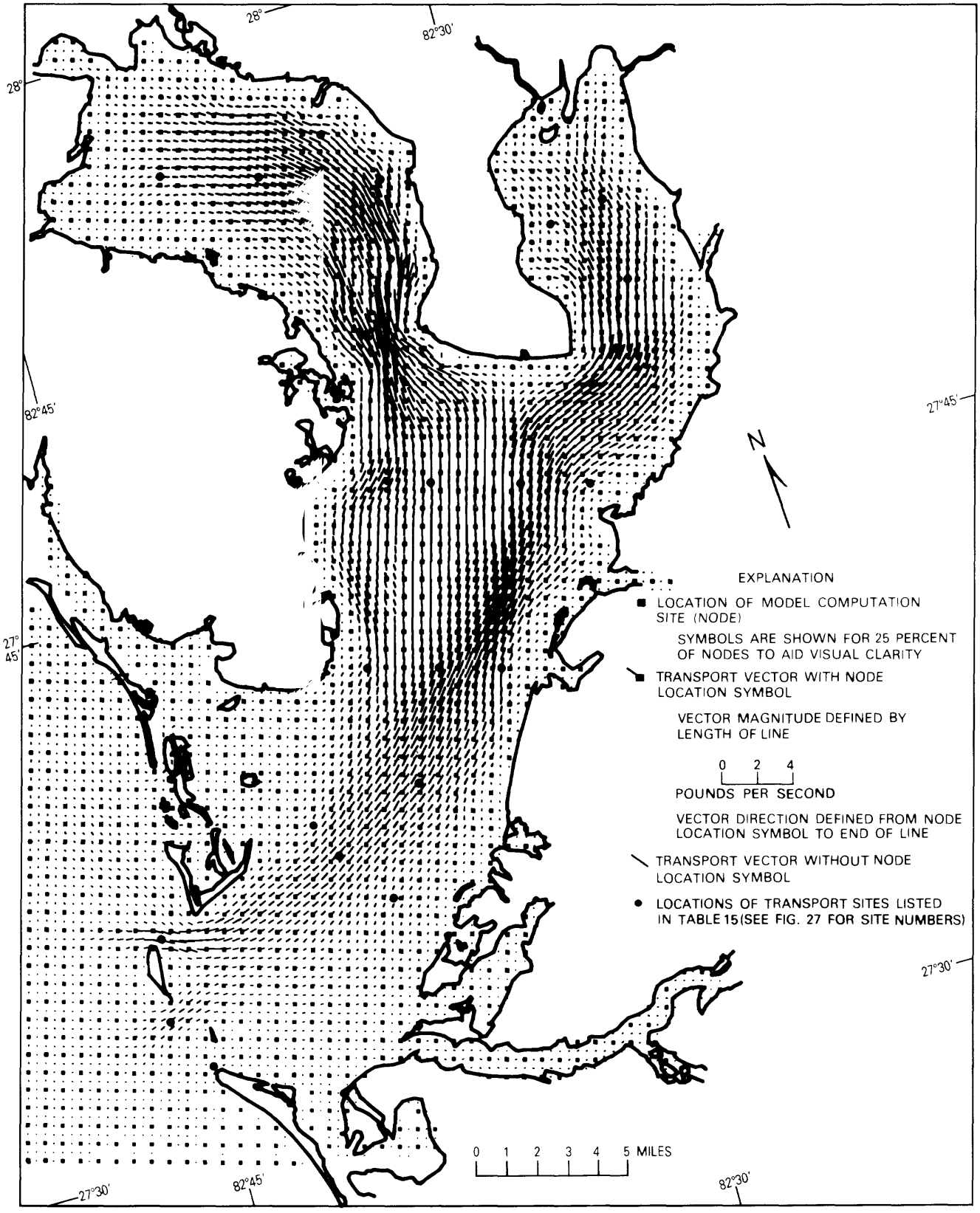

Figure 45. Constituent-transport pattern during typical floodtide in Tampa Bay for 1880 level of development.

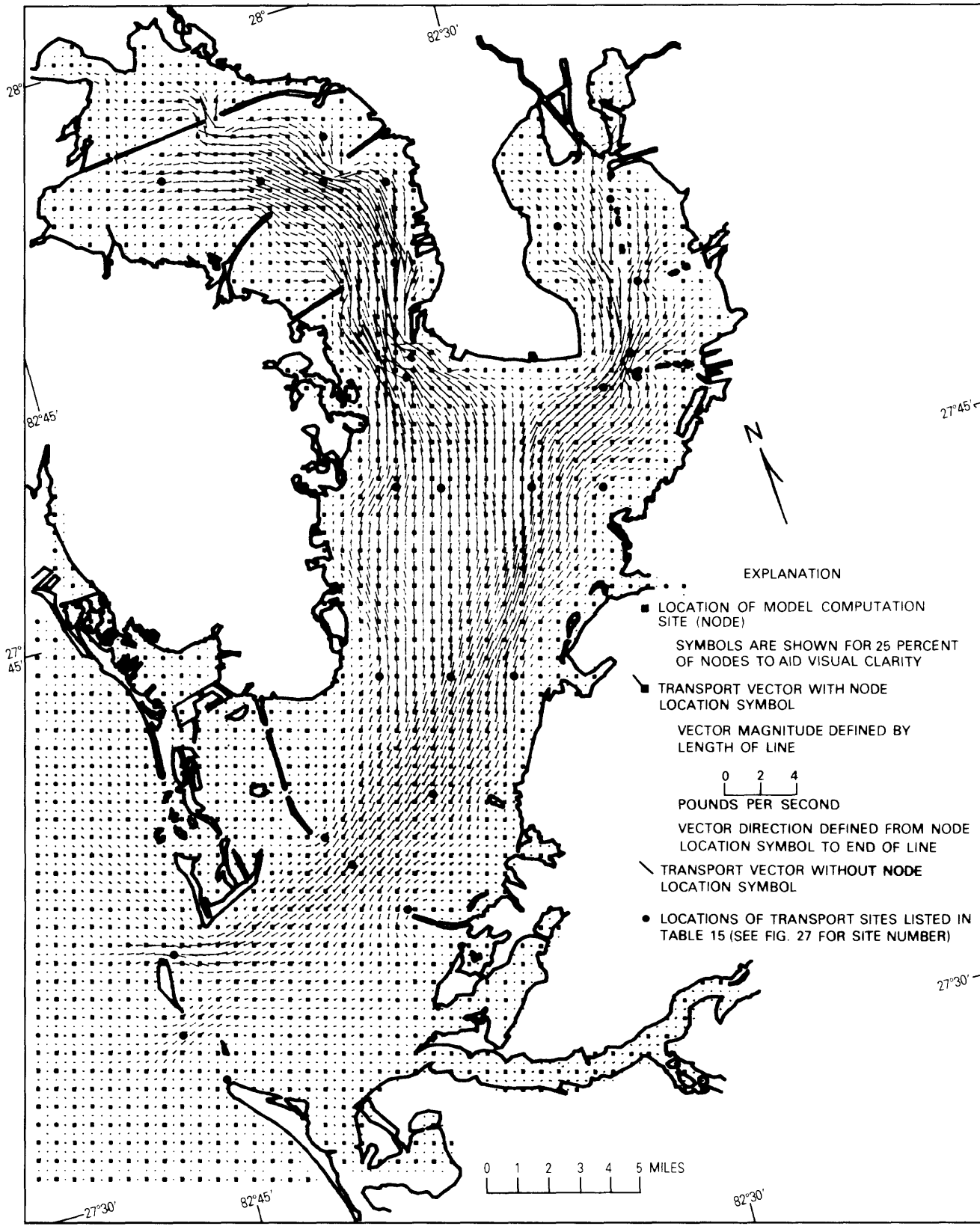

Figure 46. Constituent-transport pattern during typical floodtide in Tampa Bay for 1972 level of development.

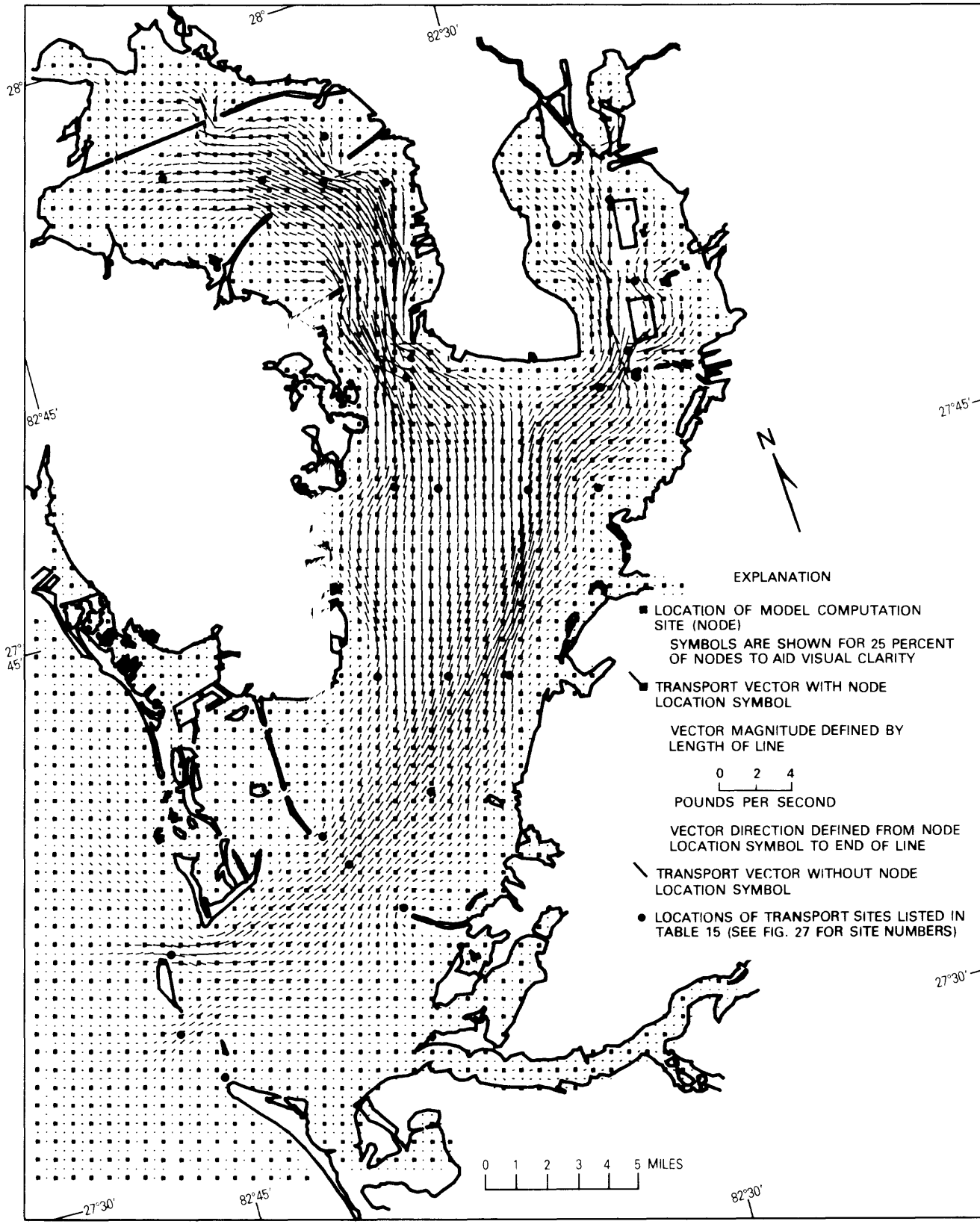

Figure 47. Constituent-transport pattern during typical floodtide in Tampa Bay for 1985 level of development.

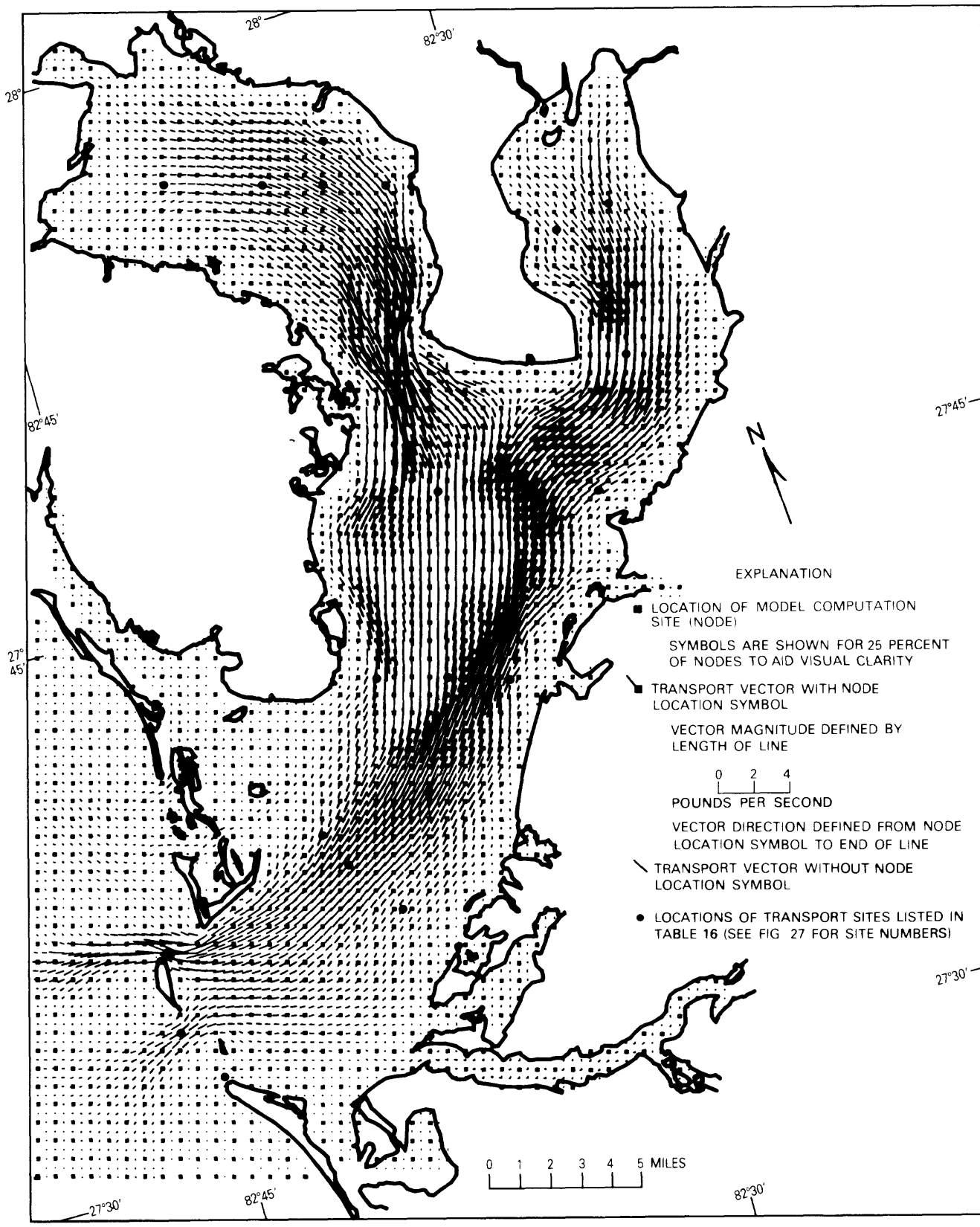

Figure 48. Constituent-transport pattern during typical ebbtide in Tampa Bay for 1880 level of development.

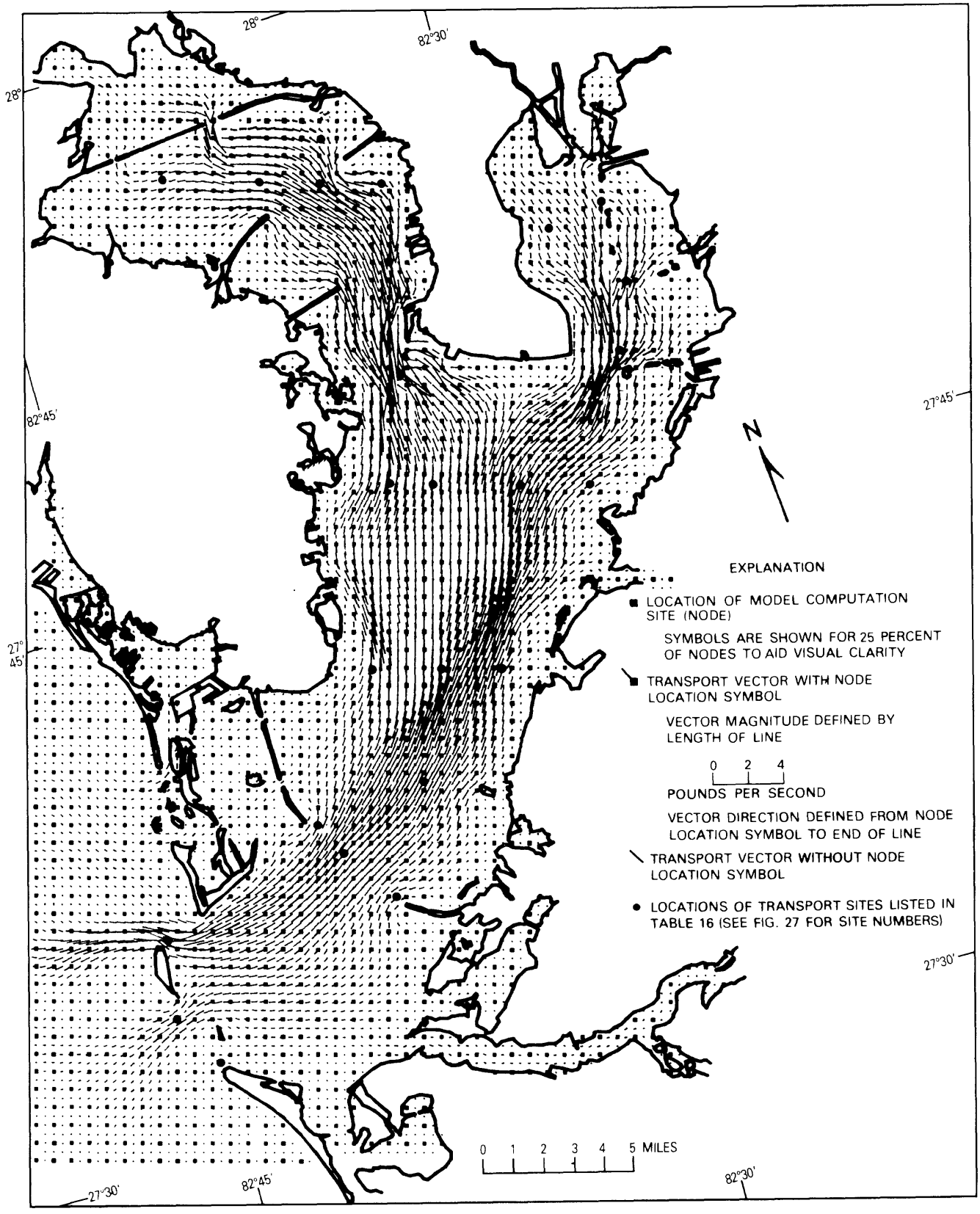

Figure 49. Constituent-transport pattern during typical ebbtide in Tampa Bay for 1972 level of development.

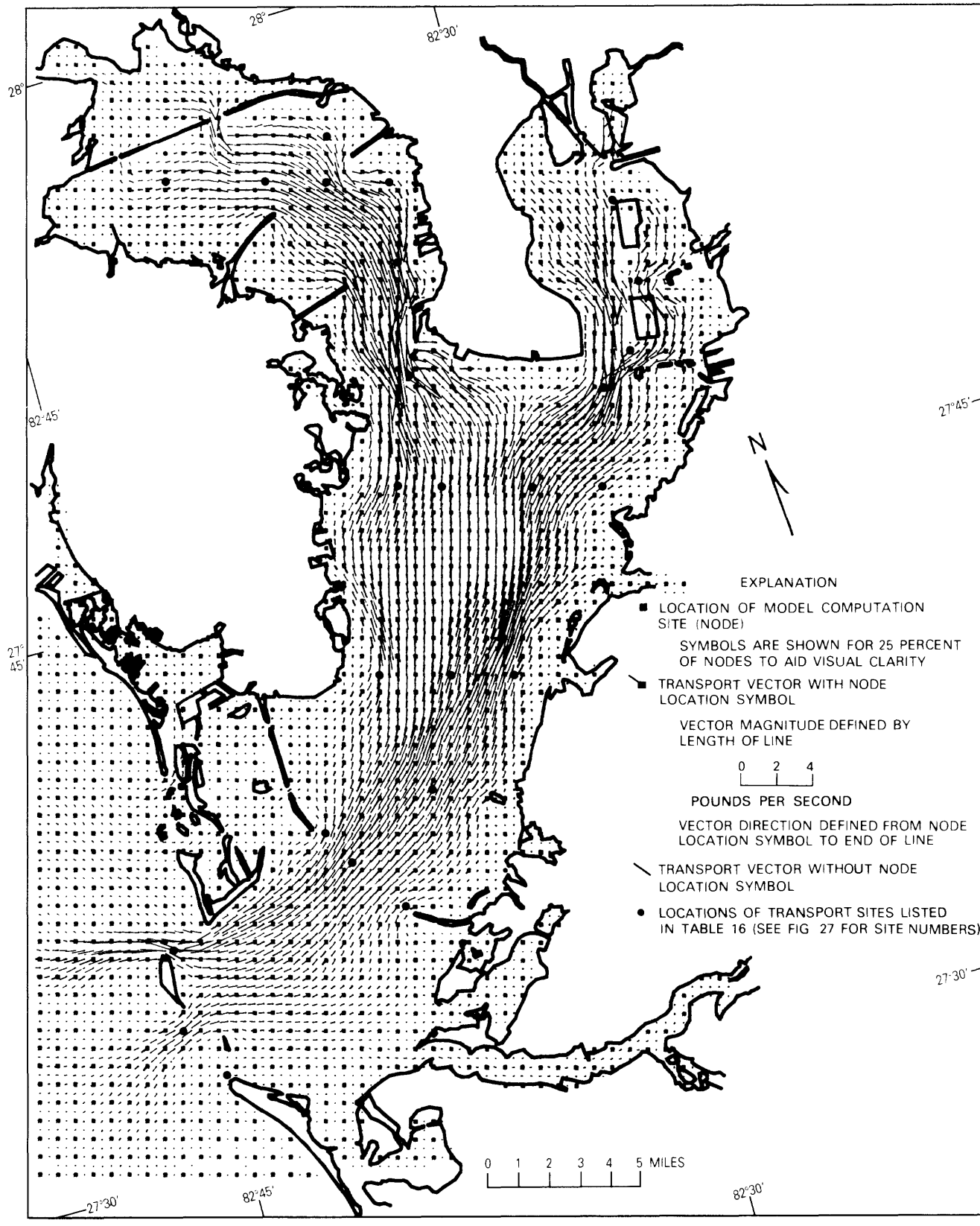

Figure 50. Constituent-transport pattern during typical ebbtide in Tampa Bay for 1985 level of development.

As with water transport, maximum constituent transport during ebbtide is substantially greater than that during floodtide because the rate of water-level decline is faster than the rate of water-level rise (fig. 22 and table 9). The magnitudes and directions of constituent-transport vectors at 25 selected sites during ebbtide are listed in table 16. Vector magnitudes through each 1,500-ft cell were nearly constant at about 1.8 lb/s at the entrance to Tampa Bay (site 1) for each level of development, varied from about 1.5 lb/s in 1880 to 1.2 lb/s in 1985 in mid-Tampa Bay (site 9), varied from 0.6 lb/s in 1880 to 0.9 lb/s in 1985 in Old Tampa Bay (site 23), and remained nearly constant at 0.4 lb/s in Hillsborough Bay (site 18).

Flood and Ebb Constituent-Transport Differences For 1880, 1972, and 1985

Transport patterns of a representative constituent during floodtide conditions for 1880, 1972, and 1985 are shown in figures 45, 46, and 47, respectively. Changes in constituent transport for a typical floodtide between 1880 and 1972 are shown in figure 51, and changes between 1972 and 1985 are shown in figure 52. Comparison of figures 51 and 52 with figures 33 and 34, respectively, shows that similar patterns of change exist between water and constituent transport during floodtide. This similarity is expected because constituent transport is the product of concentration times water transport and because the initial constituent concentrations used for each simulation were the same. The following table summarizes the total area and percentage changes for constituent transport during floodtide between 1880 and 1972 and between 1972 and 1985. The data confirm the general similarity to water transport during floodtide (see p. 49).

Constituent transport, floodtide

Percentage change	Area of change, in square miles	
	1880 to 1972	1972 to 1985
0-10	260	397
11-50	144	41
51-100	52	8
101-200	7	1
>200	1	0

Table 16. Constituent transport and direction during typical ebbtide at selected sites in Tampa Bay for 1880, 1972, and 1985 levels of development

Site no. (see fig. 27)	Transport (pounds per second)			Direction (degrees, clockwise from north)		
	1880	1972	1985	1880	1972	1985
1	1.86	1.82	1.76	290	290	290
2	.728	.712	.734	243	243	244
3	.152	.148	.150	250	250	250
4	.635	.728	.724	224	224	223
5	1.12	1.26	1.32	231	230	231
6	.353	.397	.395	229	266	266
7	1.29	1.19	.800	225	225	224
8	.977	.948	.959	206	206	206
9	1.53	1.52	1.24	206	207	211
10	.997	1.01	1.04	214	217	216
11	1.31	1.22	1.19	216	215	215
12	1.05	.979	.955	203	204	204
13	1.46	1.55	1.61	207	206	203
14	.796	.754	.721	246	247	247
15	1.92	2.55	2.42	234	227	226
16	1.59	1.92	.613	201	215	246
17	1.16	1.29	.809	187	214	199
18	.414	.379	.401	166	167	170
19	.754	.291	.311	172	168	183
20	1.78	2.49	2.44	175	179	179
21	.732	.509	.500	164	143	143
22	1.05	1.45	1.42	137	143	143
23	.593	.897	.884	122	100	100
24	.130	.276	.271	89	134	135
25	.662	.428	.421	129	150	150

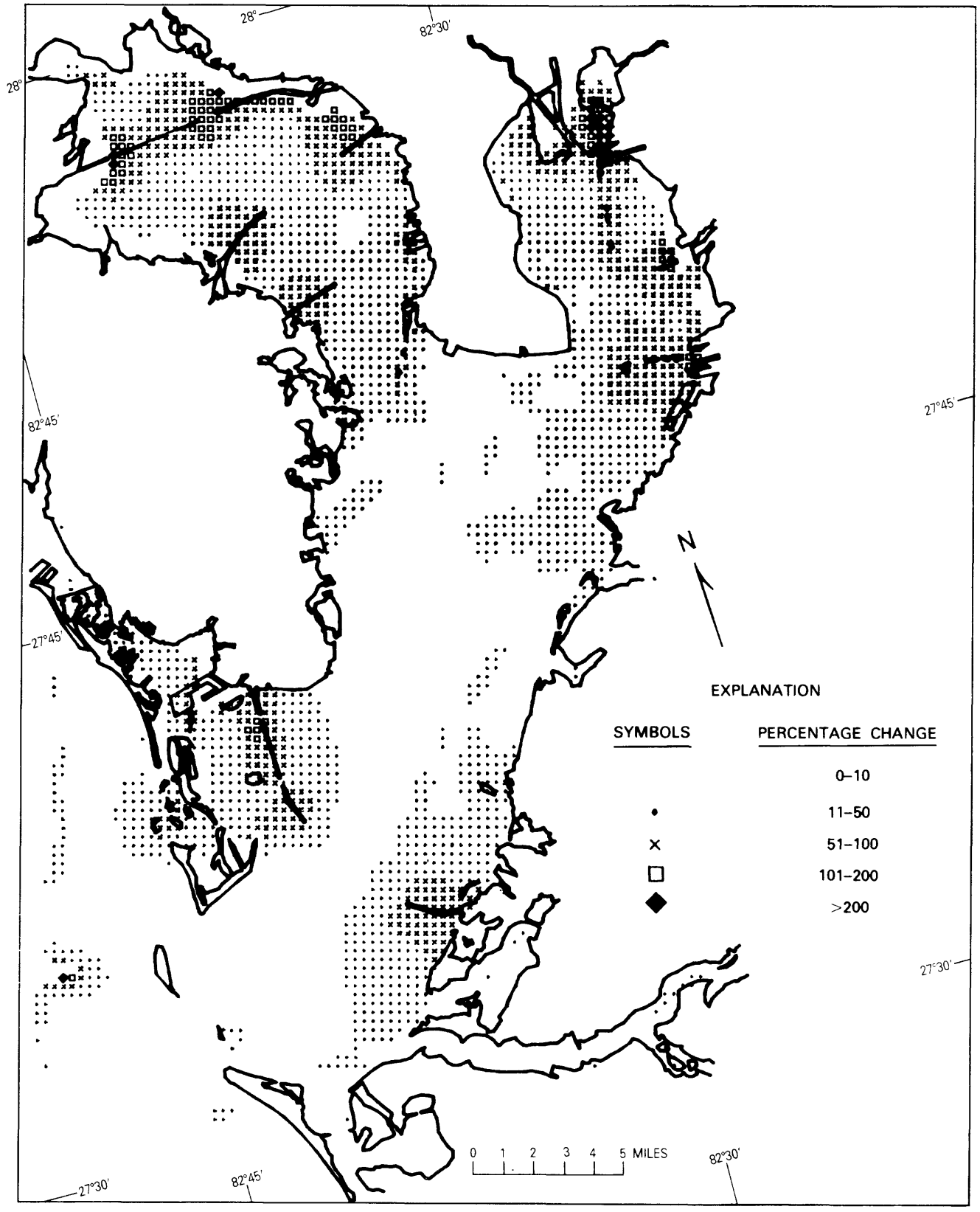

Figure 51. Changes in constituent transport in Tampa Bay for typical floodtide between 1880 and 1972 levels of development.

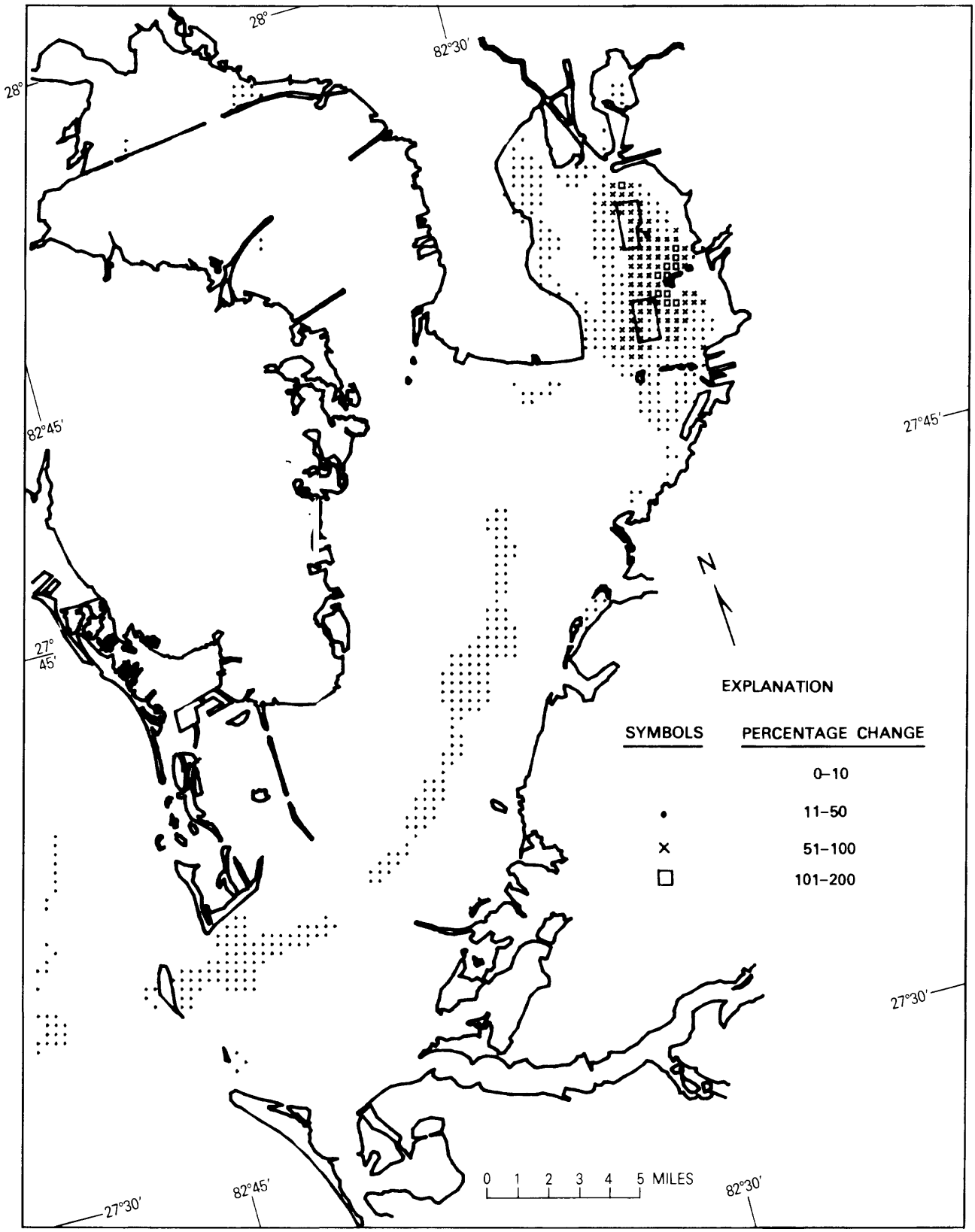

Figure 52. Changes in constituent transport in Tampa Bay for typical floodtide between 1972 and 1985 levels of development.

Transport patterns of a representative constituent during ebbtide conditions for 1880, 1972, and 1985 are shown in figures 48, 49, and 50, respectively. Figure 53 shows changes in constituent transport between 1880 and 1972, and figure 54 shows changes between 1972 and 1985. As with floodtide conditions, ebbtide conditions produce patterns of constituent-transport change that are similar to patterns of water-transport change (see figs. 35 and 36). The following table summarizes the total area and percentage changes for constituent transport during ebbtide. The values are generally comparable to those for water transport at ebbtide.

Constituent transport, ebbtide

Percentage change	Area of change, in square miles	
	1880 to 1972	1972 to 1985
0–10	276	399
11–50	121	31
51–100	53	7
101–200	6	1
>200	0	0

Figure 55 shows flood and ebb constituent transport for each cross section along longitudinal summary lines (see fig. 26) for 1880, 1972, and 1985 levels of development. Typical ebb constituent transport is shown to be low at the Gulf of Mexico but increases to a maximum of about 32 lb/s for 1880 and 30 lb/s for 1985 at mi 25 at the upper end of zone 4, where subsequent transport is divided between zones 5 and 7. Constituent transport decreases to zero at the head of zones 6 and 8. Typical flood constituent transport (see fig. 55) has a longitudinal distribution that is very similar to but of lesser magnitude than that for ebb conditions. Maximum values reach about 24 lb/s for 1880 and 22 lb/s for 1985. The change in transport at mi 37 in figure 55 for 1972 and 1985 conditions corresponds to the location where tide-induced circulation in 1972 and 1985 increased significantly over that for 1880 conditions (see fig. 44).

Progressive constituent-transport reductions throughout the bay over time (fig. 55) are largely caused by similar reductions in water transport (fig. 37). Constituent-transport values and percentage changes among levels of development are given in table 17 for the seaward end of each bay subarea. Comparison of percentage-change figures between water and constituent transport, tables 12 and 17, respectively, shows a substantial difference only at the seaward end of Hillsborough Bay between 1880 and 1972. This difference indicates that constituent concentrations in Hillsborough Bay during the simulation period of 48 hours were reduced more for 1972 and 1985 conditions than for 1880 conditions. Simulations were not sufficiently long, however, to determine equilibrium concentrations for each level of development.

Residual Constituent Transport

Figures 56, 57, and 58, show residual constituent-transport patterns for 1880, 1972, and 1985 levels of development, respectively. Each map shows the same series of circulatory features or gyres found for residual water transport (see figs. 38–40). Vector magnitudes defining constituent-transport gyre intensity are different than those defining water-transport gyre intensity because of the influence of the concentration distribution. The most intense constituent-transport gyres occur in the upper parts of Tampa Bay in areas of high concentrations.

Residual constituent-transport vector magnitudes and directions are given in table 18 for 25 selected sites (see fig. 27 for location of sites). Vector magnitudes were computed to be about 0.17 lb/s at the entrance to Tampa Bay (site 1) for all three levels of development, to range from 0.04 lb/s in 1880 to 0.03 lb/s in 1985 in mid-Tampa Bay (site 9), to range from 0.03 lb/s in 1880 to 0.07 lb/s in 1985 in Old Tampa Bay (site 23), and to range from 0.06 lb/s in 1880 to 0.07 lb/s in 1985 in Hillsborough Bay (site 18).

Table 17. Flood and ebb constituent transport and percentage changes in Tampa Bay for 1880, 1972, and 1985 levels of development

Area	Constituent transport (pounds per second)			Percentage change		
	1880	1972	1985	1880 to 1972	1972 to 1985	1880 to 1985
During typical floodtide, computed at the seaward end						
Lower Tampa Bay	5.22	4.93	4.89	− 5.6	−0.8	− 6.3
Middle Tampa Bay	13.7	13.1	13.0	− 4.4	− .8	− 5.1
Old Tampa Bay	13.9	13.3	13.2	− 4.3	− .8	− 5.0
Hillsborough Bay	9.46	8.29	7.71	−12.4	−7.0	−18.5
During typical ebbtide, computed at the seaward end						
Lower Tampa Bay	9.94	9.65	9.44	− 2.9	−2.2	− 5.0
Middle Tampa Bay	21.5	20.9	20.5	− 2.8	−1.9	− 4.7
Old Tampa Bay	15.6	14.8	14.6	− 5.1	−1.4	− 6.4
Hillsborough Tampa Bay	14.5	13.1	12.3	− 9.7	−6.1	−15.2

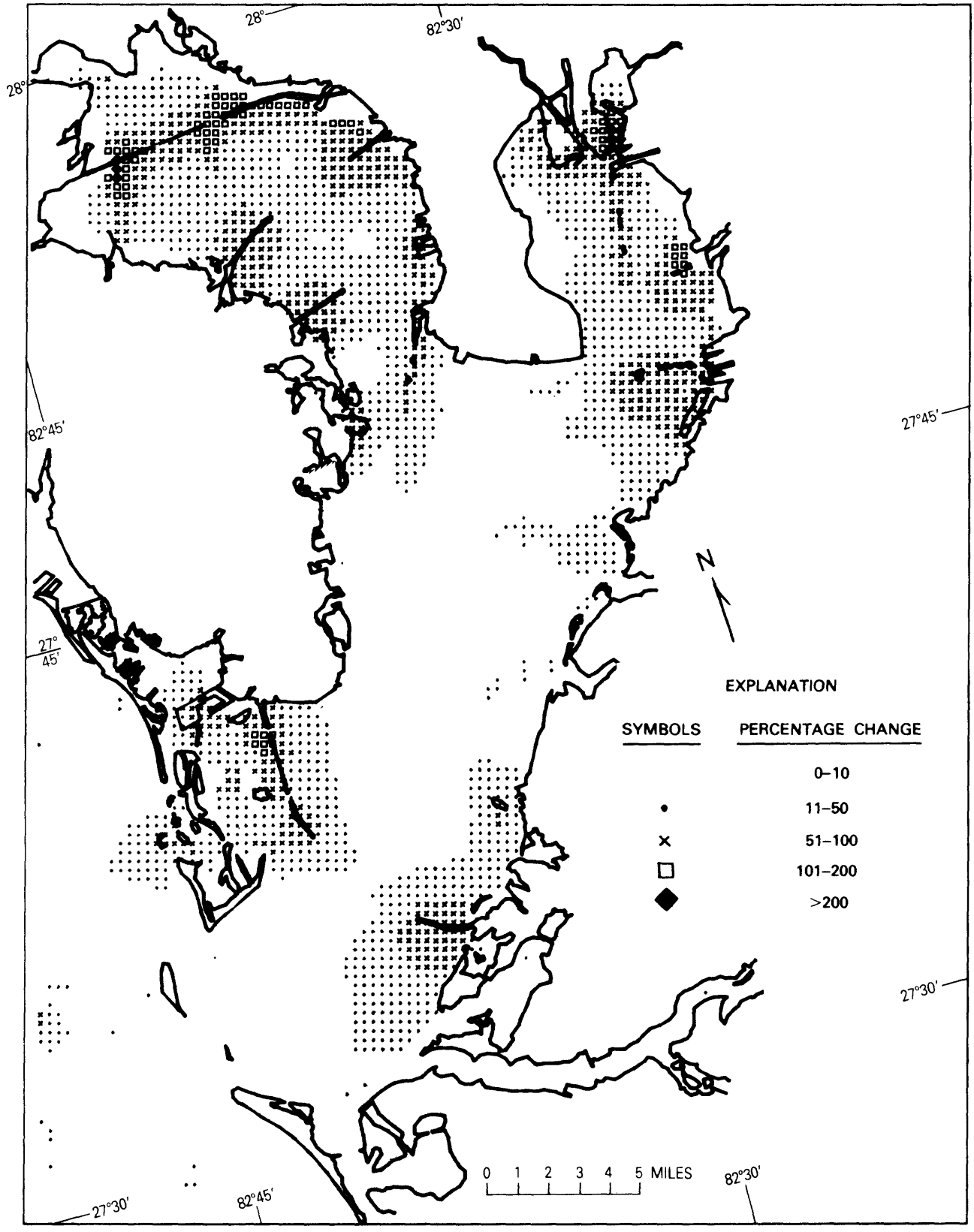

Figure 53. Changes in constituent transport in Tampa Bay for typical ebbtide between 1880 and 1972 levels of development.

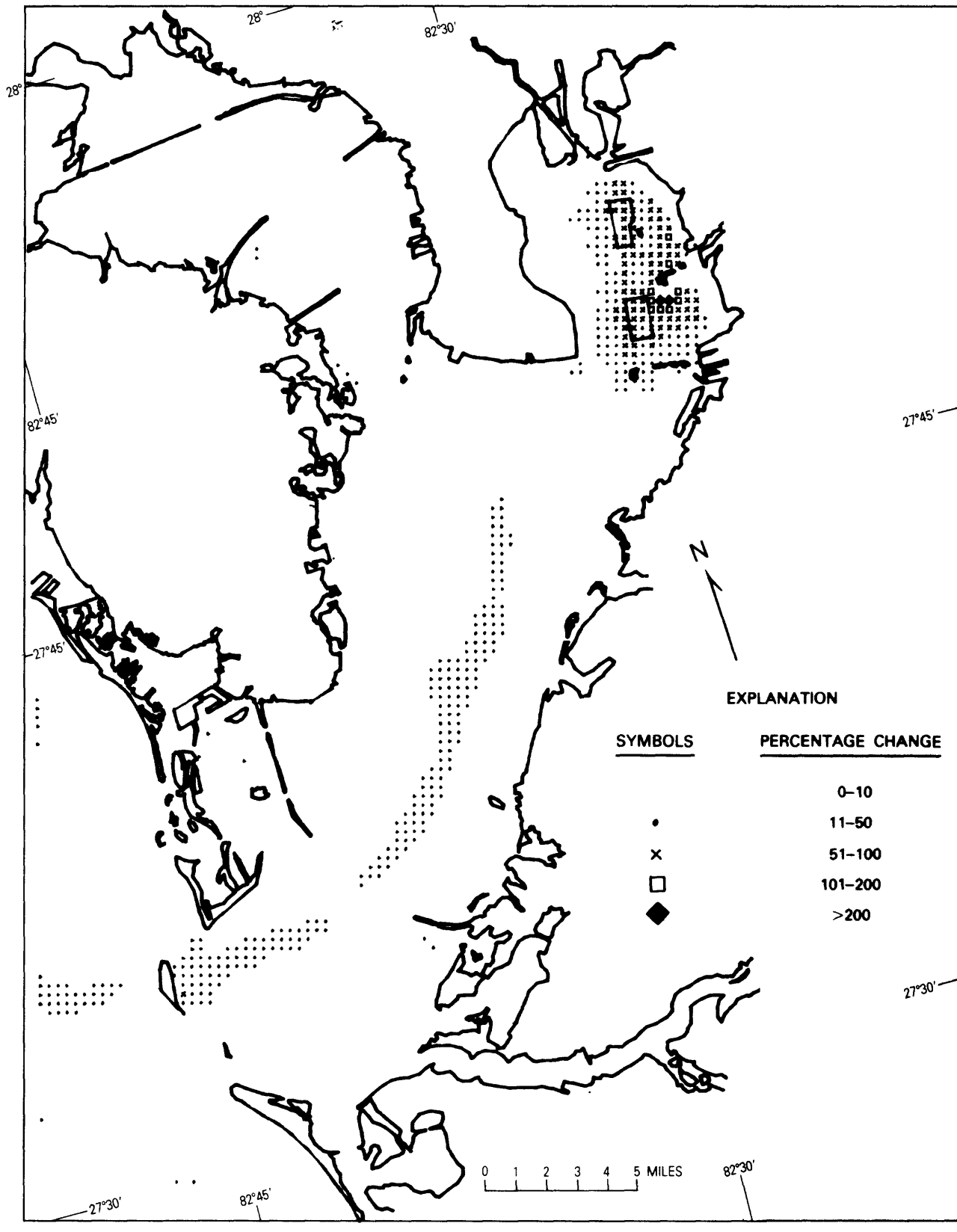

Figure 54. Changes in constituent transport in Tampa Bay for typical ebbtide between 1972 and 1985 levels of development.

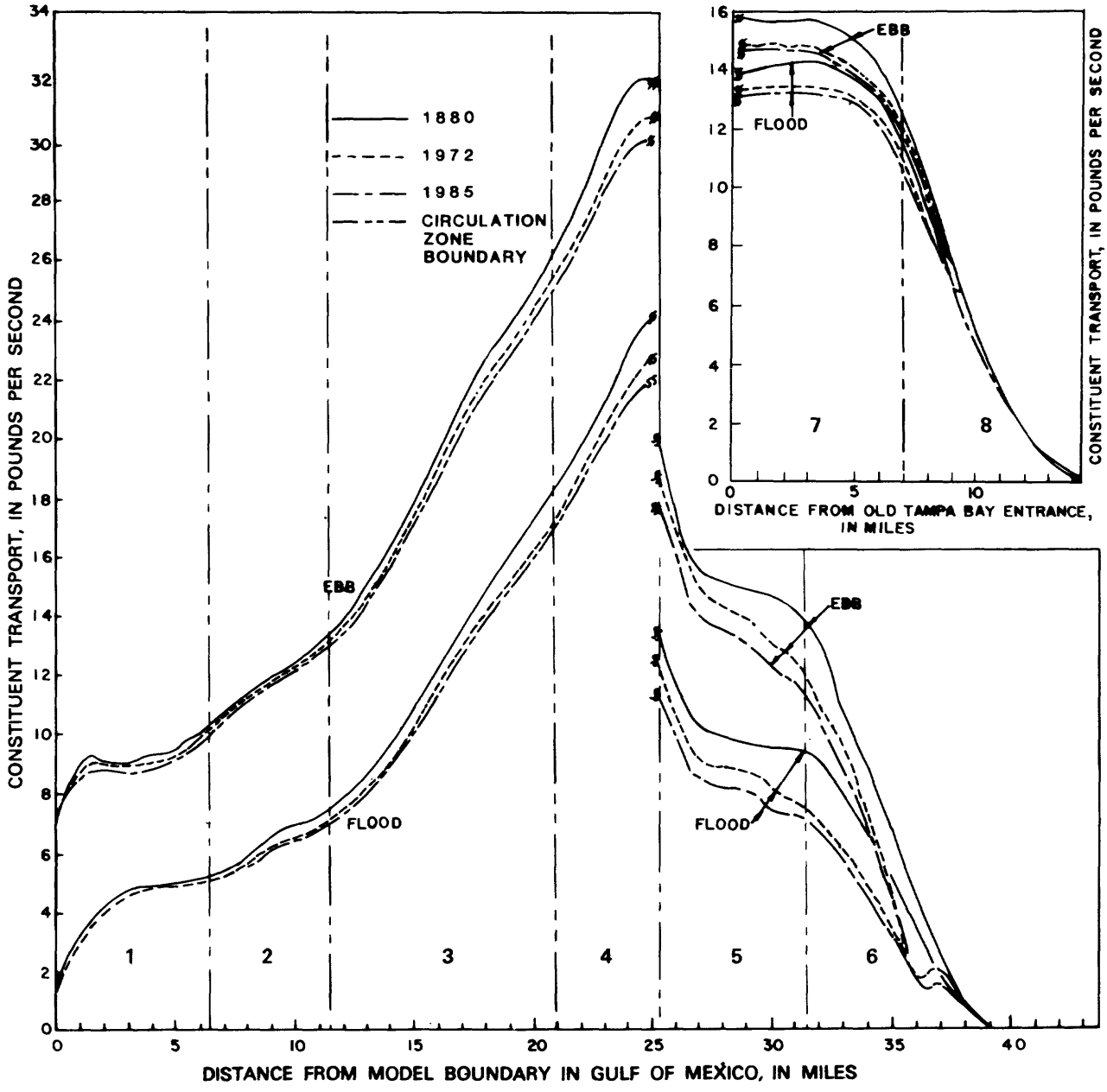

Figure 55. Constituent transport along longitudinal summary lines (see fig. 26) during typical floodtide and ebbtide in Tampa Bay for 1880, 1972, and 1985 levels of development.

Residual Constituent-Transport Differences For 1880, 1972, and 1985

Figures 56, 57, and 58 show patterns of residual constituent transport for 1880, 1972, and 1985 levels of development, respectively. Areas of change in residual constituent transport between 1880 and 1972 are shown in figure 59, and changes between 1972 and 1985 are shown in figure 60. As with previously discussed difference patterns (p. 71 and 74), residual water-transport and residual constituent-transport changes are similar. Comparison of figures 59 and 60 with figures 42 and 43, respectively, shows the similarity of patterns. The following table summarizes the total area and percentage changes in residual constituent transport. The values confirm the general similarity with areas of change computed for residual water transport (p. 61).

Residual constituent transport

Percentage change	Area of change, in square miles	
	1880 to 1972	1972 to 1985
0-10	98	241
11-50	166	144
51-100	83	32
101-200	72	24
>200	45	6

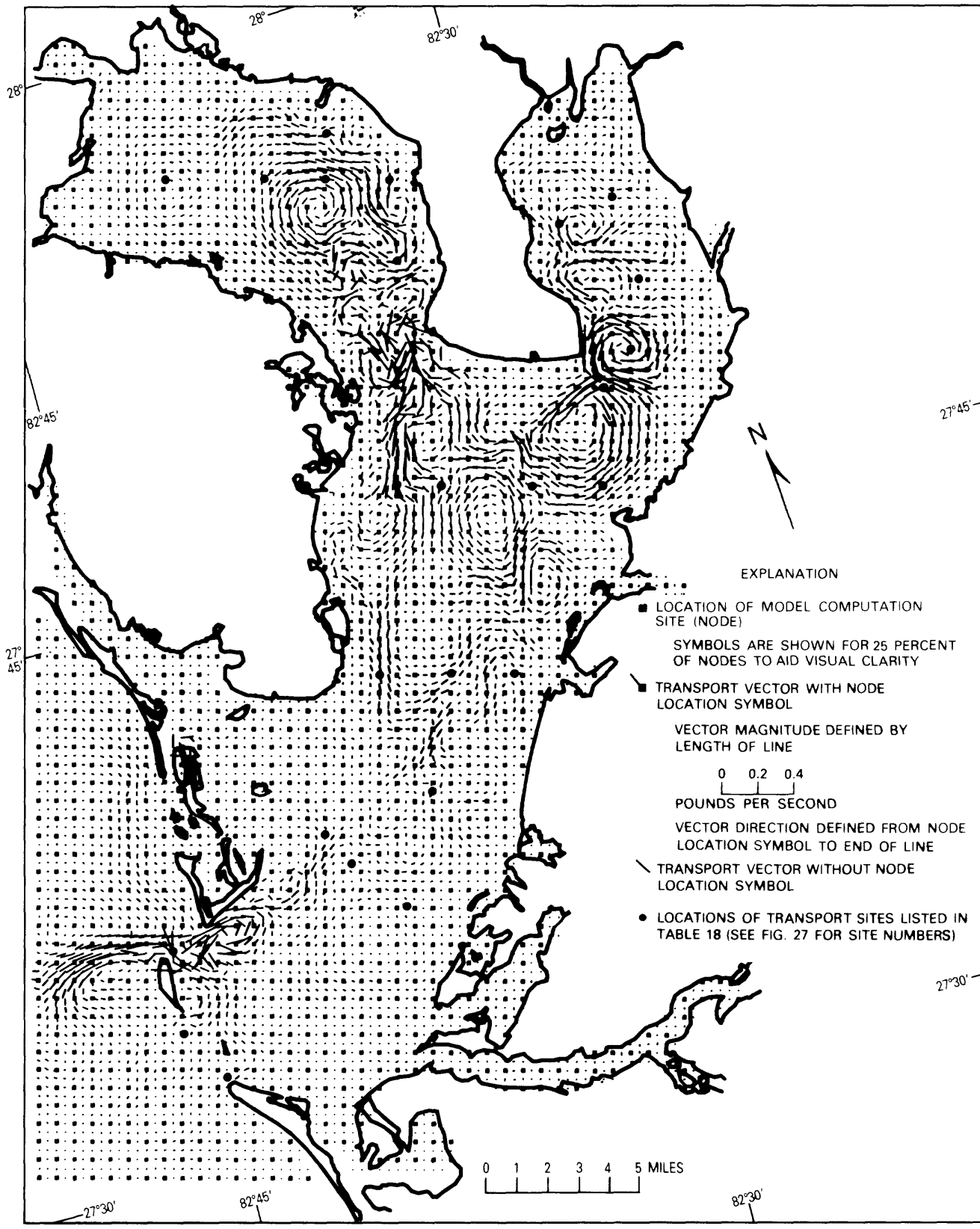

Figure 56. Residual constituent-transport pattern in Tampa Bay for 1880 level of development.

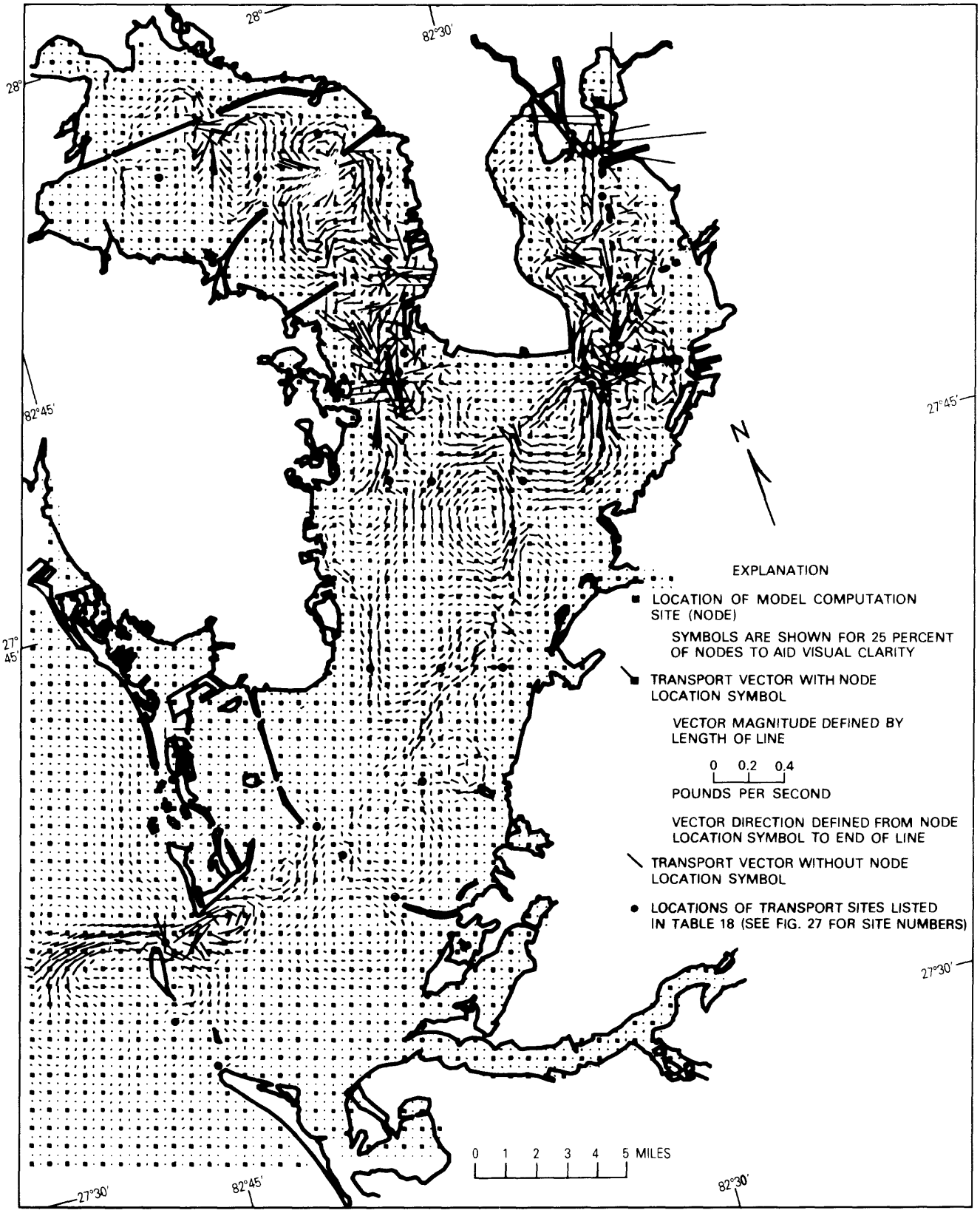

Figure 57. Residual constituent-transport pattern in Tampa Bay for 1972 level of development.

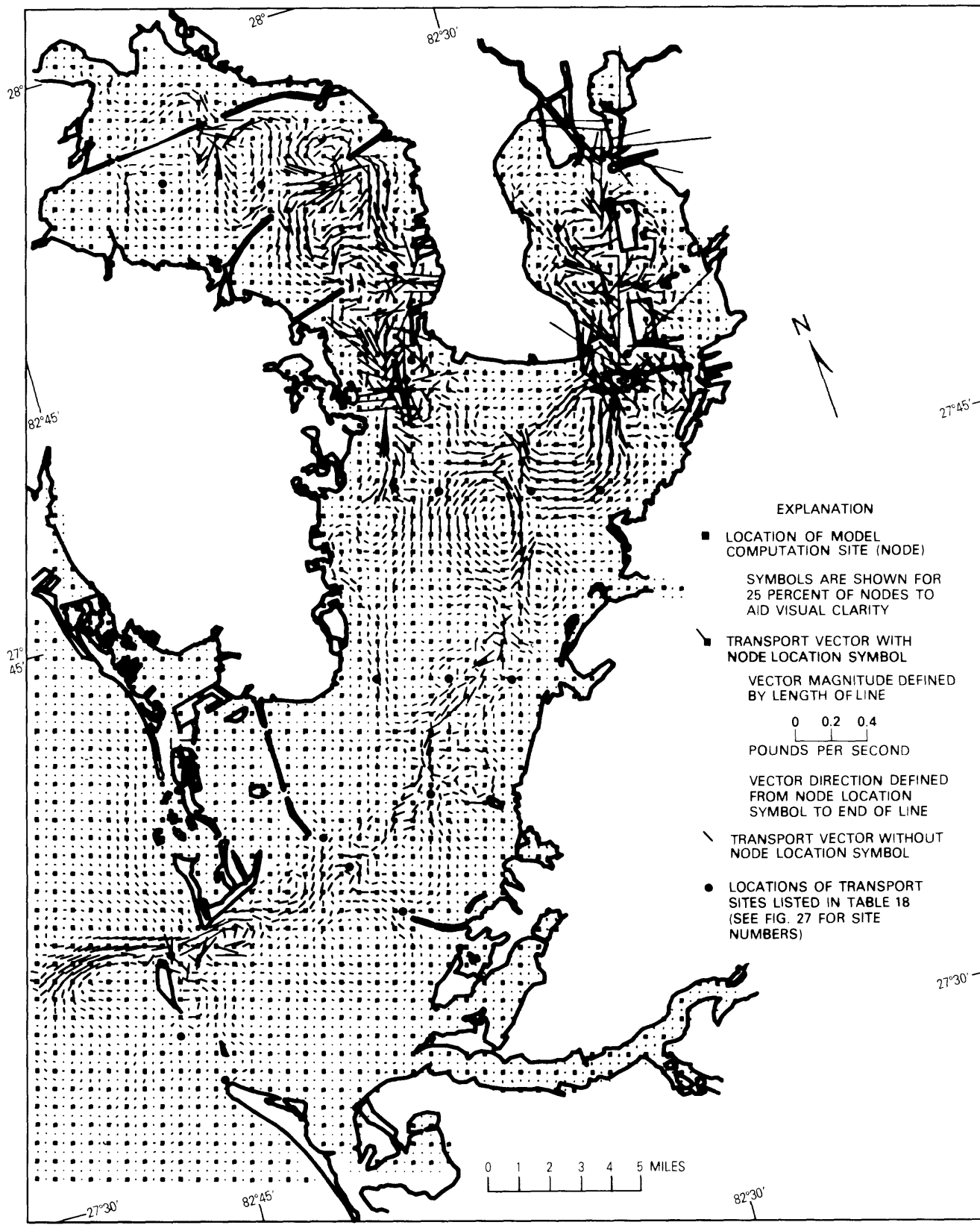

Figure 58. Residual constituent-transport pattern in Tampa Bay for 1985 level of development.

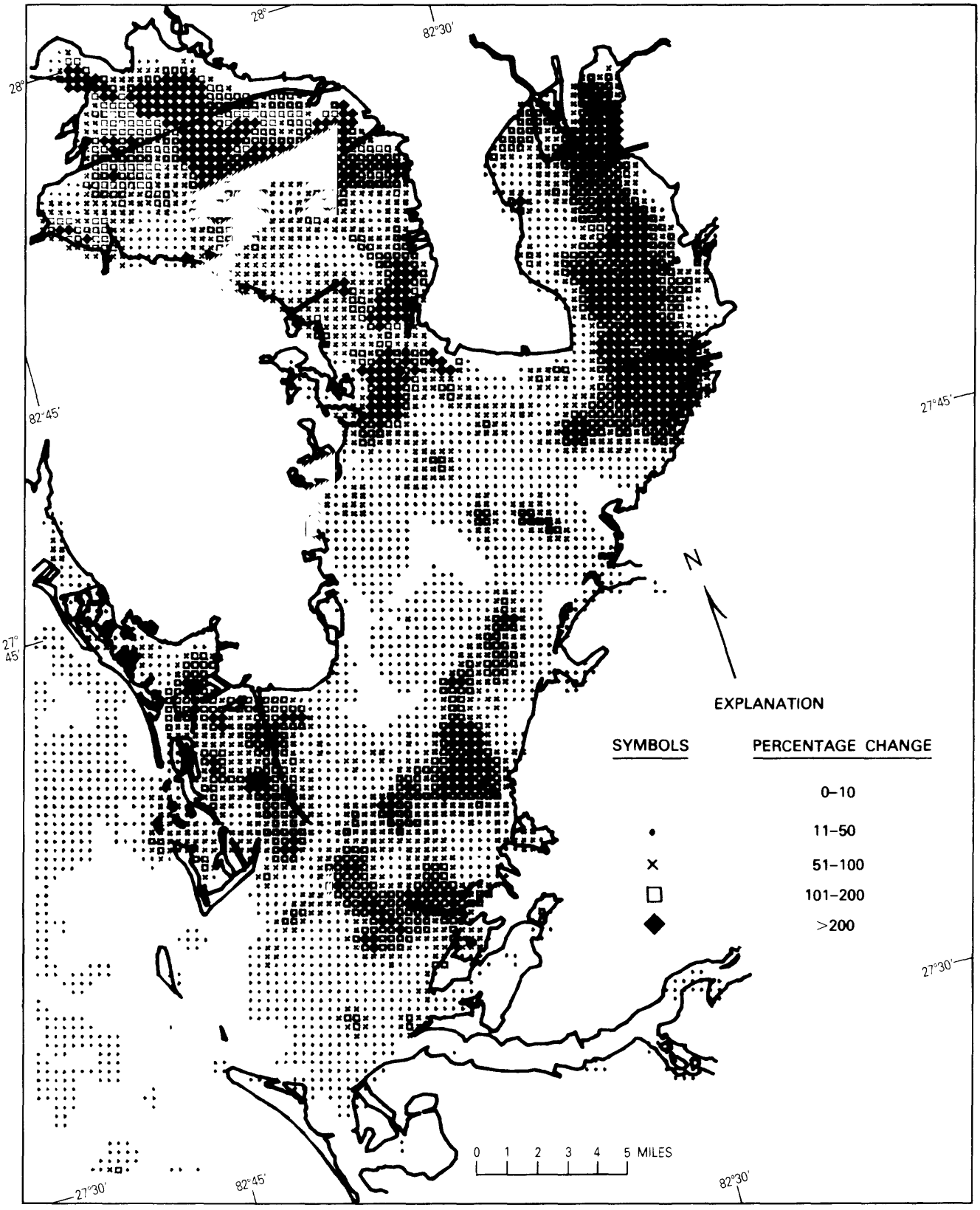

Figure 59. Changes in residual constituent transport in Tampa Bay between 1880 and 1972 levels of development.

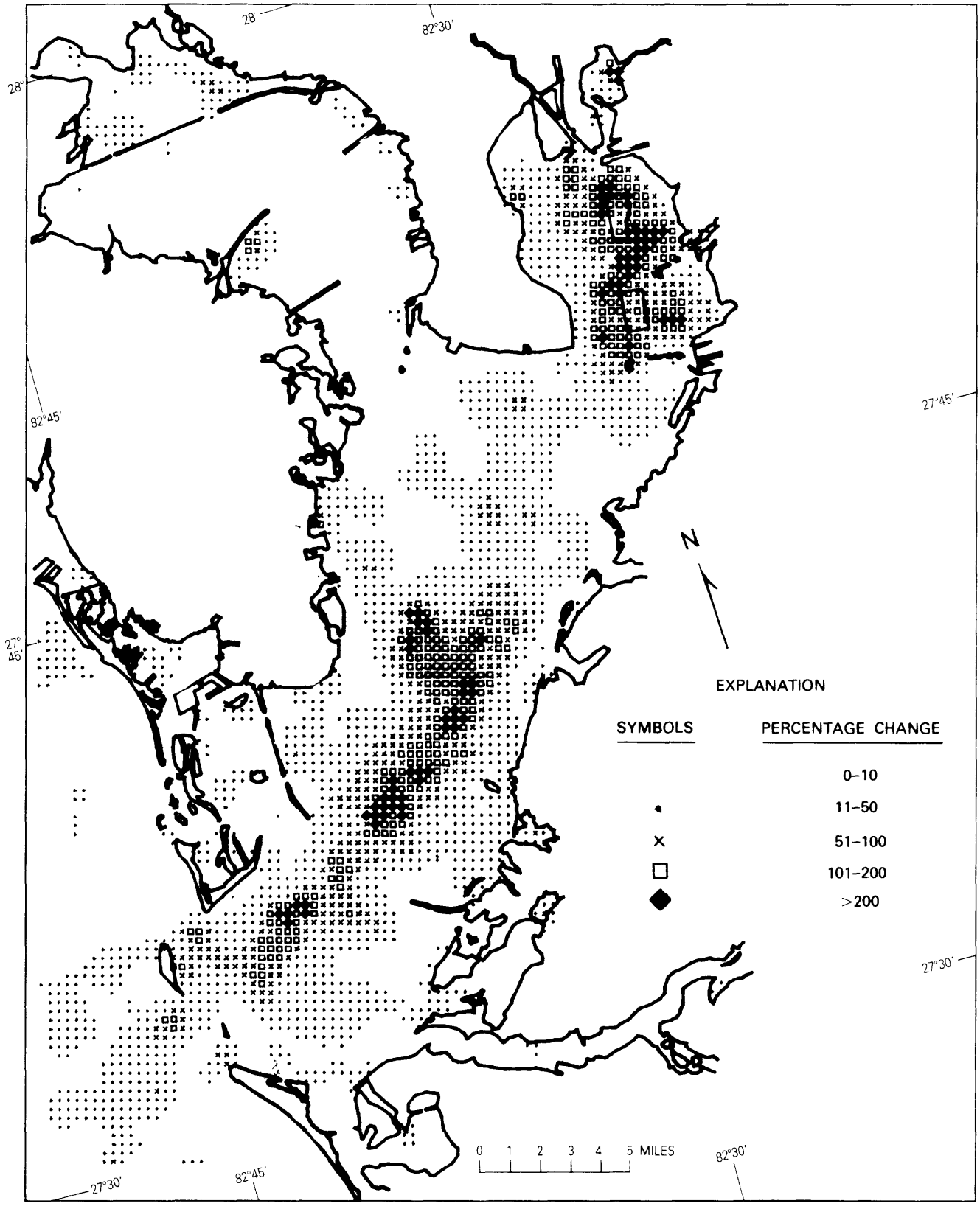

Figure 60. Changes in residual constituent transport in Tampa Bay between 1972 and 1985 levels of development.

Table 18. Residual constituent transport and direction at selected sites in Tampa Bay for 1880, 1972, and 1985 levels of development

Site no. (see fig. 27)	Transport (pounds per second)			Direction (degrees, clockwise from north)		
	1880	1972	1985	1880	1972	1985
1	0.177	0.168	0.167	288	287	285
2	.032	.031	.028	119	118	130
3	.025	.024	.023	60	60	60
4	.019	.018	.017	207	199	198
5	.015	.023	.040	334	309	290
6	.006	.034	.032	291	265	264
7	.034	.032	.027	226	257	227
8	.056	.054	.050	179	177	177
9	.038	.040	.029	72	63	220
10	.022	.043	.038	310	286	289
11	.076	.079	.075	205	212	210
12	.040	.037	.033	192	228	219
13	.057	.071	.072	344	357	9
14	.072	.072	.068	261	259	257
15	.117	.125	.139	153	174	176
16	.032	.380	.774	83	59	59
17	.020	.043	.145	3	229	280
18	.064	.059	.071	188	173	176
19	.025	.032	.088	284	149	74
20	.070	.111	.108	58	194	195
21	.047	.078	.077	32	26	26
22	.093	.203	.201	290	282	283
23	.028	.071	.070	179	78	78
24	.019	.066	.064	210	189	189
25	.043	.072	.071	278	86	86

Tide-induced flushing, for purposes of this report, can be defined as total constituent flushing (see Longitudinal Summary section, p. 37), minus the constituent transport caused by tributary streamflow. Figure 61 shows both computed tide-induced and streamflow flushing for 1880, 1972, and 1985 levels of development. Results are not given for Old Tampa Bay because tide-induced flushing is effectively zero due to the nearly constant constituent distribution (see fig. 23). For the constituent used in this study, concentrations are highest near the head of Hillsborough Bay (see fig. 23) and decrease toward the Gulf of Mexico. Such a distribution produces larger flushing by streamflow in Hillsborough Bay than in lower Tampa Bay (fig. 61).

For the example constituent, tide-induced flushing is generally low, between 2,000 and 6,000 lb/d in zones 1, 2, and 3 for all three levels of development (table 19). Zone 4 is an area of high tide-induced flushing, and zones 5 and 6 are areas of progressively lower flushing. Tide-induced flushing for 1972 and 1985 conditions is generally greater than for 1880 conditions. Average flushing for each zone in the bay and percentage changes among 1880, 1972, and 1985 are given in table 19 (see fig. 26 for location of zones).

Average tide-induced flushing changes in zones 1, 2, and 3 are generally consistent with tide-induced circulation changes shown in table 14. An overall tide-induced flushing decrease of less than 1 percent occurred in zone 1; an increase of about 41 percent occurred in zone 2, and an increase of about 16 percent occurred in zone 3. For the example constituent distribution, a flushing minimum occurred in zone 2 in the lower part of Tampa Bay (fig. 61 and table 19), whereas a circulation minimum occurred in zone 3 (fig. 44 and table 14).

A computed 14-percent increase (table 19) in tide-induced flushing between 1880 and 1972 in zone 4 is difficult to understand because computed tide-induced circulation decreased by about 8 percent in the zone during the same period (table 14). The cause for this condition is apparently linked to increases in circulation in zone 5, and possibly zone 7, between 1880 and 1972. Tide-induced flushing is determined both by circulation and the distribution of constituent carried by the circulating water. Therefore, the amounts of constituent material

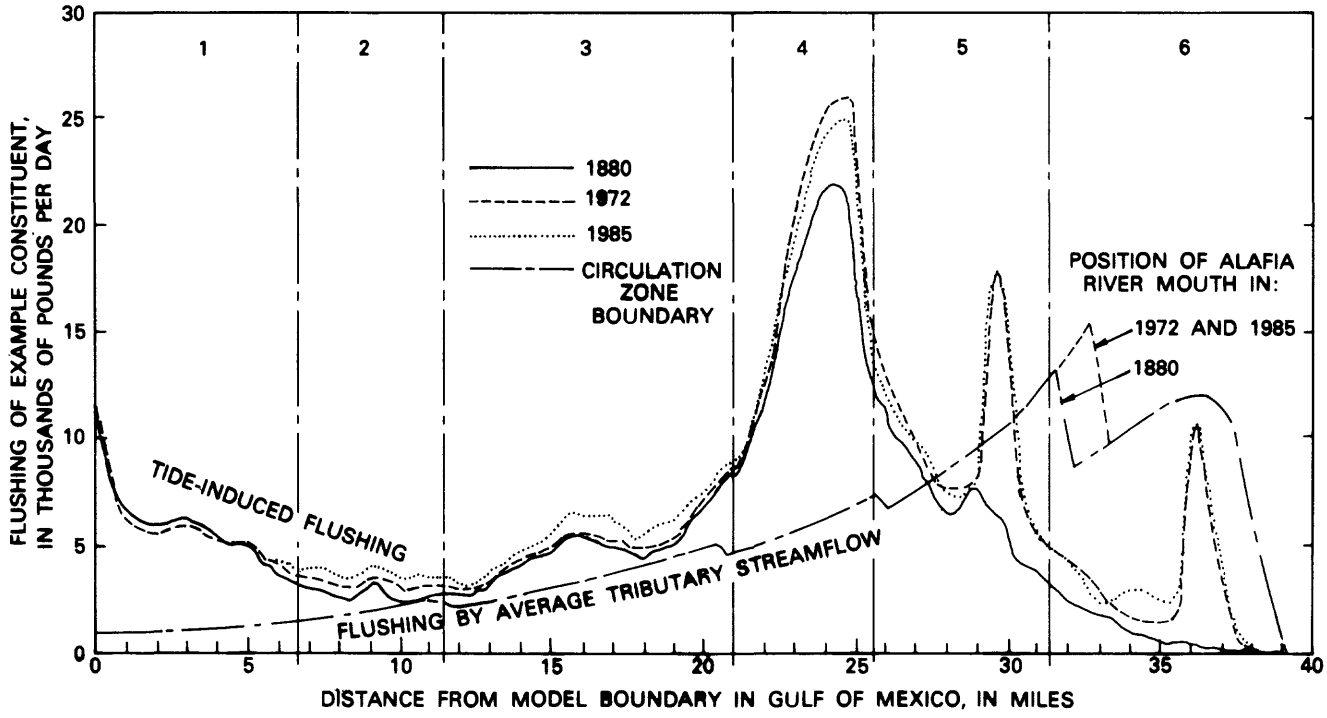

Figure 61. Tide-induced and streamflow flushing of example constituent along longitudinal summary line (see fig. 26) from lower Tampa Bay to Hillsborough Bay for 1880, 1972, and 1985 levels of development.

flushed into zone 4 from zones 5 and 7 probably caused significantly different constituent distributions in 1972 and 1880. The computed 1972 distribution was apparently sufficient to more than offset the reduced 1972 circulation. A 4-percent reduction in tide-induced flushing occurred in zone 4 between 1972 and 1985.

In zone 5, streamflow and tide-induced circulation produce about equal rates of flushing for the example constituent. Computations indicate that powerplant cooling-water circulation and other physical changes will produce an overall increase in tide-induced flushing of about 37 percent by 1985.

In 1880, the primary flushing mechanism in zone 6 was tributary streamflow. Powerplant cooling-water circulation at mi 36 (see fig. 61), ship-channel construction, and shoreline filling expected through 1985 contribute to tide-induced flushing increases of more than 250 percent between 1880 and 1985. Streamflow, however, remained the dominant flushing mechanism in zone 6.

This analysis shows that changes to Tampa Bay since 1880 have generally increased tide-induced flushing of a hypothetical constituent having a concentration distribution similar to that shown in figure 23. Most increases were caused by physical changes in the bay between 1880 and 1972. Assuming that streamflow and upland constituent inflow remain constant, this greater rate of flushing will cause lower concentration levels throughout the bay. Greater flushing also will cause a rise in concentration levels of constituents that have seaward sources.

SUMMARY

Changes in two-dimensional tidal flow, circulation, and flushing caused by dredge and fill construction in Tampa

Table 19. Tide-induced flushing and percentage changes in Tampa Bay for 1880, 1972, and 1985 levels of development

Circulation zone (see fig. 26)	Average tide-induced flushing (pounds per day)			Percentage change		
	1880	1972	1985	1880 to 1972	1972 to 1985	1880 to 1985
1	5,930	5,830	5,890	− 1.7	+ 1.0	− 0.7
2	2,560	3,320	3,740	+ 25.3	+12.6	+ 41.1
3	4,910	5,180	5,720	+ 5.5	+10.4	+ 16.5
4	16,300	18,560	17,900	+ 13.9	− 3.6	+ 9.8
5	7,070	9,830	9,650	+ 39.0	− 1.8	+ 36.5
6	1,150	3,950	4,100	+243	+ 3.8	+257

Bay are determined in this study by using finite-difference computer simulation techniques. Three levels of development were chosen for comparison:

1. conditions in 1880 prior to any significant manmade physical changes to the bay;
2. conditions in 1972 after construction of numerous causeways, islands, shoreline fills, and a series of ship channels serving the Port of Tampa; and
3. conditions projected for 1985 after completion of a Federal dredging project that requires excavation and deposition of about 70 million yd^3 of material.

Physical changes to Tampa Bay since 1880 have caused a progressive reduction in the quantity of water that enters and leaves the bay. Flow reductions that averaged about 4 percent from 1880 to 1972 and 1 percent from 1972 to 1985 are a result of reductions in intertidal water volume, or tidal prism, caused by filling of the bay. Hillsborough Bay has had the largest changes in tidal flows. Flow reductions into and out of Hillsborough Bay were computed to be about 8 percent from 1880 to 1972 and about 7 percent from 1972 to 1985. Hillsborough Bay also had the largest percentage reduction in tidal prism.

Dredged and filled areas have changed the magnitude and direction of tidal floodflows and ebbflows in large parts of the bay. Areas near islands, causeways, channels, and shoreline fills have been affected most. Total flood and ebb transport were changed by more than 50 percent over about 58 mi^2 of the bay from 1880 to 1972. Similar changes from 1972 to 1985 occurred over only 8 mi^2.

Residual water-transport maps for each level of development show a sequence of about 20 circulatory features, or gyres, that are thought to either control or have a large influence on the long-term interchange of water and constituents between sections of Tampa Bay and between the bay and the Gulf of Mexico. The overall circulation patterns in 1880, 1972, and 1985 are visually similar, with some areas of obvious differences, mostly at and near areas of physical change. Gyre intensity can be reduced or increased, gyre location can be shifted, new gyres can be created, old gyres can be destroyed, and gyre shape can be distorted by these physical changes.

Areas of residual water-transport change are several times larger than those computed for tidal flood- and ebb-transport change. Residual changes of more than 50 percent occurred in about 167 mi^2 from 1880 to 1972. About 57 mi^2 were changed by the same amount from 1972 to 1985. Between 1880 and 1972, large residual water-transport changes occurred throughout most of Hillsborough and Old Tampa Bays due to dredge and fill activity. Another area of large residual change from 1880 to 1972 was lower Tampa Bay; the increase was due to residential, causeway, and ship-channel construction. From 1972 to 1985, Hillsborough and lower Tampa Bays also had large residual changes, as a result of ship-channel and island construction.

Similarities among computed tide-induced circulation for the three levels of development that were studied in Tampa Bay are evident. In an area that includes the entrance to the bay, computed circulation was very high and ranged from 45,500 ft^3/s (1880) to 41,000 ft^3/s (1985). Computed circulation between middle and lower Tampa Bays, an area of apparent circulation constriction, ranged from 4,900 ft^3/s (1880) to 6,300 ft^3/s (1985), lower than circulation computed for adjacent bayward and seaward areas. Circulation in an area seaward of the entrances to both Hillsborough and Old Tampa Bays ranged from 8,600 ft^3/s (1880) to 7,800 ft^3/s (1985). Circulation decreased to zero at the heads of Hillsborough and Old Tampa Bays.

Eight zones have been identified on the basis of tide-induced circulation characteristics in Tampa Bay. Three three-zone sequences have also been identified and associated with the three named bays within the Tampa Bay system. Tampa Bay, Hillsborough Bay, and Old Tampa Bay each appear to have a zone of high circulation either at or seaward of their respective bay entrances. Each also has a zone of low circulation at some distance bayward of their entrances. A zone of transition separates each high and low circulation zone.

Tide-induced circulation increased throughout most of Tampa Bay in response to physical changes made since 1880. The greatest circulation increase, 225 percent, occurred in the upper part of Hillsborough Bay from 1880 to 1972. A 15-percent increase was computed for that area for 1972 to 1985. In the zone of circulation constriction, between middle and lower Tampa Bay, increases of 6 and 22 percent occurred from 1880 to 1972 and from 1972 to 1985, respectively. Large localized increases in circulation were caused by pumping for powerplant cooling-water systems. A reduction of about 4 percent in tide-induced circulation occurred near the mouth of Tampa Bay from 1880 to 1972. A reduction of about 6 percent occurred from 1972 to 1985.

Transport and flushing of a representative constituent was investigated in this study. The constituent distribution used in the model approximated that of phosphorus measured in July 1975. Highest concentrations, 1.5–2.5 mg/L, were in Hillsborough Bay. Concentrations were nearly constant at 0.8 mg/L in Old Tampa Bay and decreased to less than 0.2 mg/L at the entrance to Tampa Bay.

Flood and ebb constituent transport reached maximum values of about 24 lb/s and 32 lb/s, respectively, in the upper part of middle Tampa Bay in 1880 and decreased toward the Gulf and toward the heads of Hillsborough and Old Tampa Bays. Physical changes since 1880 caused reductions in flood and ebb constituent transport, similar to those for flood and ebb water transport, because of reductions in tidal prism as a result of manmade intertidal fills.

Residual constituent-transport maps show gyre features similar to those computed for residual water transport. Vector magnitudes are proportionately larger, however, for those gyres in regions of high constituent concentration and proportionately smaller in regions of low concentration. Areas of computed change in flood, ebb, and residual constituent transport are in all respects very similar to the corresponding changes computed for flood, ebb, and residual water transport.

In most areas of Tampa Bay, constituent flushing of the example constituent induced by the tide is greater than that induced by streamflow. In most of Hillsborough Bay, particularly the upper part, flushing by streamflow is larger than tide-induced flushing for all three levels of development. Tide-induced constituent flushing increased throughout most of the bay in response to physical changes that have been made since 1880. The greatest tide-induced flushing increase, 243 percent, occurred in Hillsborough Bay from 1880 to 1972. A 4-percent increase occurred in Hillsborough Bay from 1972 to 1985. In a zone of apparent flushing constriction in the middle of lower Tampa Bay, tide-induced flushing increased 25 percent from 1880 to 1972 and 13 percent from 1972 to 1985. Large local increases in flushing were caused by pumping for powerplant cooling-water systems.

As a result of increases in tide-induced circulation and flushing due to physical changes to Tampa Bay made since 1880, the bay can now more rapidly transfer waterborne constituents that have landward sources to the Gulf of Mexico. Conversely, the bay can also more rapidly transfer constituents that have their source in the Gulf into the upper parts of the bay.

SELECTED REFERENCES

April, G. C., Hill, D. O., and Liu, Hua-An, 1975, Hydrodynamic and material transport model for Mobile Bay, Alabama, *in* Symposium on modeling techniques: American Society of Civil Engineers Conference, San Francisco, Calif., September 3-5, 1975, Proceedings, p. 764-782.

Beauchamp, C. H., and Spaulding, M. F., 1978, Tidal circulation in coastal seas, *in* Verification of mathematical and physical models in hydraulic engineering: American Society of Civil Engineers Specialty Conference, College Park, Md., August 9-11, 1978, Proceedings, p. 518-528.

Buchanan, T. J., and Somers, W. P., 1969, Discharge measurements at gaging stations: U.S. Geological Survey Techniques of Water-Resources Investigations Book 3, Chap. A8, 65 p.

Cheng, R. T., and Casulli, Vincenzo, 1982, On Lagrangian residual currents with applications in south San Francisco Bay, California: Water Resources Research, v. 18, no. 6, p. 1652-1662.

Cheng, R. T., and Gartner, J. W., 1985, Harmonic analysis of tides and tidal currents in South San Francisco Bay, California: Estuarine, Coastal, and Shelf Science, London, Academic Press, v. 21, p. 52-74.

Dinardi, D. A., 1978, Tampa Bay circulatory survey 1963: National Ocean Survey Oceanographic Circulatory Survey Report No. 2, National Oceanic and Atmospheric Administration, 39 p.

Dronkers, J. J., 1964, Tidal computations: Amsterdam, North Holland Publishing Company, 518 p.

Elder, J. W., 1959, The dispersion of marked fluid in turbulent shear flow: Journal of Fluid Mechanics, v. 5, p. 544-560.

Fischer, H. B., List, J. E., Imberger, Jorg, and Brooks, N. H., 1979, Mixing in inland and coastal waters: New York, Academic Press, 483 p.

Giovannelli, R. F., 1981, Relation between freshwater flow and salinity distributions in the Alafia River, Bullfrog Creek, and Hillsborough Bay, Florida: U.S. Geological Survey Water-Resources Investigations 80-102, 68 p.

Goetz, C. L., and Goodwin, C. R., 1980, Water quality of Tampa Bay, Florida: June 1972-May 1976: U.S. Geological Survey Water-Resources Investigations 80-12, 55 p.

Goodwin, C. R., 1977, Circulation patterns for historical, existing, and proposed channel configurations in Hillsborough Bay, Florida: International Navigation Congress, 24th, subject 4, sec. 4, Proceedings, p. 167-179.

———1980, Preliminary simulated tidal flow and circulation patterns in Hillsborough Bay, Florida: U.S. Geological Survey Open-File Report 80-1021, 28 p.

Goodwin, C. R., and Michaelis, D. M., 1976, Tides in Tampa Bay, Florida: June 1971 to December 1973: U.S. Geological Survey Open-File Report FL-75004, 338 p.

———1984, Appearance and water quality of turbidity plumes produced by dredging in Tampa Bay, Florida: U.S. Geological Survey Water-Supply Paper 2192, 66 p.

Goodwin, C. R., Rosenshein, J. S., and Michaelis, D. M., 1974, Water quality of Tampa Bay, Florida: Dry weather conditions, June 1971: U.S. Geological Survey Open-File Report FL-74026, 85 p.

———1975, Water quality of Tampa Bay, Florida: Wet-weather conditions, October 1971: U.S. Geological Survey Open-File Report FL-75005, 88 p.

Gren, G. G., 1976, Hydraulic dredges, including boosters, *in* Dredging and its environmental effects: American Society of Civil Engineers Specialty Conference, Mobile, Ala., January 26-28, 1976, Proceedings, p. 115-124.

Heath, R. C., and Conover, C. S., 1981, Hydrologic almanac of Florida: U.S. Geological Survey Open-File Report 81-1107, 239 p.

Holley, E. R., 1969, Unified view of diffusion and dispersion: American Society of Civil Engineers, v. 95, no. HY2, Proceedings, p. 621-631.

Leendertse, J. J., 1970, A water-quality simulation model for well-mixed estuaries and coastal seas: Volume I, Principles of computation: Santa Monica, Calif., The Rand Corporation, RM-6230-RC, 71 p.

———1972, A water-quality simulation model for well-mixed estuaries and coastal seas: Volume IV, Jamaica Bay tidal flows: New York, The New York City Rand Institute, R-1009-NYC, 48 p.

Leendertse, J. J., and Gritton, E. C., 1971, A water-quality simulation model for well-mixed estuaries and coastal seas: Volume II, Computation procedures: New York, The New York City Rand Institute, R-708-NYC, 48 p.

Leendertse, J. J., and Liu, Shiao-Kung, 1974, A water-quality simulation model for well-mixed estuaries and coastal seas: Volume VI, Simulation observation and state estimation: New York, The New York City Rand Institute, R-1586-NYC, 103 p.

Lewis, R. R., and Whitman, R. L., 1985, A new geographic description of the boundaries and subdivisions of Tampa Bay, *in* Tampa Bay Area Scientific Information Symposium, May 1982: Tampa, Fla., Proceedings, p. 10–17.

Masch, F. D., and Brandes, R. J., 1975, Simulation of tidal hydrodynamics—Masonboro Inlet, *in* Symposium on modeling techniques: American Society of Civil Engineers Conference, San Francisco, Calif., September 3–5, 1975, Proceedings, p. 220–239.

Prandle, David, and Crookshank, N. L., 1974, Numerical model of St. Lawrence River estuary: Journal of the Hydraulics Division, American Society of Civil Engineers, v. 100, no. HY4, p. 517–529.

Reid, R. O., and Bodine, B. R., 1968, Numerical model for storm surges in Galveston Bay: Journal of the Waterways and Harbors Division, American Society of Civil Engineers, v. 94, no. WWI, p. 33–57.

Rosenshein, J. S., Goodwin, C. R., and Jurado, Antonio, 1977, Bottom configuration and environment of Tampa Bay: Photogrammetric Engineering and Remote Sensing, v. 43, no. 6, p. 693–699.

Ross, B. E., 1973, The hydrology and flushing of the bays, estuaries, and nearshore areas of the eastern Gulf of Mexico, *in* A summary of knowledge of the eastern Gulf of Mexico: St. Petersburg, Fla., Florida Institute of Oceanography, p. IID-1–IID-45.

Ross, B. E., and Anderson, M. W., 1972 Courtney-Campbell Causeway tidal flushing study: Report to the Florida Department of Transportation, Tampa Bay Regional Planning Council, St. Petersburg, Fla., 16 p.

Saloman, C. H., Finucane, J. H., and Kelly, J. A., Jr., 1964, Hydrographic observations of Tampa Bay, Florida, and adjacent waters, August 1961 through December 1962: U.S. Fish and Wildlife Service, Bureau of Commercial Fisheries Data Report 4, 112 p.

Schaffranek, R. W., and Baltzer, R. A., 1975, Compiling bathymetry for flow simulation models, *in* Symposium on modeling techniques: American Society of Civil Engineers Conference, San Francisco, Calif., September 3–5, 1975, Proceedings, p. 1329–1346.

Thompson, R. B., ed., 1980, Florida statistical abstract: Gainesville, The University Presses of Florida, 695 p.

U.S. Department of Commerce, 1951, Tidal current charts—Tampa Bay: Coast and Geodetic Survey, 12 p.

———1971, Tide tables 1972—High and low water predictions—East coast of North and South America including Greenland: National Oceanic and Atmospheric Administration, National Ocean Service, 290 p.

———1982a, Tide tables 1983—High and low water predictions—East Coast of North and South America including Greenland: National Oceanic and Atmospheric Administration, National Ocean Service, 285 p.

———1982b, Tidal current tables 1983—Atlantic Coast of North America: National Oceanic and Atmospheric Administration, National Ocean Service, 234 p.

U.S. Department of the Interior, 1969, Problems and management of water quality in Hillsborough Bay, Florida: Federal Water Pollution Control Administration, 88 p.

U.S. Geological Survey, 1977, Water resources data for Florida, water year 1976: U.S. Geological Survey Water-Data Report FL-76-3, v. 3, Southwest Florida, 1,070 p.

Van der Ree, W. J., Voogt, J., and Leendertse, J. J., 1978, A tidal survey for a model of an offshore area, *in* Proceedings of the Sixteenth Coastal Engineering Conference: New York, American Society of Civil Engineers, p. 2656–2670.

Wang, J. D., 1978, Verification of finite element hydrodynamic model cafe, *in* Verification of mathematical and physical models in hydraulic engineering: American Society of Civil Engineers Specialty Conference, College Park, Md., August 9–11, 1978, Proceedings, p. 500–508.

Woodward-Clyde Consultants, 1979, Egmont Channel, Tampa, Florida, tidal height study: Final report contract DACW17-79-C-0020 to U.S. Army Corps of Engineers, Jacksonville, Fla., 17 p.

GLOSSARY OF SELECTED TERMS

Constituent transport. The rate and direction of movement of a quantity of constituent material dissolved in water, expressed in weight per unit time.

Dissolved constituent. Any material that is in true solution as distinguished from material that is in suspension.

Gyre. An area of rotational water flow that is characterized by little or no motion near its center and generally circular or eliptical motion elsewhere.

Mean lower low water. A tidal datum computed as the average of the lowest low water altitude of each tidal day observed over a given period of time, generally an 18.6-year tidal epoch.

Tidal prism. The volume of water that enters or leaves a tidal water body between high slack water and low slack water. This is approximately equal to the surface area of the water body multiplied by the tidal range between high tide and low tide.

Tide-induced circulation. In general, the tidally averaged, long-term water motion that occurs because of the existence of alternating flood and ebb (inward and outward) movement of the tide over an irregularly shaped bottom. More specifically, the tidally averaged rate of inward-flowing water defined at any cross section within a tidal water body, expressed in volume per unit time. Due to continuity, this is also equal to the tidally averaged rate of outward-flowing water minus the average tributary streamflow.

Water transport. The rate and direction of movement of a quantity of water, expressed in volume per unit time.

Abbreviations and Conversion Factors

Factors for converting inch-pound units used in this report to International System of Units (SI) are listed below.

Multiply inch-pound unit	By	To obtain SI unit
inch (in.)	25.4	millimeter (mm)
foot (ft)	0.3048	meter (m)
mile (mi)	1.609	kilometer (km)
square mile (mi^2)	2.590	square kilometer (km^2)
cubic foot (ft^3)	0.02832	cubic meter (m^3)
cubic yard (yd^3)	0.7646	cubic meter (m^3)
foot per second (ft/s)	0.3048	meter per second (m/s)
mile per hour (mi/h)	1.609	kilometer per hour (km/h)
pound per second (lb/s)	0.4536	kilogram per second (kg/s)
pound per day (lb/d)	0.4536	kilogram per day (kg/d)
square foot per second (ft^2/s)	0.09290	square meter per second (m^2/s)
cubic foot per second (ft^3/s)	0.02832	cubic meter per second (m^3/s)
foot per square second (ft/s^2)	0.3048	meter per square second (m/s^2)
pound per square foot (lb/ft^2)	4.882	kilogram per square meter (kg/m^2)
pound•square second per $foot^4$ ($lb \cdot s^2/ft^4$)	515.2	kilogram per cubic meter (kg/m^3)
micromho per centimeter at 25°C (μmho/cm)	1.000	microseimens per centimeter at 25°C (μS/cm)

National Geodetic Vertical Datum of 1929 (NGVD of 1929).—A geodetic datum derived from a general adjustment of the first-order level nets of both the United States and Canada, formerly called mean sea level.

☆ U S GOVERNMENT PRINTING OFFICE 1987 - 181-407 - 226/40110